

General guarantees for randomized benchmarking with random quantum circuits

Markus Heinrich¹, Martin Kliesch^{1,2}, and Ingo Roth³

¹Institute for Theoretical Physics, Heinrich Heine University Düsseldorf, Düsseldorf, Germany

²Institute for Quantum-Inspired and Quantum Optimization, Hamburg University of Technology, Germany

³Quantum research centre, Technology Innovation Institute, Abu Dhabi, United Arab Emirates

In its many variants, randomized benchmarking (RB) is a broadly used technique for assessing the quality of gate implementations on quantum computers. A detailed theoretical understanding and general guarantees exist for the functioning and interpretation of RB protocols if the gates under scrutiny are drawn *uniformly* at random from a compact group. In contrast, many practically attractive and scalable RB protocols implement random quantum circuits with local gates randomly drawn from some gate-set. Despite their abundance in practice, for those *non-uniform* RB protocols, general guarantees for gates from arbitrary compact groups under experimentally plausible assumptions are missing. In this work, we derive such guarantees for a large class of RB protocols for random circuits that we refer to as *filtered RB*. Prominent examples include linear cross-entropy benchmarking, character benchmarking, Pauli-noise tomography and variants of simultaneous RB. Building upon recent results for random circuits, we show that many relevant filtered RB schemes can be realized with random quantum circuits in linear depth, and we provide explicit small constants for common instances. We further derive general sample complexity bounds for filtered RB. We show filtered RB to be sample-efficient for several relevant groups, including protocols addressing higher-order cross-talk. Our theory for non-uniform filtered RB is, in principle, flexible enough to design new protocols for non-universal and analog quantum simulators.

Contents

1	Introduction	2
2	The filtered randomized benchmarking protocol	5
3	Summary of results	9
4	Preliminaries	11
4.1	Operators, superoperators and norms	11
4.2	Representation theory	12
4.3	Fourier transform on compact groups	14
4.4	ρ -designs, moment operators, and random walks	16
4.5	The Heisenberg-Weyl and Clifford group	20
5	Results	21
5.1	Setting and noise model	21
5.2	The effective measurement frame	21

Markus Heinrich: markus.heinrich@hhu.de, corresponding author

Martin Kliesch: martin.kliesch@tuhh.de

Ingo Roth: ingo.roth@tii.ae

5.3	Signal guarantees for filtered randomized benchmarking	24
5.4	Sampling complexity of filtered randomized benchmarking	33
5.5	Sufficient sequence lengths	41
5.6	Comparison of bounds to typical random circuit decays	46
5.7	Application to common random circuits	48
5.8	Towards better filter functions	53
5.9	Detailed comparison to related works	56
6	Conclusion	58
7	Acknowledgements	59
8	Acronyms	59
	References	59
A	Different estimators and their variances	66
B	Matrix perturbation theory	67
C	Sampling complexity for ideal implementations	72
C.1	Second moment for unitary 3-designs	72
C.2	Second moment for local unitary 3-designs	77
C.3	Second moment for the Heisenberg-Weyl/Pauli group	79

1 Introduction

Assessing the quality of quantum gate implementations is a crucial task in developing quantum computers [1, 2]. Arguably, the most widely employed protocols for this task are randomized benchmarking (RB) [3–8] and its many variants (see Ref. [9] for a recent overview) including linear cross-entropy benchmarking (XEB) [10]. The basic idea of RB is to measure the accuracy of random gate sequences of different lengths. Typically, this results in an experimental signal described by (a mixture of) exponential decays. Stronger noise results in faster decays with smaller decay parameters. Hence, those decay parameters are used to capture the average fidelity of the implemented quantum gates. A crucial advantage of these methods besides their experimental efficiency is that the reported decay parameters are robust against state preparation and measurement (SPAM) errors.

Generally speaking, many experimental signatures can be rather well fitted by an exponential decay. Experimentally observing an exponential decay in an RB experiment does by itself not justify the interpretation of the decay parameter as a measure for the quality of the gates. In addition, RB requires a well-controlled theoretical model that explains the observed decays under realistic assumptions and provides the desired interpretation of the decay parameters.

Extensive research has already established a solid theoretical foundation for RB, particularly when the gates comprising the sequences are drawn *uniformly* at random from a compact group. Generalizing the arguments of Refs. [8, 11–14], Helsen et al. [9] derived general guarantees for the signal form of the entire zoo of RB protocols with finite groups (which readily generalizes to compact groups [15]): If the noise of the gate implementation is sufficiently small (in a precise sense), each decay parameter is associated to an irreducible representation (irrep) of the group generated by the gates. (To be precise, the decay parameter is the dominant eigenvalue of a generalized Fourier transform of the noisy implementation.) Thus, the decay parameter indeed quantifies the average deviation of the gate implementation from their ideal action on the subspace carrying the irrep. For example, the ‘standard’ RB protocol draws random multi-qubit gates uniformly from the Clifford group, except for the last gate of the sequence, which is supposed to restore the initial state. This protocol results in a single decay parameter associated with the irreducible action on traceless matrices and related to the average gate fidelity.

In practice, however, the suitability of *uniform* RB protocols for holistically assessing the quality of noisy and intermediate-scale quantum (NISQ) hardware is restricted. On currently available hardware, sufficiently long sequences of multi-qubit Clifford unitaries lead to way too fast decays to be accurately estimated for already moderate qubit counts. More scalable RB protocols *directly* draw sequences of local random gates, implementing a *random circuit* [16–19]. We refer to those protocols that use a non-uniform probability distribution over a compact group as *non-uniform* RB protocols. Arguably, the most prominent example of non-uniform RB is the *linear cross-entropy benchmarking (XEB)* protocol, which was used for the first demonstration of a quantum computational advantage in sampling tasks [10, 20].

Establishing theoretical guarantees for non-uniform RB is considerably more subtle. Roughly speaking, the interpretation of the decay parameter is more complicated as one additionally witnesses the convergence of the non-uniform distribution to the uniform one with the sequence length—causing a superimposed decay in the experimental data. These obstacles are well-known in the RB literature [17, 21] and have raised suspicion in the context of linear XEB [22, 23]. If not carefully considered, one easily ends up significantly overestimating the fidelity of the gate implementations. In the context of their *universal randomized benchmarking* framework, Chen, Ding, and Huang [24] have given a comprehensive analysis of non-uniform RB protocols using random circuits which form approximate unitary 2-designs. As such, the results in Refs. [24] are e.g. applicable to linear XEB with universal gate sets or with gates from the Clifford group [25].

The original theoretical analysis of linear XEB relies on the assumption that for every circuit, one observes an ideal implementation up to global depolarizing noise [10]. Building more trust in linear XEB has motivated a line of theoretical research, introducing different heuristic estimators [22] and analyzing the behaviour of different noise models in random circuits [26, 27] using mappings of random circuits to statistical models [28]. But general guarantees that work under minimal plausible assumptions on the gate implementation and for random circuits generating arbitrary compact groups—akin to the framework [9, 15] for uniform RB and going beyond unitary 2-designs [24, 25] — are missing. Moreover, the sampling complexity of protocols like linear XEB for non-uniform distributions and general gate-dependent noise remains unclear.

In this work, we close these gaps by developing a general theory of *filtered randomized benchmarking* with *random circuits* using gates from *arbitrary compact groups* under arbitrary gate-dependent (Markovian and time-stationary) noise. Under minimal assumptions, we guarantee the functioning of the protocol, and give explicit bounds on sufficient sequence lengths as well as on the number of samples. Moreover, we specialize our general findings to concrete groups and random circuits, and give explicit constants.

Besides linear XEB, *filtered RB* [9] encompasses character benchmarking [29], matchgate benchmarking [30], and Pauli-noise tomography [31] as well as variants of simultaneous [32] and correlated [33] RB as additional examples.

Filtered RB protocols deviate from standard RB by omitting the last gate that inverts the sequence and instead perform a computational basis measurement. This approach simplifies the experimental procedure and is arguably a core requirement for experimentally scalable *non-uniform* RB. The last inversion gate is calculated in the classical post-processing of the data. At this stage, the experimental data can be additionally filtered to show only specific decays (associated with an individual irrep) of potentially overlapping decays arising for smaller groups.

The filtering allows for a more fine-grained perspective on the perturbative argument at the heart of the framework of Ref. [9] such that the different irreps of a group can be analyzed individually. In this way, we derive new perturbative bounds based on the harmonic analysis of compact groups that can be naturally combined with results from the theory of random circuits, thereby treating uniform and non-uniform RB on the same footing.

More precisely, our guarantees assume that the *error of the average implementation (per irrep)* of only the gates actually appearing in the random circuit is sufficiently small compared to a corresponding spectral gap of the random circuit. Then, the signal of filtered RB is well-described by a suitable exponential decay after a sufficient circuit depth. The required depth depends inversely on the spectral gap and logarithmically on the dimension of the irrep. We show that for practically relevant examples, our results imply that a *linear* circuit depth in the number of qubits suffices for filtered RB.

Omitting the inversion gate comes at the price that the simple arguments for the sample-

efficiency of standard randomized benchmarking do not longer apply to filtered RB. As in shadow estimation for quantum states [34], the post-processing introduces estimators that are generally only bounded exponentially in the number of qubits. Thus, the precise convergence of estimators calculated from polynomially many samples is a priori far from clear.

Generalizing our perturbative analysis of the filtered RB signal to its variance, we derive general expressions for the sample complexity of filtered RB. In particular and under essentially the same assumptions that guarantee the signal form of the protocol, filtered RB is as sample-efficient as the analogous protocol that uses uniformly distributed unitaries. Again important examples are found to be already sample-efficient using linear circuit depth. Perhaps surprisingly, we find that filtered RB without entangling gates has constant sampling complexity independent of the non-trivial support of the irreps. This finding is in contrast to the related results in state shadow estimation.

To showcase the general results, we explicitly discuss the cases where the random circuit generates the Clifford group, the local Clifford group, or the Pauli group. Moreover, we discuss common families of random circuits and summarize spectral gap bounds with explicit, small constants from the literature and our own considerations [35–39].

Finally, it is an open question whether the post-processing of filtered RB can be modified so that meaningful decay constants can be extracted already from *constant depth* circuits. In the context of linear XEB, Ref. [22] introduces a heuristic so-called ‘unbiased’ estimator to this end. Using the general perspective of filtered RB, we sketch two general approaches to construct modified linear estimators for constant-depth circuits. The first approach introduces a more costly computational task in the classical post-processing. The second approach requires that the random distribution of circuits is locally invariant of local Clifford gates. We formally argue that these estimators work under the assumption of global depolarizing noise, putting them at least on the same footing as existing theoretical proposals. However, we leave a detailed perturbative analysis to future work.

We expect that the theory of non-uniform filtered RB can be applied to many more practically relevant benchmarking schemes and bootstraps the development of new RB schemes. In fact, one of our main motivations for deriving the flexible theoretical framework is its applications for the characterization and benchmarking of non-universal and analog quantum computing devices—consolidating and extending existing proposals [40, 41] in future work.

On a technical level, we develop tools to analyze noisy random circuits using harmonic analysis on compact groups and matrix perturbation theory. We expect that this perturbative description also finds applications in quantum computing beyond the randomized benchmarking of quantum gates. The tools and results might, in principle, be applicable to analyze the noise-robustness of any scheme involving random circuits, e.g. randomized compiling [42], shadow tomography and randomized measurements [43] or error mitigation [44]. As a by-product, our variance bounds take a more direct representation-theoretic approach working with tensor powers of the adjoint representation rather than exploiting vector space isomorphisms and invoking Schur-Weyl duality [45]. This approach also opens up a complimentary, illuminating perspective on the sample-efficiency of estimation protocols based on random sequences of gates more generally.

Prior and related work. Already one of the first RB proposals, NIST RB [7] classifies as non-uniform RB and was later thoroughly analyzed and compared to standard Clifford RB [21]. A first discussion of the obstacles arising from decays associated with the convergence to the uniform measure was then given in Ref. [21]. Further non-uniform RB protocols are approximate RB [16] and direct RB [17] (sometimes called *generator RB*). The original guarantees for these protocols rely on the closeness of the probability distribution to the uniform one in total variance distance, thus generally requiring long sequences. Direct RB ensures this closeness by starting from a random stabilizer state as the initial state—assumed noiseless in the analysis, which is additionally restricted to Pauli-noise. The restriction can be justified with randomized compiling [42, 46, 47], which essentially requires the perfect implementation of Pauli unitaries.

The work by Helsen et al. [9] unifies and generalizes the guarantees for these schemes to gate-dependent noise but still works with convergence in total variation distances. The approach of Ref. [9] extends previous arguments for the analysis of gate-dependent noise by Wallman [13] using the language of Fourier transforms of finite groups introduced to RB by Merkel *et al.* [14]. The argument straightforwardly carries over to compact groups [15]. The assumptions on the gate

implementation required for the guarantees of Ref. [9], closeness in average diamond norm error over all irreps, are too strong to yield practical circuit depths for RB with random circuits.

This obstacle has been overcome in the *universal randomized benchmarking* framework by Chen, Ding, and Huang [24]. There, the authors are able to relax the assumption on the probability measure for the above protocols (“twirling schemes” in Ref. [24]) and only require that the channel twirl over this measure is within unit distance from the Haar-random channel twirl (in induced diamond norm or spectral norm). Hence, it is sufficient for these schemes to implement random circuits which form approximate unitary 2-designs w.r.t. the relevant norm. As such, it is necessary that the used distributions have support on groups which are unitary 2-designs, such as the unitary or the Clifford group [25].

The logic of our proofs follows the established outline of using matrix perturbation theory as in Refs. [9, 15, 24], and combines this with harmonic analysis. Thus, our work can be seen as generalization of the main results in these works to arbitrary compact groups and non-uniform measures thereon, although with some notable technical innovations. By more carefully controlling the perturbation of the Fourier transform per irrep in spectral norm specifically for filtered RB, we can directly study the noise perturbation of the moment operators associated with random circuits. Moreover, we go beyond these works by deriving general bounds on the required sequence lengths, analyzing the sampling complexity of filtered RB, and proposing changes to our protocol which may lead to sub-linear circuits. We discuss the similarities and differences to Refs. [9, 15, 24, 25] in more detail in Sec. 5.9.

Filtered RB, as formulated in Ref. [9], is a variant of character RB [29]. Linear XEB [10], when averaged over multiple circuits, can be seen as the special case of filtered RB when the group generated by the circuits is a unitary 2-design. Ref. [9] analyzes linear XEB, including variance bounds, but only for uniform measures, not for random circuits. Ref. [26] puts forward a different perturbative analysis for filtered randomized benchmarking schemes by carefully tracing the effect of individual Pauli-errors in random circuits. To our understanding, the argument, however, crucially relies on the heuristic estimator proposed in Ref. [22]. See also the review [20] for a detailed literature overview on linear XEB. Hybrid benchmarking [19] involves the measurement of random Pauli observables at the end of gate sequences, followed by suitable post-processing in order to avoid the inversion gate. For sequences from arbitrary probability measures and gate-dependent noise, the hybrid benchmarking signal is then shown to consist of linear combinations of (exponentially) many decays with complex poles [18, 19]. Estimating these poles, however, is typically infeasible, see the detailed discussion in Ref. [9]. This further illustrates the importance of the perturbative approach that justifies the approximation by *few* decay parameters for understanding practical benchmarking schemes. Hybrid benchmarking can also be understood within our filtered RB framework. In particular, our analyses indicate that the Monte-Carlo sampling in Ref. [19] can be avoided, resulting in an improved sampling complexity.

The here discussed filtered RB protocols for circuits generating local groups is an alternative to simultaneous [32] and correlated [33] RB but is in addition capable of estimating higher-order correlations. A randomized benchmarking scheme with the Heisenberg-Weyl group is also proposed in Ref. [48].

Alternative approaches to filtered non-uniform RB aiming at better scalability of randomized benchmarking protocols are cycle RB [49, 50], averaged circuit eigenvalue sampling (ACES) [51] and the recent RB with mirror circuits [52].

2 The filtered randomized benchmarking protocol

We start by describing and motivating the general protocol of *non-uniform filtered randomized benchmarking (RB)*. The general version of this protocol has been described in Refs. [9, 53]. Many already existing protocols naturally fall into this class or can be reformulated to do so.

We consider a quantum device with state space modelled by a d -dimensional Hilbert space \mathcal{H} . Filtered RB aims at assessing the quality of the implementation of a set of coherent operations on the device that constitute a compact group $G < \text{U}(\mathcal{H})$. The random operations that are actually applied in the experiment are specified by a probability measure ν on G . For example, ν can be a uniform measure on a subset of operations generating G that are ‘native’ to the device.

The protocol of *non-uniform filtered RB* can be divided into two distinct phases: The *data acquisition phase* in which experimental data is collected, and the *post-processing phase* in which this data is processed and the decay parameters are extracted.

Data acquisition. A key feature of filtered RB is that the experimental prescription is simple and already routinely implemented in many experiments. The protocol for the data acquisition phase repeats the following primitive for different sequence lengths m : Prepare a fixed initial state ρ , apply independent and identically distributed gates $g_1, \dots, g_m \sim \nu$ and perform a measurement in a fixed basis $E_i := |i\rangle\langle i|$ for $i \in [d] = \{1, \dots, d\}$. The output of a single run of this primitive is a tuple $(i, g_1, \dots, g_m) \in [d] \times G^m$ where i is the observed measurement outcome.

The setting differs from the standard RB protocol in two major aspects: First, we allow that the gates g_i are drawn from a suitable probability measure which does not need to be the Haar measure nor a unitary 2-design. In particular, it is explicitly allowed to draw them from a set of generators of the group G . Precise conditions on the measure will be formulated and discussed later. Second, we omit the *end* or *inversion gate* $g_{\text{end}} = (g_m \cdots g_1)^{-1}$ at the end of the sequence and record a basis measurement outcome. From a practical point of view, this is advantageous since even if the individual gates g_1, \dots, g_m have short circuit implementations, this is not necessarily true for g_{end} . Instead, the inversion gate is effectively accounted for in the post-processing of the obtained samples [9].

Post-processing. At the heart of *filtered RB* is the idea of analyzing the performance of the implementation of the group for individual irreducible representations (irreps). This allows one to isolate single exponential decays in the post-processing giving rise to crucial simplifications of the experimental signatures [9]. The device is intended to implement a certain *target* or *reference* representation ω of G . For all practical purposes, ω is given as the conjugation representation $\omega(g) = U_g(\cdot)U_g^\dagger$ acting on $\text{End}(\mathcal{H})$, the linear operators on \mathcal{H} , and U_g is the representation of G on the Hilbert space \mathcal{H} . The representation ω has a decomposition into irreducible subrepresentations (irreps) depending on the choice of G . We will quantify the quality of implementing ω by assessing the implementation for each of its irreps in the post-processing. For example for $G = \text{U}(d)$, ω has two irreps: The trivial action on the subspace spanned by the identity and the action on the subspace of traceless matrices.

To describe the post-processing in detail, we introduce the quantum channel

$$S := \int_G \omega(g)^\dagger M \omega(g) d\mu(g), \quad M(X) := \sum_{i \in [d]} \text{tr}[E_i X] E_i. \quad (1)$$

Here, μ is the Haar (uniform) probability measure on G . Thus, S is the *channel twirl* w.r.t. to G applied to the completely dephasing channel M in the measurement basis $\{|i\rangle\}_{i \in [d]}$. Given an irrep τ_λ of G labelled by λ , we denote by P_λ the projector onto the irrep τ_λ in $\text{End}(\mathcal{H})$. Finally, we define a *filter function* $f_\lambda : [d] \times G \rightarrow \mathbb{C}$ by

$$f_\lambda(i, g) := \text{tr}[E_i \omega(g) S^+ P_\lambda(\rho)], \quad (2)$$

where S^+ is the Moore-Penrose pseudoinverse of S . As we see later, S is positive semi-definite and thus S^+ is simply the superoperator given by inverting all non-zero eigenvalues of S .

The first step of the post-processing is to calculate the mean estimator of f_λ evaluated on the samples collected in the data acquisition. Say, we collected a number of N samples $(i^{(l)}, g_1^{(l)}, \dots, g_m^{(l)})$. Then, we evaluate

$$\hat{F}_\lambda(m) = \frac{1}{N} \sum_{l=1}^N \overline{f_\lambda(i^{(l)}, g_1^{(l)} \cdots g_m^{(l)})}. \quad (3)$$

We refer to $\hat{F}_\lambda(m)$ as the RB signal and denote its expected value as

$$F_\lambda(m) := \mathbb{E}[\hat{F}_\lambda(m)]. \quad (4)$$

The main result of this work lies in deriving conditions that guarantee an exponential fitting model for the expected RB signal $F_\lambda(m)$ and the variance of $\hat{F}_\lambda(m)$. This justifies to fit an exponential decay $a_\lambda r_\lambda^m$ to the RB signal and obtain the decay parameter r_λ , the result of the RB protocol.

The post-processing involves evaluating f_λ and, thus, basically simulating the sequence of gates restricted to the irrep under consideration. This may require run-time and memory scaling exponentially in the number of qubits.

The ideal signal. To motivate our choice of filter function, let us consider an ideal and noise-free implementation, and gates that are drawn uniformly from G . For a given sequence of gates, the data acquisition phase produces samples from the distribution given by the Born probabilities

$$p(i|g_1, \dots, g_m) = \text{tr}[E_i \omega(g_m) \cdots \omega(g_1)(\rho)] = \text{tr}[E_i \omega(g)(\rho)], \quad g := g_m \cdots g_1.$$

Hence, we are effectively measuring ρ with respect to the positive operator-valued measure (POVM) $(i, g) \mapsto \omega(g)^\dagger(E_i) d\mu(g)$. Let us, for the sake of the argument, assume that the POVM is *informationally complete*, i.e. the operators $\omega(g)^\dagger(E_i)$ span the full operator space $\text{End}(\mathcal{H})$. As this span is exactly the range of S , it is invertible and the pseudoinverse is the inverse, $S^+ = S^{-1}$. We observe that the filtered RB signal (4) becomes

$$\begin{aligned} F_\lambda(m) &= \sum_{i \in [d]} \int_{G^m} \text{tr}[\rho P_\lambda S^{-1} \omega(g_1 \cdots g_m)^\dagger(E_i)] \text{tr}[E_i \omega(g_1 \cdots g_m)(\rho)] d\mu(g_1, \dots, g_m) \\ &= \text{tr}\left[\rho P_\lambda S^{-1} \int_G \omega(g)^\dagger M \omega(g) d\mu(g)(\rho)\right] = \text{tr}[\rho P_\lambda(\rho)]. \end{aligned} \quad (5)$$

Hence, we have found that $F_\lambda(m)$ is exactly the overlap of ρ with the irrep τ_λ . In the case that the POVM is not informationally complete, the result is $\text{tr}[\rho P_\lambda S^+ S(\rho)]$, where $S^+ S$ is exactly the projector onto the span of the POVM.

Example: Linear XEB as filtered randomized benchmarking. The perhaps most prominent example of filtered RB is linear cross-entropy benchmarking (XEB), as already observed in Ref. [9, Sec. VIII.C]. Originally, the linear cross-entropy was proposed as a proxy to the cross-entropy between the output probability distribution of an *individual* generic quantum circuit and its experimental implementation, designed to specifically discriminate against a uniform output distribution [10]. The theoretical motivation, however, already stems from considering an ensemble of random unitaries and the original analysis of linear XEB is based on typicality statements that hold on average or (by concentration of measure) with high-probability over the ensemble. When also explicitly *taking the average* of the linear cross-entropy estimates of random instances from an ensemble of unitaries, linear XEB becomes a randomized benchmarking scheme, more precisely, a *non-uniform filtered randomized benchmarking for the full unitary group*. Let us reproduce this argument in a slightly more general form.

In linear XEB on n qubits, a random unitary U , sampled according to some probability measure ν on $U(2^n)$, is applied to the initial state $\rho := |0\rangle\langle 0|$, followed by a computational basis measurement described by projectors $\{E_x := |x\rangle\langle x|\}_{x \in \mathbb{F}_2^n}$, where \mathbb{F}_2 denotes the binary field. Having observed outcomes $x^{(1)}, \dots, x^{(N)}$ for unitaries $U^{(1)}, \dots, U^{(N)}$, one computes the estimator

$$\hat{F}_{\text{XEB}} = \frac{1}{N} \sum_{i=1}^N (d p_{\text{ideal}}(x^{(i)} | U^{(i)}) - 1), \quad (6)$$

where $d = 2^n$ and $p_{\text{ideal}}(x|U) := |\langle x | U | 0 \rangle|^2$ is the ideal, noiseless outcome distribution of the circuit U . As before, let $p(x|U)$ be the actual outcome distribution in the presence of noise. Then, the

expected value of the linear XEB estimator (6) reads

$$\begin{aligned}
F_{\text{XEB}} &= \sum_{x \in \mathbb{F}_2^n} \int_{\text{U}(2^n)} p(x|U) (d p_{\text{ideal}}(x|U) - 1) \, d\nu(U), \\
&= d \sum_{x \in \mathbb{F}_2^n} \int_{\text{U}(2^n)} p(x|U) \left(\text{tr}(|x\rangle\langle x| \omega(U)(\rho)) - \frac{1}{d} \right) \, d\nu(U) \\
&= d \sum_{x \in \mathbb{F}_2^n} \int_{\text{U}(2^n)} \text{tr}(|x\rangle\langle x| \omega(U) P_{\text{ad}}(\rho)) p(x|U) \, d\nu(U) \\
&= \frac{d}{d+1} \sum_{x \in \mathbb{F}_2^n} \int_{\text{U}(2^n)} f_{\text{ad}}(x|U) p(x|U) \, d\nu(U) \\
&= \frac{d}{d+1} F_{\text{ad}}(1).
\end{aligned}$$

Here, we inserted our definition of the filtered RB signal (4), using that the projector onto the traceless irrep of the unitary group is $P_{\text{ad}}(X) = X - \text{tr}(X)\mathbb{1}/d$ and the operator S is such that $S^{-1}P_{\text{ad}} = (d+1)P_{\text{ad}}$ (as derived later in Sec. 5.2). Moreover, we used that f_{ad} is real-valued.

This argument can easily be adapted to the case where a random quantum circuit is used. If the random circuit has m layers and every layer is sampled according to the measure ν , then, F_{XEB} reads instead

$$\begin{aligned}
F_{\text{XEB}} &= \frac{d}{d+1} \sum_{x \in \mathbb{F}_2^n} \int_{\text{U}(2^n)} f_{\text{ad}}(x|U_1 \cdots U_m) p(x|U_1, \dots, U_m) \, d\nu(U_1) \cdots d\nu(U_m) \\
&= \frac{d}{d+1} F_{\text{ad}}(m).
\end{aligned}$$

Thus, we observe that linear XEB is in fact performing a filtered RB protocol for the unitary group $G = \text{U}(d)$. Note that the discrepancy in the prefactor stems from the fact that F_{XEB} uses a different normalization. Nevertheless $\frac{d}{d+1} \approx 1$ for a moderate number of qubits.

3 Summary of results

Having introduced the protocol, we aim to give a slightly more technical summary of our main results in this section. To this end, we sketch the line of argument of this work while avoiding unnecessary technicalities.

We model the imperfect implementation of gates on the quantum device by a so-called *implementation map* ϕ on G such that $\phi(g)$ is completely positive and trace non-increasing for all $g \in G$. In particular, the existence of such a map requires that the gate noise is *Markovian and time-stationary*, although generalizations are conceivable [54]. In the absence of noise, the implementation map should be exactly given by the *reference representation* ω of G . As noted above, the reference representation is simply $\omega(g) = U_g(\cdot)U_g^\dagger$, where U_g is the representation of G on the Hilbert space \mathcal{H} . We consider the filtered RB signal of a non-trivial irrep τ_λ of ω .

Generalizing the argumentation leading to Eq. (5), we show that non-uniform filtered RB assesses the eigenvalues of the linear map $\widehat{\phi\nu}[\tau_\lambda] = \int_G \tau_\lambda(g)^\dagger(\cdot)\phi(g)d\nu(g)$. The notation stems from the fact that this map can be identified with an operator-valued Fourier transform on G , applied to ϕ and the measure ν . We treat $\widehat{\phi\nu}[\tau_\lambda]$ as a perturbation of the Fourier transform $\widehat{\omega\nu}[\tau_\lambda] = \int_G \tau_\lambda(g)^\dagger(\cdot)\omega(g)d\nu(g)$ for the ideal implementation $\phi = \omega$. The map $\widehat{\omega\nu}[\tau_\lambda]$ is related to the well-known *channel twirl* w.r.t. the measure ν , and obtained from the latter by projecting onto the irrep τ_λ . Particularly crucial for our arguments, $\widehat{\omega\nu}[\tau_\lambda]$ has the form of a (second-order) *moment operator* associated with the measure ν , and the convergence rate of the random circuit generated by ν to the uniform measure on G is controlled by the spectral gap Δ_λ of $\widehat{\omega\nu}[\tau_\lambda]$. Using matrix perturbation theory, we then find an explicit expression for the signal form of filtered RB:

Theorem (Signal form of filtered RB, informal). *Assume τ_λ is multiplicity-free in ω and suppose there is a $\delta_\lambda > 0$ such that*

$$\|\widehat{\phi\nu}[\tau_\lambda] - \widehat{\omega\nu}[\tau_\lambda]\|_\infty \leq \delta_\lambda < \frac{\Delta_\lambda}{5}.$$

Then, $\mathbb{E}[\hat{F}_\lambda(m)] = A_\lambda I_\lambda^m + \text{tr}(B_\lambda O_\lambda^m)$ where $1 - 2\delta < I_\lambda \leq 1$ captures the average gate noise, independent of SPAM, and the second term is suppressed as

$$|\text{tr}(B_\lambda O_\lambda^m)| \leq c_\lambda (1 - \Delta_\lambda + 2\delta_\lambda)^m, \quad (7)$$

with a constant c_λ depending on the irrep, measurement basis, and SPAM. Typically, we have $c_\lambda = O(d_\lambda)$.

Note that we here assumed that τ_λ is multiplicity-free for the sake of brevity. Thm. 8 in Sec. 5 provides the more general statement including multiplicity, yielding i.a. a *matrix-exponential* RB signal with the multiplicity determining the matrix dimension.

A similar perturbative approach is taken in Ref. [9], however our analysis is able to focus on individual irreps, and our guarantees depend only on irrep-specific quantities. Moreover, we only require that the measure ν ‘approximates Haar moments’ of the irrep of G , a significantly weaker assumption than, e.g. approximation in total variation distance used in Ref. [9].

Let us take a closer look at the theorem’s statement: Our guarantee assumes that the *error of the average implementation* of the gates (per irrep) is sufficiently small compared to a irrep-specific spectral gap of the random circuit. Importantly, only the error of the gates which actually appear in the random circuit matter. We provide a detailed discussion of the assumption in Sec. 5.3.1 and connect the assumption to error measures of the individual gates. Provided the perturbation assumption holds, the filtered RB signal is well-described by an exponential decay $A_\lambda I_\lambda^m$, provided the circuit is sufficiently deep to suppress the second sub-dominant term $\text{tr}(B_\lambda O_\lambda^m)$. By Eq. (7), these subdominant terms essentially reflect the mixing process of the random circuit with convergence rate $1 - \Delta_\lambda$. The prefactor c_λ can be improved further for concrete examples: For the non-trivial action of a unitary 2-group on a d -dimensional Hilbert space (e.g. the Clifford group), we have $c_\lambda \in O(d^{3/2})$. For a direct product of unitary 2-groups and an irrep acting non-trivially on s subsystems of local dimension p , we have $c_\lambda \in O(p^{3s/2})$. For the Heisenberg-Weyl/Pauli group acting locally, we find $c_\lambda = 1$.

We work out explicit sufficient conditions on the sequence length in Sec. 5.5. We find that the following sequence length is typically sufficient to suppress the subdominant terms by α :

$$m \geq 2\Delta_\lambda^{-1}(\log(d_\lambda) + \log(1/\alpha) + 1.8), \quad (8)$$

Brickwork circuit (BWC)	$9.8n$
Clifford generators BWC*	$470n$
Local random circuit (LRC)	$4.2n^2$
LRC nearest-neighbor (NN)	$17.5n^2$
Clifford generator LRC	$49n^2$
Clifford generator LRC NN	$49.5n^2$

Table 1: Sufficient circuit lengths for filtered RB with different circuit architectures with 2-qubit gates on n qubits. The bound * is expected to be highly non-optimal.

again with slightly better constants for concrete examples.

By evaluating the bound (8) using results on random quantum circuits [35–39], we arrive at concrete scalings of the circuit depth for some specific examples in Sec. 5.7. The derived scalings are summarized in Tab. 1. Our result implies that for brickwork circuits *linear* circuit depth $m = O(n)$ in the number of qubits n suffices for filtered RB even if one directly draws generators, either from the unitary or from the Clifford group.

For ‘large’ irreps, the range of the estimator $\hat{F}_\lambda(m)$ can scale exponentially in the number of qubits. For this reason, additional effort is required to establish efficient sample-complexity bounds. To this end, we derive bounds on the variance of $\hat{F}_\lambda(m)$ through a perturbative expansion of the second moment, Thm. 10. This allows us to give general expressions for the sample complexity of filtered RB in terms of the corresponding second moments of the noise-free and uniformly random implementation. Again, sub-dominant terms appearing in the perturbative expansion become negligible if the sequence length m is chosen large enough. Typically, this requires that m has to be chosen approximately *twice as large* compared to the bound (8), but in most relevant cases the overhead is smaller. Denote by $\mathbb{E}[f_\lambda^2]_{\text{ideal}}$ the second-moment of the filter function when the implementation is noise-free and the gates are drawn uniformly from the group. We prove the following statement:

Theorem (Sampling complexity of filtered RB, informal). *Choose the sequence length m such that the subdominant terms are bounded by α . If the number of samples fulfills $N \geq (\mathbb{E}[f_\lambda^2]_{\text{ideal}} + \alpha)\varepsilon^{-2}\delta^{-1}$, then the mean estimator $\hat{F}_\lambda(m)$ is ε -precise with probability at least δ .*

The result allows us to derive sample complexity bounds for filtered RB by calculating the moments of the analogous protocol using noise-free, uniformly distributed unitaries. We give the results for groups that form global unitary 3-designs, local unitary 3-designs, and the Heisenberg-Weyl group in Prop. 13. Perhaps surprisingly, we find that filtered RB with single-qubit gates coming from a unitary 3-design (e.g. the Clifford group) has constant sampling complexity irrespective of the size of the non-trivial support of the irreps. Interestingly, a similar result in local dimension $q > 2$ does not hold. More generally, if the group G contains the Heisenberg-Weyl group, Prop. 12 gives an upper and lower bound for the ideal second moment, generalizing the explicit calculations leading to Prop. 13.

On a more technical level, we find that the role of SPAM in the derivation of the sampling complexity is considerably more intricate than in the one of the signal form. As a first step, we bound the perturbation expansion of the second moment $\mathbb{E}[f_\lambda^2]$ appearing in the variance of the mean estimator $\hat{F}_\lambda(m)$ in terms of the second moment of the ideal implementation, but including SPAM, $\mathbb{E}[f_\lambda^2]_{\text{SPAM}}$. To this end, we assume a non-negativity condition on the involved coefficients. Prop. 14 ensures non-negativity in the absence of SPAM and we argue that even with SPAM noise this is likely to still hold. Furthermore, for the case that the Heisenberg-Weyl group is a subgroup of G , we show in Prop. 11 that the effect of SPAM is to reduce the absolute value of the involved coefficients.

Finally, in Sec. 5.8, we propose two potential modifications of filtered RB that can improve over the above scalings and yield meaningful decay parameter already from *constant-depth* circuits at least under simplifying assumptions on the noise.

4 Preliminaries

In the following we introduce the mathematical definitions required for the precise statement and derivation of our results.

4.1 Operators, superoperators and norms

Linear operators. Consider a finite-dimensional Hilbert space \mathcal{H} over the field $\mathbb{F} = \mathbb{C}$ or $\mathbb{F} = \mathbb{R}$. Then, the vector space $\text{End}(\mathcal{H})$ of linear operators on \mathcal{H} is by itself a finite-dimensional Hilbert space over \mathbb{F} with the *Hilbert-Schmidt inner product*:

$$(X|Y) := \text{tr}(X^\dagger Y).$$

Here, X^\dagger is the adjoint operator defined w.r.t. the (complex or real) inner product on \mathcal{H} . As in the usual Dirac notation, we can use the Hilbert-Schmidt inner product to define *operator kets and bras* by $|Y) \equiv Y$ and $(X| : Y \mapsto (X|Y)$. Likewise, we can define outer products $|X)(Y|$ which form linear maps on $\text{End}(\mathcal{H})$ acting as $A \mapsto (Y|A)X$. Following a common nomenclature, we refer to such linear maps as *superoperators* (on \mathcal{H}). As $\text{End}(\mathcal{H})$ is again a Hilbert space, it should not come as a surprise that the vector space of superoperators, $\text{End End}(\mathcal{H}) = \text{End}^2(\mathcal{H})$, can again be endowed with a Hilbert space structure using an analogue inner product. By slightly overloading notation, we use $(\mathcal{X}|\mathcal{Y})$ to also denote the Hilbert-Schmidt inner product between superoperators $\mathcal{X}, \mathcal{Y} \in \text{End}^2(\mathcal{H})$. Likewise, we denote outer products by $|\mathcal{X})(\mathcal{Y}|$, which are linear operators on superoperators and thus lie in $\text{End}^3(\mathcal{H})$.¹

We also consider linear maps $\mathcal{V} \rightarrow \mathcal{W}$ between different Hilbert spaces \mathcal{V} and \mathcal{W} over \mathbb{F} . Analogue to above, these form a Hilbert space $\text{Hom}(\mathcal{V}, \mathcal{W})$ with the Hilbert-Schmidt inner product $(X|Y) := \text{tr}(X^\dagger Y)$ where $X^\dagger : \mathcal{W} \rightarrow \mathcal{V}$ is the adjoint of X defined by $\langle w, X(v) \rangle_{\mathcal{W}} = \langle X^\dagger(w), v \rangle_{\mathcal{V}}$.

Moore-Penrose pseudoinverse. Given a linear operator $X \in \text{End } \mathcal{H}$, the restricted linear map $\tilde{X} : (\ker X)^\perp \rightarrow \text{ran } X$ is an isomorphism and we define the *Moore-Penrose pseudoinverse*, or simply *pseudoinverse* of X to be the linear operator X^+ which is \tilde{X}^{-1} on $\text{ran } X$ and identically zero on $(\text{ran } X)^\perp$. In a basis, X^+ can be computed using the singular value decomposition $X = U\Sigma V^\dagger$ as the matrix $X^+ := V\Sigma^+U^\dagger$, where Σ^+ is the diagonal matrix obtained from Σ by inverting all non-zero singular values. Note that if X is a real matrix, then the singular value decomposition is $X = O\Sigma T^\dagger$ where O and T are orthogonal matrices; in particular, X^+ is a real matrix, too.

Norms. Throughout this paper, we use *Schatten p -norms* which are defined for any linear map $X \in \text{Hom}(\mathcal{V}, \mathcal{W})$ between Hilbert spaces \mathcal{V} and \mathcal{W} and $p \in [1, \infty]$ as

$$\|X\|_p := \left(\text{tr}|X|^p \right)^{\frac{1}{p}} = \left(\sum_{i=1}^d \sigma_i^p \right)^{\frac{1}{p}},$$

where $|X| := \sqrt{X^\dagger X} \in \text{End}(\mathcal{V})$ and $\sigma_i \geq 0$ are the singular values of X , i.e. the square roots of the eigenvalues of the positive semidefinite operator $X^\dagger X$. In particular, we use the *trace norm* $p = 1$, the *spectral norm* $p = \infty$, as well as the *Hilbert-Schmidt norm* $p = 2$ which is simply the norm induced by the Hilbert-Schmidt inner product. The definition of Schatten norms only relies on the Hilbert space structure of the underlying vector space, thus these norms can be defined for operators, superoperators, and even higher-order operators alike.

Hermiticity-preserving maps. The Hilbert space of linear operators $\text{End}(\mathcal{H})$ over $\mathbb{F} = \mathbb{C}$ has a real structure in the sense that it decomposes as a direct sum $\text{End}(\mathcal{H}) = \text{Herm}(\mathcal{H}) \oplus i \text{Herm}(\mathcal{H})$, where $\text{Herm}(\mathcal{H})$ is the real Hilbert space of Hermitian matrices on \mathcal{H} . The associated antilinear involution is given by the adjoint \dagger with $\text{Herm}(\mathcal{H})$ as its fixed point space. We call a linear map $\phi : \text{End}(\mathcal{H}) \rightarrow \text{End}(\mathcal{H})$ *Hermiticity-preserving* if it commutes with \dagger , i.e. it maps $\text{Herm}(\mathcal{H})$ to itself. Naturally, such a map induces a real linear map $\phi_{\mathbb{R}}$ on $\text{Herm}(\mathcal{H})$ by restriction. Note that ϕ

¹We resist the urge to call these *super duper operators* in public.

is Hermiticity-preserving if and only if it is represented by a real matrix in some basis of Hermitian matrices for $\text{End}(\mathcal{H})$ (and ϕ and $\phi_{\mathbb{R}}$ have the same matrix representation).

Finally, suppose $\phi : \text{End}(\mathcal{H}) \rightarrow \text{End}(\mathcal{H})$ is Hermiticity-preserving, then so is its pseudoinverse ϕ^+ . To see this, choose a basis of Hermitian matrices for $\text{End}(\mathcal{H})$ and let A be the matrix representation of ϕ in this basis. Since ϕ is Hermiticity-preserving, A is real-valued and we find the singular value decomposition $A = O\Sigma T^\dagger$ with orthogonal matrices O and T . Next, note that the action of O and T on the complex Hilbert space $\text{End}(\mathcal{H})$ is unitary and hence this is also the singular value decomposition of A seen as a complex matrix. In particular, the matrix representation of ϕ^+ is the real matrix $A^+ = T\Sigma^+O^\dagger$ and hence ϕ^+ is Hermiticity-preserving.

Isomorphisms. Finally, we mention certain non-canonical isomorphisms between the different “levels” in the hierarchy of linear maps. For a complex Hilbert space \mathcal{V} , the inner product does not induce a *linear* isomorphism between \mathcal{V} and its dual \mathcal{V}^* , but instead an anti-linear one. However, any choice of orthonormal basis $(v_i)_i$ of \mathcal{V} gives rise to an isomorphism $\mathcal{V} \rightarrow \mathcal{V}^*$ by $|v_i\rangle \mapsto \langle v_i|$. Having fixed an orthonormal basis $(w_j)_j$ of another Hilbert space \mathcal{W} , this induces an isometry $\text{vec} : \text{Hom}(\mathcal{V}, \mathcal{W}) \simeq \mathcal{W} \otimes \mathcal{V}$, and $\text{Hom}(\mathcal{W}, \mathcal{V}) \simeq \mathcal{V} \otimes \mathcal{W}$, commonly called (*row-wise*) vectorization, by the mapping $|w_j\rangle\langle v_i| \mapsto |w_j\rangle \otimes |v_i\rangle$ and $|v_j\rangle\langle w_i| \mapsto |v_j\rangle \otimes |w_i\rangle$ for all i, j .

Next, let us consider a linear map $\phi : \text{Hom}(\mathcal{V}, \mathcal{W}) \rightarrow \text{Hom}(\mathcal{V}', \mathcal{W}')$ which acts as $\phi(X) = AXB$ for some $B \in \text{Hom}(\mathcal{V}', \mathcal{V})$ and $A \in \text{Hom}(\mathcal{W}, \mathcal{W}')$. Under isometries of the above type, ϕ is then isomorphic to $\text{vec}(\phi) = \text{vec}(A(\cdot)B) := A \otimes B^\top \in \text{Hom}(\mathcal{W} \otimes \mathcal{V}, \mathcal{W}' \otimes \mathcal{V}')$ where the transposition $B^\top \in \text{Hom}(\mathcal{V}, \mathcal{V}')$ is with respect to the chosen basis. This induced isomorphism vec is necessarily an isometry, in particular $\text{vec}(\phi^\dagger) = \text{vec}(A^\dagger(\cdot)B^\dagger) = A^\dagger \otimes \bar{B} = (A \otimes B^\top)^\dagger$. Among others, this implies that the Schatten p -norms are preserved under the isomorphism, $\|\text{vec}(\phi)\|_p = \|\phi\|_p$.

4.2 Representation theory

In this section, we briefly review some basic concepts from the representation theory of compact groups and introduce the relevant notation. For more details, we refer the interested reader to standard text books [55–58].

A *topological group* G is a group which is endowed with a topology such that group multiplication and inversion are continuous maps. We call a topological group *compact* if it is a compact topological Hausdorff space. A compact group comes with a unique Borel measure μ , called the *Haar measure*, which is left and right invariant under group multiplication, $\mu(gA) = \mu(A) = \mu(Ag)$ for all $g \in G$ and open sets $A \subset G$, and normalized as $\mu(G) = 1$.

Given a compact group G , a finite-dimensional *unitary representation* of G is a pair (ρ, V) where V is a finite-dimensional Hilbert space and $\rho : G \rightarrow \text{U}(V)$ is a group homomorphism such that the map $G \times V \rightarrow V$ given by $(g, v) \mapsto \rho(g)v$ is continuous. In general, we call two representations (ρ, V) and (ρ', V') *isomorphic* or *equivalent* if there is a unitary isomorphism $U : V \rightarrow V'$ such that $\rho(g) = U^\dagger \rho'(g)U$ for all $g \in G$. A subspace $W \subset V$ is called *invariant* w.r.t. ρ if $\rho(g)(W) = W$ for all $g \in G$. We call ρ an *irreducible representation* or short *irrep* if the only invariant subspaces are $\{0\}$ and V itself. Otherwise, we call ρ *reducible*. It is well-known that any finite-dimensional unitary representation (ρ, V) of G is *completely reducible*, i.e. we can write the vector space V as a direct sum of invariant subspaces V_i ,

$$V = \bigoplus_i V_i, \quad (9)$$

such that each restriction $\rho_i := \rho|_{V_i}$ is irreducible. We can then write $\rho = \oplus_i \rho_i$. However, the decomposition (9) is in general not unique. This is the case if two irreps ρ_i and ρ_j with $i \neq j$ are *isomorphic*. Then, the possible ways of decomposing the representation $\rho_i \oplus \rho_j$ into irreps corresponds exactly to a $\text{U}(2)$ symmetry.

More generally, we call a representation *isotypic* if it is a direct sum of mutually isomorphic irreps. Let us denote by $\text{Irr}(G)$ the set of *inequivalent* irreducible unitary representations of G and note that these are necessarily finite-dimensional for a compact group G . Given an irrep $\tau \in \text{Irr}(G)$, the τ -isotype of a representation (ρ, V) is defined as the subspace $V(\tau) \subset V$ given as the ordinary sum of all irreducible subspaces isomorphic to τ . One can show that the orthogonal projection

onto $V(\tau)$ is given by the formula

$$P_\tau := \dim(\tau) \int_G \overline{\chi_\tau}(g) \rho(g) d\mu(g). \quad (10)$$

Here, $\chi_\tau(g) := \text{tr}(\tau(g))$ is the character of the irrep τ and μ is the Haar measure on G . In particular, we have the canonical decomposition into isotypes as follows

$$V = \bigoplus_{\tau \in \text{Irr}(G)} V(\tau).$$

Note that $V(\tau) = \{0\}$ if τ is not contained in ρ . Hence, the sum actually runs over the inequivalent irreps of ρ , which we denote by $\text{Irr}(\rho)$. The dimension of $V(\tau)$ is given as $n_\tau \dim(\tau)$ where n_τ is the *multiplicity* of τ : it is the unique number of copies of τ that appear in any decomposition of ρ . For some choice of irrep decomposition we have

$$V(\tau) \simeq V_\tau^{\oplus n_\tau} \simeq V_\tau \otimes \mathbb{C}^{n_\tau},$$

where V_τ is the Hilbert space on which τ acts. The corresponding decomposition of $\rho|_{V(\tau)}$ is $\tau^{\oplus n_\tau}$ under the first identification and $\tau \otimes \text{id}_{n_\tau}$ under the second one. The factor \mathbb{C}^{n_τ} is sometimes called the *multiplicity space*.

For any compact group G , the vector space of square-integrable complex functions on G , $L^2(G, \mu) \equiv L^2(G)$, is a Hilbert space endowed with the inner product

$$\langle f, g \rangle := \int_G \overline{f(t)} g(t) d\mu(t).$$

An important example of functions in $L^2(G)$ are the characters $\chi_\rho(g) = \text{tr}(\rho(g))$, where ρ is a finite-dimensional (not necessarily irreducible) unitary representation. Characters are very useful in the representation theory of compact groups, hence let us summarize a few important facts. Here, ρ and ρ' are two finite-dimensional unitary representations.

- (i) ρ and ρ' are isomorphic if and only if their characters agree.
- (ii) ρ is irreducible if and only if $\langle \chi_\rho, \chi_\rho \rangle = 1$.
- (iii) Characters of inequivalent irreps are orthogonal: $\langle \chi_\tau, \chi_{\tau'} \rangle = 0$ for all $\tau, \tau' \in \text{Irr}(G)$ with $\tau \neq \tau'$.
- (iv) For any $\tau \in \text{Irr}(G)$, $n_\tau = \langle \tau, \rho \rangle$ is the multiplicity of τ in ρ (see e.g. [55, Corollary 2.16]).

The Hilbert space $L^2(G)$ has more interesting properties on which we comment in more detail in Sec. 4.3.

Real representations. Let $\rho : G \rightarrow \text{GL}(W)$ be a representation on a *real* vector space W . Then, its *complexification* $\rho_{\mathbb{C}}$ is a representation on the complex vector space $W_{\mathbb{C}} := W \oplus iW$. Conversely, if ω is a representation on the *complex* vector space V , and there is a real structure $V = W \oplus iW$ and a representation $\rho : G \rightarrow \text{GL}(W)$ such that $\rho_{\mathbb{C}} = \omega$, then ω is also called a *real representation*. These concepts can be used to study the relations between real and complex irreps. Importantly, the real irreps of ρ may become reducible under complexification. In particular, the irrep structure of ρ and $\rho_{\mathbb{C}} = \omega$ may not be the same. However, when complexifying a real irrep τ , only three cases can occur. Here and in the following, we only consider the case that $\tau_{\mathbb{C}}$ is of *real type*, meaning that $\tau_{\mathbb{C}}$ is again irreducible as a complex representation.

Notation. For $G = \text{U}(d)$, we denote by $g \mapsto U_g$ its defining representation as unitary matrices on \mathbb{C}^d . Likewise, we use the same notation for the restriction to a subgroup $G \subset \text{U}(d)$. In the following and throughout this paper, we assume that all representations are finite-dimensional and unitary, if not stated otherwise.

4.3 Fourier transform on compact groups

Given a function $f \in L^2(G)$, we can construct its *Fourier transform* \widehat{f} which maps an irrep τ_λ of G to an operator on the representation space V_λ as follows [59]:

$$\mathcal{F}(f)[\tau_\lambda] := \widehat{f}[\tau_\lambda] := \int f(g) \tau_\lambda(g)^\dagger d\mu(g) \in \text{End}(V_\lambda). \quad (11)$$

It is a classic result in harmonic analysis that \mathcal{F} induces an algebra isomorphism $L^2(G) \simeq \bigoplus_{\lambda \in \text{Irr}(G)} \text{End}(V_\lambda)$; this is one incarnation of the famous *Peter-Weyl theorem*.

In the following, we introduce a generalization of the Fourier transform to operator-valued functions $\phi : G \rightarrow \text{End}(V)$ which can be understood as the component-wise application of the above Fourier transform. This has been studied in the mathematical literature [60] and introduced to the randomized benchmarking literature in Refs. [9, 14].

Definition 1 (Fourier transform). *Let $\phi : G \rightarrow \text{End}(V)$ be a square-integrable operator-valued function on a compact group G with Haar measure μ . Let $\lambda \in \text{Irr}(G)$ label the inequivalent irreducible representations $(V_\lambda, \tau_\lambda)$ of G . Then, for any $\lambda \in \text{Irr}(G)$, we define a linear operator $\text{Hom}(V, V_\lambda) \rightarrow \text{Hom}(V, V_\lambda)$ as follows:*

$$\mathcal{F}(\phi)[\tau_\lambda] := \widehat{\phi}[\tau_\lambda] := \int_G \tau_\lambda(g)^\dagger (\cdot) \phi(g) d\mu(g). \quad (12)$$

Note that our definition of Fourier transform differs a bit from the one in Refs. [9, 14]. The reason for this is that there is a certain ambiguity in defining the Fourier transform, even for ordinary functions as in Eq. (11). We think that, for our purposes, Definition 1 is suited best, although other, equivalent formulations can be useful in certain contexts. Thus, let us briefly comment on these.

We have a canonical isomorphism

$$\text{End}(\text{Hom}(V, V_\lambda)) \simeq (V_\lambda \otimes V^*) \otimes (V_\lambda \otimes V^*)^* \simeq (V_\lambda \otimes V_\lambda^*) \otimes (V \otimes V^*) \simeq \text{End}(V_\lambda \otimes V)$$

with respect to which Eq. (12) becomes

$$\widehat{\phi}[\tau_\lambda] \simeq \int_G \tau_\lambda(g)^\dagger \otimes \phi(g) d\mu(g) \in \text{End}(V_\lambda \otimes V).$$

However, this fails to be a proper \dagger -isomorphism for the operator algebra since the order of composition is exchanged on one factor. This can be accounted for by applying a suitable algebra anti-automorphism to the first factor. Up to a choice of basis, there is a unique one which preserves the properties of the Fourier transform, namely the transposition:

$$\widehat{\phi}[\tau_\lambda] \simeq \int_G \bar{\tau}_\lambda(g) \otimes \phi(g) d\mu(g) \in \text{End}(V_\lambda \otimes V) \quad (13)$$

This is exactly the definition of the Fourier transform used in Refs. [9, 14]. Note that the proper isomorphism is similar to the *vectorization* which is prominently used in quantum information to represent a unitary channel $\rho \mapsto U\rho U^\dagger$ as the operator $U \otimes \bar{U}$.

It is convenient to slightly extend the notation above and use the defining Eq. (12) even if the argument is not an irrep τ_λ . For an arbitrary representation $\rho \simeq \bigoplus_\lambda \tau_\lambda^{\oplus n_\lambda} \simeq \bigoplus_\lambda \tau_\lambda \otimes \text{id}_{n_\lambda}$, we then obtain, in the light of the above isomorphisms,

$$\widehat{\phi}[\rho] \simeq \bigoplus_\lambda \widehat{\phi}[\tau_\lambda]^{\oplus n_\lambda} \simeq \bigoplus_\lambda \widehat{\phi}[\tau_\lambda] \otimes \text{id}_{n_\lambda}. \quad (14)$$

For example, if $\omega(g) = U_g(\cdot)U_g^\dagger$ is acting by conjugation, $\widehat{\omega}[\omega]$ is a convenient notation of what in quantum information is referred to as the *channel twirl*.

We proceed by proving a property of the Fourier transform which we will frequently use. It is a direct consequence of Schur's lemma.

Proposition 2 (Fourier transform of representations). *Let $\rho : G \rightarrow \text{U}(V)$ be a representation of G . Then, $\widehat{\rho}[\tau_\lambda]$ is an orthogonal projection and its rank is the multiplicity n_λ of the irrep τ_λ in ρ . More precisely, if the τ_λ -isotypic component in V is $V(\lambda) \simeq V_\lambda \otimes \mathbb{C}^{n_\lambda}$ with $n_\lambda \neq 0$, then $\widehat{\rho}[\tau_\lambda]$ is block-diagonal w.r.t. the induced decomposition and the only non-zero block is*

$$\widehat{\rho}[\tau_\lambda] \simeq d_\lambda^{-1} |\text{id}_\lambda\rangle \langle \text{id}_\lambda| \otimes \text{id}_{n_\lambda}^*,$$

where $\text{id}_{n_\lambda}^*$ is the identity on the dual multiplicity space $(\mathbb{C}^{n_\lambda})^*$.

Proof. If $\rho : G \rightarrow \text{U}(V)$ is a representation, then we have

$$\widehat{\rho}[\tau_\lambda]^2 = \int \int \tau_\lambda(g)^\dagger \tau_\lambda(g')^\dagger (\cdot) \rho(g') \rho(g) d\mu(g) d\mu(g') = \int_G \tau_\lambda(g)^\dagger (\cdot) \rho(g) d\mu(g) = \widehat{\rho}[\tau_\lambda].$$

Hence, $\widehat{\rho}[\tau_\lambda]$ is a projector. Moreover, $\widehat{\rho}[\tau_\lambda]$ is also self-adjoint:

$$(\widehat{\rho}[\tau_\lambda](X)|Y) = \text{tr} \left(\int_G \rho(g)^\dagger X^\dagger \tau_\lambda(g) d\mu(g) Y \right) = \text{tr} \left(X^\dagger \int_G \tau_\lambda(g) Y \rho(g)^\dagger d\mu(g) \right) = (X|\widehat{\rho}[\tau_\lambda](Y)).$$

In the last step, we use that the Haar measure is invariant under inversion. Thus, $\widehat{\rho}[\tau_\lambda]$ is an *orthogonal* projector and its rank is

$$\text{rank } \widehat{\rho}[\tau_\lambda] = \text{tr } \widehat{\rho}[\tau_\lambda] = \int_G \overline{\text{tr } \tau_\lambda(g)} \text{tr } \rho(g) d\mu(g) = \langle \chi_\lambda, \text{tr } \rho \rangle = n_\lambda.$$

We can now explicitly compute $\widehat{\rho}[\tau_\lambda]$ by decomposing ρ into irreps as follows:

$$\widehat{\rho}[\tau_\lambda] = \int_G \tau_\lambda(g)^\dagger (\cdot) \rho(g) d\mu(g) \simeq \bigoplus_{\lambda' \in \text{Irr}(\rho)} \int_G \tau_\lambda(g)^\dagger (\cdot) \tau_{\lambda'}(g) \otimes \text{id}_{n_{\lambda'}} d\mu(g).$$

On every λ' block, the integral on the right hand side is exactly the projection onto operators X which are equivariant, i.e. $\tau_\lambda(g)X = X(\tau_{\lambda'}(g) \otimes \text{id}_{n_{\lambda'}})$ for all $g \in G$. By Schur's lemma, such an operator has to be trivial if $\lambda \neq \lambda'$ and otherwise we can write it as $X = \text{id}_\lambda \otimes x_\lambda^*$ for some $x_\lambda^* \equiv \langle x_\lambda | \in (\mathbb{C}^{n_\lambda})^*$. An orthogonal basis for the subspace of these operators is given by $\text{id}_\lambda \otimes e_{\lambda,i}^*$ where $(e_{\lambda,i})_{i \in [n_\lambda]}$ is a basis for \mathbb{C}^{n_λ} . With respect to the second isomorphism in Eq. (14), the Fourier transform then becomes

$$\widehat{\rho}[\tau_\lambda] \simeq d_\lambda^{-1} \sum_{i=1}^{n_\lambda} |\text{id}_\lambda \otimes e_{\lambda,i}^*\rangle \langle \text{id}_\lambda \otimes e_{\lambda,i}^*| = d_\lambda^{-1} |\text{id}_\lambda\rangle \langle \text{id}_\lambda| \otimes \text{id}_{n_\lambda}^*,$$

where $\text{id}_{n_\lambda}^*$ denotes the identity on the dual multiplicity space $(\mathbb{C}^{n_\lambda})^*$. \square

For our purposes, it will be convenient to consider Fourier transforms where the integration is performed with respect to another measure than the Haar measure μ . As we will see in a moment, this is captured by a generalization of Fourier analysis from functions to measures. For simplicity, let us return to the ordinary Fourier transform of a function $f \in L^2(G)$. We can effectively change the measure by multiplying f with a density $\varphi \in L^1(G)$:

$$\widehat{f\varphi}[\tau_\lambda] = \int \tau_\lambda(g)^\dagger f(g) \varphi(g) d\mu(g) = \int \tau_\lambda(g)^\dagger f(g) d(\varphi\mu)(g).$$

However, this does not allow us to consider measures on G which do not have a density w.r.t. the Haar measure μ , for instance discrete measures.² Nevertheless, we can instead interpret \widehat{f} as a transformation of the complex measure $f\mu$ and notice that this transformation is still well-defined if we replace $f\mu$ by a suitable (complex) measure ν on G . More precisely, we denote by $\text{Borel}(G)$ the Borel σ -algebra on G , i.e. the one generated by the open sets of G . We consider measures on $\text{Borel}(G)$ called (complex) *Radon measures* and denote the vector space of complex Radon measures by $\mathcal{M}(G)$. This space is canonically isomorphic to the continuous linear functionals $C(G)^*$ where

²Admittedly, the conceptually difficult bit would be the singular continuous part of the measure.

the isomorphism is given by the integration of a continuous function $f \in C(G)$ w.r.t. to a Radon measure. Note that for the typical groups which we are considering, namely finite or compact Lie groups, any *finite* measure on $\text{Borel}(G)$ is a Radon measure.³ Then, we define the Fourier transform of $\nu \in \mathcal{M}(G)$ as

$$\widehat{\nu}[\tau_\lambda] := \int \tau_\lambda(g)^\dagger d\nu(g).$$

In this way, we can treat continuous and discrete measures on the same footing and recover the Fourier transform of functions for $\nu = f\mu$. To generalize this discussion to operator-valued functions, we define *operator-valued measures* in a natural way.

Definition 3 (Operator-valued measure). *A map $\nu : \text{Borel}(G) \rightarrow \text{End}(V)$ taking values in the linear operators on a finite-dimensional real/complex Hilbert space V is called an operator-valued measure (OVM) if for all $v, w \in V$ the function*

$$\text{Borel}(G) \ni A \mapsto \langle v | \nu(A) | w \rangle,$$

is a real/complex Radon measure on G .

Suppose f is a function on G which is integrable w.r.t. the measures $\nu_{ij}(A) := \langle e_i | \nu(A) | e_j \rangle$ for some orthonormal basis $\{e_i\}$ of V . For instance, this is always the case if f is continuous. Then, we can define the integral of f with respect to the operator-valued measure ν ,

$$\int_G f(g) d\nu(g) \in \text{End}(V),$$

which is a well-defined linear operator on V .

Definition 4 (Fourier transform of OVMs). *Let ν be an operator-valued measure on a compact group G taking values in $\text{End}(V)$. As above, let $\lambda \in \text{Irr}(G)$ label the inequivalent irreducible representations $(V_\lambda, \tau_\lambda)$ of G . Then, for any $\lambda \in \text{Irr}(G)$, we define the following operator on $\text{Hom}(V, V_\lambda)$:*

$$\widehat{\nu}[\tau_\lambda] := \int_G \tau_\lambda(g)^\dagger (\cdot) d\nu(g).$$

We recover the Fourier transform for operator-valued functions ϕ in Def. 1 by considering the OVM $\nu_\phi := \phi\mu$ where μ is the Haar measure on G . For this paper, we exclusively consider OVMs of the form $\nu_\phi := \phi\nu$ where $\nu \in \mathcal{M}(G)$ is a Radon probability measure on G .

It is important to notice that Prop. 2 does only hold for the Fourier transform in the sense of Def. 1 since it relies on the properties of the Haar measure. In the next section, we introduce the definitions to capture the structure of the Fourier transform for specific measures ν more generally.

4.4 ρ -designs, moment operators, and random walks

In this section, we introduce the concept of *designs* and thereby adapt a quite general definition of this term from Ref. [61]. We then proceed by discussing the relation of designs to the previously introduced Fourier transform and summarize a few properties of *moment operators*.

For reference, recall that a probability measure $\nu \in \mathcal{M}(\text{U}(d))$ on the unitary group $\text{U}(d)$ is called a *unitary t -design* if the following equality holds:

$$\int_{\text{U}(d)} U_g^{\otimes t}(\cdot) (U_g^{\otimes t})^\dagger d\nu(g) = \int_{\text{U}(d)} U_g^{\otimes t}(\cdot) (U_g^{\otimes t})^\dagger d\mu(g),$$

where μ is again the normalized Haar measure on $\text{U}(d)$. In the following, we use a generalization of this definition where $\text{U}(d)$ is replaced by an arbitrary compact group G and likewise the representation $\tau^{(t)}(g) := U_g^{\otimes t}(\cdot) (U_g^{\otimes t})^\dagger$ is replaced by an arbitrary representation ρ of G .

Definition 5 (ρ -design). *Let (V, ρ) be a representation of G and let $\nu \in \mathcal{M}(G)$ be a probability measure on G .*

³More generally, this is true if our compact group G is also second-countable.

(i) ν is called a ρ -design if and only if

$$\mathbf{M}_\rho(\nu) := \int_G \rho(g) d\nu(g) = \int_G \rho(g) d\mu(g) = \mathbf{M}_\rho(\mu).$$

The linear operator $\mathbf{M}_\rho(\nu)$ is called the moment operator of ν (w.r.t. ρ). For any set Λ of G -representations, we call ν a Λ -design if ν is a ρ -design for all $\rho \in \Lambda$.

(ii) Let $\|\cdot\|$ be an arbitrary norm on $\text{End}(V)$ and $\varepsilon > 0$. Then, we call ν an ε -approximate ρ -design w.r.t. $\|\cdot\|$ if $\|\mathbf{M}_\rho(\nu) - \mathbf{M}_\rho(\mu)\| < \varepsilon$. If the norm is not further specified, we mean the spectral norm $\|\cdot\| = \|\cdot\|_\infty$.

If the representation ρ is reducible, say $\rho \simeq \sigma \oplus \eta$, then the moment operator $\mathbf{M}_\rho(\nu)$ is block-diagonal:

$$\mathbf{M}_\rho(\nu) \simeq \mathbf{M}_\rho(\sigma) \oplus \mathbf{M}_\rho(\eta).$$

Hence, ν is a ρ -design if and only if it is a $\{\sigma, \eta\}$ -design, and more generally a κ -design for any subrepresentation κ of ρ . In particular, if $\text{Irr}(\rho)$ labels the irreps appearing in ρ , i.e. if $\rho \simeq \bigoplus_{\lambda \in \text{Irr}(\rho)} \rho_\lambda^{\oplus n_\lambda}$, then $\mathbf{M}_\rho(\nu) \simeq \bigoplus_{\lambda \in \text{Irr}(\rho)} \mathbf{M}_\lambda(\nu)^{\oplus n_\lambda}$ and a ρ -design is exactly a $\text{Irr}(\rho)$ -design.

Let us briefly specialize this notion to unitary t -designs which, in the notation of Def. 5, are exactly $\tau^{(t)}$ -designs for the compact group $G = \text{U}(d)$ and the representation $\tau^{(t)}(g) = U_g^{\otimes t}(\cdot)(U_g^{\otimes t})^\dagger$. From the representation theory of the unitary group, we know that each of its irreps is labelled by a non-increasing integer sequence $\lambda_1 \geq \dots \geq \lambda_d$ (see e.g. Ref. [58, Thm. 38.3]). In particular, the irreps appearing in $\tau^{(t)}$ are exactly labelled by those sequences for which the sum of positive elements λ^+ is equal to the absolute sum of negative elements λ^- , and bounded by t , i.e. $\lambda^+ = \lambda^- \leq t$ [62–64] (see also [65]). Let us define the set of such sequences as

$$\nearrow_d^t := \{\lambda \in \mathbb{Z}^d \mid \lambda_1 \geq \dots \geq \lambda_d, \lambda^+ = \lambda^- \leq t\}.$$

Then, a unitary t -design is exactly a \nearrow_d^t -design in the sense of Def. 5. From the definition, we directly find $\nearrow_d^{t-1} \subset \nearrow_d^t$, and hence we recovered the well-known fact that any unitary t -design is also a $(t-1)$ -design.

Consider a fixed representation ω of a compact group G (later called the *reference representation*) and some probability measure $\nu \in \mathcal{M}(G)$. The Fourier transform of the operator-valued measure $\omega\nu$ is by Def. 4 given as

$$\widehat{\omega\nu}[\tau_\lambda] = \int_G \tau_\lambda(g)^\dagger(\cdot) \omega(g) d\nu(g) \equiv \mathbf{M}_\rho(\nu),$$

i.e. $\widehat{\omega\nu}[\tau_\lambda]$ is the *moment operator* of ν w.r.t. the representation $\rho = \tau_\lambda^\dagger(\cdot)\omega$. Hence, ν is a ρ -design if and only if $\widehat{\omega\nu}[\tau_\lambda] = \widehat{\omega}[\tau_\lambda]$.

In the following, we discuss some properties of moment operators $\mathbf{M}_\rho(\nu)$ for a certain family of probability measures ν .

Definition 6. Let $\nu \in \mathcal{M}(G)$ be a Radon measure on a compact group G .

- (i) ν is called *symmetric* if it is invariant under inversion.
- (ii) We say that ν has *support on generators* if there is a set \mathcal{G} of generators for G such that every open neighbourhood of a generator $g \in \mathcal{G}$ has non-zero measure, i.e. $\mathcal{G} \subset \text{supp } \nu$.
- (iii) Suppose ν is a probability measure. The random walk generated by ν is the stochastic process $(g_m)_{m \in \mathbb{N}}$ on G defined by the transition rule $g_{m+1} = hg_m$ where $h \sim \nu$. Equivalently, the random variables g_m are distributed as ν^{*m} for all $m \in \mathbb{N}$.

Note that having support on generators is not much of a restriction on ν since we can always consider the subgroup $G' \subset G$ generated by $\text{supp}(\nu)$ instead. If G' is dense in G , then we will abuse terminology a bit and still say that ν has support on generators of G , because this detail does not affect our arguments. In fact, this is a practically relevant situation as e.g. $G = \text{U}(d)$ is not finitely generated, but has finitely generated dense subgroups. For instance, a measure which

has support on generators of $U(d)$ in the broad sense, is given by drawing from a finite, universal gate set.

Furthermore, we will encounter important examples of measures that are *not* symmetric. Most of the following discussion and all results in Sec. 5 also hold for non-symmetric probability measures. Nevertheless, symmetric ones have some nice properties which we need for certain conclusions. To this end, we introduce the *symmetrization trick* in the end of this section.

Let us now explore more properties of the moment operator $M_\rho(\nu)$, given a representation (V, ρ) of G , and how the concepts of Def. 6 are reflected in its spectrum (see e.g. Refs. [36, 66]). Suppose $v \in V$ is a right eigenvector of $M_\rho(\nu)$ with eigenvalue $\lambda \in \mathbb{C}$, then we find:

$$|\lambda| \|v\|_2^2 = |\langle v | M_\rho(\nu) | v \rangle| \leq \int_G |\langle v | \rho(g) v \rangle| d\nu(g) \leq \int_G \|v\|_2 \|\rho(g) v\|_2 d\nu(g) = \|v\|_2^2,$$

where we have used the Cauchy-Schwarz inequality and that the representation is unitary. This shows that the spectrum of $M_\rho(\nu)$ is contained in the unit disk $\{z \in \mathbb{C} | |z| \leq 1\}$. Next suppose $v \in V$ is a right eigenvector with eigenvalue 1. Then, we find

$$\begin{aligned} \int_G \langle v | (\text{id} - \rho(g))^\dagger (\text{id} - \rho(g)) | v \rangle d\nu(g) &= 2\|v\|_2^2 - \int_G \langle v | \rho(g)^\dagger + \rho(g) | v \rangle d\nu(g) \\ &= 2\|v\|_2^2 - \langle v | M_\rho(\nu)^\dagger + M_\rho(\nu) | v \rangle \\ &= 2(\|v\|_2^2 - \text{Re}(\langle v | M_\rho(\nu) | v \rangle)) = 0. \end{aligned}$$

Since $(\text{id} - \rho(g))^\dagger (\text{id} - \rho(g))$ is positive semidefinite, the left hand side is an integral of a non-negative function. This can only be zero if the function is zero ν -almost everywhere. Hence, $v \in V$ is a right eigenvector with eigenvalue 1 if and only if $\rho(g)v = v$ ν -almost everywhere. Put differently, the right 1-eigenspace of $M_\rho(\nu)$ is the fixed point space of $\text{supp}(\nu)$. Likewise, we find that the left 1-eigenspace corresponds to the fixed point space of $\text{supp}(\tilde{\nu})$ where $\tilde{\nu}(A) := \nu(A^{-1})$ is the inverted measure.

If ν has support on generators, the fixed point space of $\text{supp}(\nu)$ coincides with the fixed point space of the whole group G . The same holds for the fixed point space of $\text{supp}(\tilde{\nu})$, hence the left and right 1-eigenspaces of $M_\rho(\nu)$ coincide and agree with $V(1)$, the trivial isotype of the representation ρ (possibly $\{0\}$). Hence, the moment operator $M_\rho(\nu)$ can be unitarily block-diagonalized as follows:

$$M_\rho(\nu) \simeq \begin{bmatrix} \text{Id} & 0 \\ 0 & M_{\rho \ominus 1}(\nu) \end{bmatrix}, \quad (15)$$

where $\rho \ominus 1$ denotes the representation on the orthocomplement of $V(1)$. To quantify how much $M_\rho(\nu)$ differs from the moment operator $M_\rho(\mu)$ w.r.t. the Haar measure μ , one typically uses the spectral distance. Note that the $M_\rho(\mu)$ is exactly the orthogonal projection onto the trivial isotype $V(1)$ and hence we have the following relation

$$\|M_\rho(\nu) - M_\rho(\mu)\|_\infty = 1 - \Delta_\rho(\nu), \quad \Delta_\rho(\nu) := 1 - \|M_{\rho \ominus 1}(\nu)\|_\infty.$$

The number $\Delta_\rho(\nu)$ is called the *spectral gap* of ν . Its importance lies in the following observation: Suppose we draw repeatedly and independently from the measure ν , such that the product of our samples performs a *random walk* on the group G . After k steps, the distribution of the product is described by the k -fold convolution power ν^{*k} with moment operator $M_\rho(\nu^{*k}) = M_\rho(\nu)^k$. Moreover, it is straightforward to check that

$$M_\rho(\nu) M_\rho(\mu) = M_\rho(\mu) = M_\rho(\mu) M_\rho(\nu),$$

using the left and right invariance of the Haar measure. Hence, we find

$$\|M_\rho(\nu)^k - M_\rho(\mu)\|_\infty = \|[M_\rho(\nu) - M_\rho(\mu)]^k\|_\infty \leq (1 - \Delta_\rho(\nu))^k, \quad (16)$$

and hence the spectral distance decays exponentially with k , provided that $\Delta_\rho(\nu) > 0$. Therefore, a random walk ν converges to an approximate ρ -design at a $\Delta_\rho(\nu)$ -dependent rate.

Finally, let us assume that ν is in addition *symmetric*. This implies that the moment operator is self-adjoint:

$$\mathbf{M}_\rho(\nu)^\dagger = \int_G \rho(g^{-1}) d\nu(g) = \int_G \rho(g) d\nu(g^{-1}) = \mathbf{M}_\rho(\nu).$$

Hence, $\mathbf{M}_\rho(\nu)$ has a spectral decomposition and real eigenvalues $\lambda \in [-1, 1]$. The operator $\mathbf{M}_{\rho \ominus 1}(\nu)$ defined above is in this case given by the spectral decomposition for eigenvalues $\lambda < 1$. In particular, the spectral gap of a symmetric measure is given as $\Delta_\rho(\nu) = 1 - \max\{\lambda_2, |\lambda_{\min}|\}$, where λ_2 is the second-largest eigenvalue of $\mathbf{M}_\rho(\nu)$ and λ_{\min} is the smallest one. Moreover, for symmetric ν , we have equality in Eq. (16) as the involved operators are self-adjoint.

If ν is not symmetric, we can define the measure

$$\tilde{\nu}(A) := \nu(A^{-1}) \quad (17)$$

for any measurable set A . Then $\tilde{\nu} * \nu$ is symmetric and $\mathbf{M}_\rho(\tilde{\nu} * \nu) = \mathbf{M}_\rho(\tilde{\nu}) \cdot \mathbf{M}_\rho(\nu) = \mathbf{M}_\rho(\nu)^\dagger \cdot \mathbf{M}_\rho(\nu)$. In particular, we have

$$\|\mathbf{M}_\rho(\tilde{\nu} * \nu) - \mathbf{M}_\rho(\mu)\|_\infty = \|(\mathbf{M}_\rho(\nu)^\dagger - \mathbf{M}_\rho(\mu))(\mathbf{M}_\rho(\nu) - \mathbf{M}_\rho(\mu))\|_\infty = \|\mathbf{M}_\rho(\nu) - \mathbf{M}_\rho(\mu)\|_\infty^2,$$

where we have used $\mathbf{M}_\rho(\nu)^\dagger \mathbf{M}_\rho(\mu) = \mathbf{M}_\rho(\mu) = \mathbf{M}_\rho(\mu) \mathbf{M}_\rho(\nu)$ by the left and right invariance of the Haar measure. Hence, we find that $1 - \Delta_\rho(\tilde{\nu} * \nu) = (1 - \Delta_\rho(\nu))^2$ for the respective spectral gaps which implies the following relation:

$$\Delta_\rho(\tilde{\nu} * \nu) \geq \Delta_\rho(\nu) \geq \Delta_\rho(\tilde{\nu} * \nu)/2. \quad (18)$$

This is a common trick used for non-symmetric probability measures, cf. Ref. [67].

The above discussion holds for any representation ρ . In particular, it also applies to moment operators of the form $\widehat{\omega\nu}[\omega_\lambda]$ where $\omega_\lambda = \tau_\lambda^{\oplus n_\lambda}$ is a τ_λ -isotypic representation. However, the moment operators then have the form $\widehat{\omega\nu}[\omega_\lambda] \simeq \widehat{\omega\nu}[\tau_\lambda] \otimes \text{id}_{n_\lambda}$, see Eq. (14). Hence, the spectral gap is in this case

$$\|\widehat{\omega\nu}[\omega_\lambda] - \widehat{\omega}[\omega_\lambda]\|_\infty = \|(\widehat{\omega\nu}[\tau_\lambda] - \widehat{\omega}[\tau_\lambda]) \otimes \text{id}_{n_\lambda}\|_\infty = \|\widehat{\omega\nu}[\tau_\lambda] - \widehat{\omega}[\tau_\lambda]\|_\infty.$$

In general, the moment operator $\mathbf{M}_\rho(\nu)$ can have negative eigenvalues. If these are too negative, e.g. -1 , this can make the spectral gap very small. However, by adapting the measure ν , it is possible to evade this problem. To this end, note that the eigenvalue equation $v = -\rho(g)v$ is not fulfilled for $g = \text{id}$. Hence, if there is a neighborhood of id in $\text{supp } \nu$, then $v = -\rho(g)v$ cannot hold ν -almost everywhere and -1 is not an eigenvalue of $\mathbf{M}_\rho(\nu)$. More precisely, one can generalize Lem. 1 in Ref. [66] from finite to compact groups to obtain a lower bound on the smallest eigenvalue.

Proposition 7. *Let $\nu \in \mathcal{M}(G)$ be a symmetric probability measure. Suppose there is an open neighborhood Ω of $\text{id} \in G$ with $\nu(\Omega) < 1$. Then, the smallest eigenvalue of $\mathbf{M}_\rho(\nu)$ obeys $\lambda_{\min} \geq -1 + 2\nu(\Omega)$.*

Proof. Note that the statement is true for $\nu(\Omega) = 0$. Hence, let us assume that $1 > \nu(\Omega) > 0$. Then define the symmetric measure $\nu_\Omega(A) := \nu(A \cap \Omega)$, and

$$\xi := \frac{1}{1 - \nu(\Omega)} (\nu - \nu_\Omega).$$

Note that ξ is by construction a symmetric probability measure and thus

$$-1 \geq \lambda_{\min}(\mathbf{M}_\rho(\xi)) = \frac{1}{1 - \nu(\Omega)} (\lambda_{\min} - \lambda_{\max}(\mathbf{M}_\rho(\nu_\Omega))) \geq \frac{1}{1 - \nu(\Omega)} (\lambda_{\min} - \nu(\Omega)).$$

In the last step, we used that ν_Ω is not a probability measure as $\nu_\Omega(G) = \nu(\Omega)$ and thus, the largest eigenvalue of its moment operator is at most $\nu(\Omega)$. Rewriting the above inequality proves the claim. \square

4.5 The Heisenberg-Weyl and Clifford group

Consider the Hilbert space $\mathcal{H} = (\mathbb{C}^p)^{\otimes n}$ of n qudits of local dimension p , where we assume that p is prime. We label the computational basis $|x\rangle = \bigotimes_{i=1}^n |x_i\rangle$ by vectors $x = (x_1, \dots, x_n)$ in the discrete vector space \mathbb{F}_p^n . Here, \mathbb{F}_p is the finite field of p elements which, for concreteness, can be chosen as the residue field $\mathbb{Z}/p\mathbb{Z}$ of integers modulo p . This section roughly follows the presentation in Ref. [68]; we refer the reader to this reference for more details.

The Heisenberg-Weyl group. Let $\xi = e^{2\pi i/p}$ be a p -th root of unity. We define the n -qudit Z and X operators by their action on the computational basis:

$$Z(z)|y\rangle := \xi^{z \cdot y}|y\rangle, \quad X(x)|y\rangle := |y + x\rangle, \quad z, x, y \in \mathbb{F}_p^n.$$

Here, all operations take place in the finite field \mathbb{F}_p (i.e. modulo p), if not stated otherwise. Note that the operators $Z(z)$ and $X(x)$ are unitary and have order p except if $z = 0$ or $x = 0$, respectively. To unify the slightly different definitions for $p = 2$ and $p > 2$ in the following, we define $\tau := (-1)^p e^{i\pi/p}$ as a suitable square root of ξ . Note that for $p = 2$, $\tau = i$ has order 4 while for $p > 2$, $\tau = -e^{i\pi/p}$ has order p . Next, we group the Z and X operators and their coordinates to define the so-called *Weyl operators* indexed by $a = (a_z, a_x) \in \mathbb{F}_p^{2n}$,

$$w(a) := \tau^{-a_z \cdot a_x} Z(a_z) X(a_x). \quad (19)$$

Here, it is understood that the exponent is computed modulo 4 for $p = 2$ and modulo p in the case $p > 2$. Note that the definition in the case $p = 2$ exactly reproduces the n -qubit Pauli operators. In the quantum information literature, the Weyl operators for $p > 2$ are thus also sometimes called *generalized Pauli operators*. It is straightforward to check the following commutation relation

$$w(a)w(b) = \xi^{[a,b]} w(b)w(a), \quad [a,b] := a_z \cdot b_x - a_x \cdot b_z. \quad (20)$$

The non-degenerate, alternating form $[\cdot, \cdot]$ is the standard *symplectic form* on \mathbb{F}_p^{2n} . Furthermore, the Weyl operators are unitary, have order p , are traceless except for $w(0) = \mathbb{1}$, and form an orthogonal operator basis of $\text{End}(\mathbb{C}^p)^{\otimes n}$:

$$(w(a)|w(b)) = p^n \delta_{a,b}.$$

Finally, the *Heisenberg-Weyl group* is the group generated by Weyl operators and thus given by:

$$\text{HW}_n(p) := \langle \{w(a) \mid a \in \mathbb{F}_p^{2n}\} \rangle = \{\tau^k w(a) \mid k \in \mathbb{Z}_D, a \in \mathbb{F}_p^{2n}\}, \quad D := \begin{cases} 4 & \text{if } p = 2, \\ p & \text{else.} \end{cases}$$

Note that the center of $\text{HW}_n(p)$ is \mathbb{Z}_D . The inequivalent irreducible representations of $\text{HW}_n(p)$ are either labelled by the additive characters of the center \mathbb{Z}_D , or by additive characters of the vector space \mathbb{F}_p^{2n} , see e.g. Ref. [69]. In this paper, we encounter the second type as the irreps of the conjugation representation $\omega(g) = U_g(\cdot)U_g^\dagger$ restricted to $\text{HW}_n(p)$. From Eq. (20), it is evident that any element $\tau^k w(a) \in \text{HW}_n(p)$ acts as $\xi^{[a,b]}$ on the one-dimensional vector spaces spanned by the operators $w(b)$. Since these are orthogonal and span $\text{End}(\mathbb{C}^p)^{\otimes n}$, we have the decomposition into irreps

$$\omega|_{\text{HW}_n(p)} \simeq \bigoplus_{b \in \mathbb{F}_p^{2n}} \xi^{[\cdot, b]}. \quad (21)$$

The characters $\xi^{[\cdot, b]}$ are mutually orthogonal, thus these irreps are mutually inequivalent.

The Clifford group. is defined as the group of unitary symmetries of the Heisenberg-Weyl group:

$$\text{Cl}_n(p) := \{U \in U(p^n) \mid U \text{HW}_n(p) U^\dagger = \text{HW}_n(p)\} / U(1).$$

We take the quotient with respect to irrelevant global phases in order to render the Clifford group a finite group.⁴ It is well-known that the Clifford group forms a unitary 2-design for all primes

⁴Strictly speaking, we are here considering the *projective* Clifford group. While it is possible to define a finite, non-projective version by restricting the matrix entries to $\mathbb{Q}[\chi]$ where χ is a suitable root of unity depending on p [70, 71], these details are not needed for this paper.

p and even a unitary 3-design for $p = 2$ [5, 71–75]. In fact, the Clifford group is the canonical example for a unitary design forming a group [76, 77], see also Ref. [37, Sec. V].

The above definition of the Clifford group can be generalized to the case when the local dimension is a prime power, $q = p^k$, by using arithmetic in the finite field \mathbb{F}_q . The so-obtained groups $\text{Cl}_n(p^k)$ are subgroups of $\text{Cl}_{nk}(p)$, and form unitary 2-designs, but not 3-designs for any p and $k > 1$ [74].

It is well-known that $\omega(g) = U_g(\cdot)U_g^\dagger$ decomposes as a representation of $\text{U}(d)$ as $\omega = 1 \oplus \text{ad}$ where 1 is the trivial irrep supported on the identity matrix $\mathbb{1}$, and ad is the *adjoint irrep* supported on the traceless matrices. The unitary 2-design property implies that ω decomposes into the same irreps over the Clifford group than over the unitary group.

The general representation theory of the Clifford group is significantly more difficult than the one of the unitary group. For tensor power representations, a duality theory has been developed in a recent series of papers [78, 79].

5 Results

To set the stage for our results we first briefly state the setting and noise model we are considering. If not mentioned otherwise, these hold throughout the remainder of this work.

5.1 Setting and noise model

In the following, G is a compact group (finite or infinite), $\mu \in \mathcal{M}(G)$ is the normalized Haar measure on G , and $\nu \in \mathcal{M}(G)$ is a probability measure with support on generators of G .

We fix a finite-dimensional unitary representation ω , called the *reference representation*, on the operator space $V := \text{End}(\mathcal{H})$ where $\mathcal{H} \simeq \mathbb{C}^d$ is a suitable d -dimensional Hilbert space. We want ω to represent possible unitary dynamics of the system \mathcal{H} , hence it has the form $\omega(g) = \eta(g)(\cdot)\eta(g)^\dagger$, where η is a suitable unitary representation of G on \mathcal{H} . Typically, we have $G \subset \text{U}(\mathcal{H})$ and $\eta(g) = U_g$ is simply the defining representation of $\text{U}(\mathcal{H})$ restricted to G . The representation ω has an isotypic decomposition $\omega = \bigoplus_\lambda \omega_\lambda$ where $V = \bigoplus_\lambda V(\lambda)$ and the subrepresentations are of the form $\omega_\lambda \simeq \tau_\lambda^{\oplus n_\lambda}$ for irreps τ_λ with multiplicities n_λ . The dimension of τ_λ is $d_\lambda := \dim(\tau_\lambda)$. Note that by construction, the trivial irrep is contained in ω at least once.

Importantly, ω is Hermiticity-preserving and thus a real representation w.r.t. the real structure $\text{End}(\mathcal{H}) = \text{Herm}(\mathcal{H}) \oplus i \text{Herm}(\mathcal{H})$. Eventually, we are only interested in the action of ω and its irreps on the real subspace $\text{Herm}(\mathcal{H})$. To avoid technicalities, we assume that all irreps of ω are of real type such that they are simply the complexification of the real irreps of ω restricted to $\text{Herm}(\mathcal{H})$. In particular, the complex representation spaces $V(\lambda)$ can be written as $V(\lambda) = H(\lambda) \oplus iH(\lambda)$ where $H(\lambda) \subset \text{Herm}(\mathcal{H})$ carries the real part of the representation ω_λ .

We assume the existence of an *implementation function* $\phi : G \rightarrow \text{End}(V)$ which should be understood as a noisy implementation of ω . This assumes in particular that the noisy implementation does not depend on the history of the experiment, nor does it change with time. Hence, we assume *Markovian, time-stationary* (but otherwise arbitrary) noise. We assume that ϕ is integrable w.r.t. the measure ν and that $\phi(g)$ is a completely positive, trace non-increasing superoperator for any $g \in G$. Finally, we fix an *initial state* $\rho \in V$ and a measurement basis $|i\rangle \in \mathcal{H}$ and write $E_i := |i\rangle\langle i| \in V$. We define $M = \sum_{i=1}^d |E_i\rangle\langle E_i|$ to be the completely dephasing channel in this basis. We denote by $\tilde{\rho} = \mathcal{E}_{\text{SP}}(\rho)$, $\tilde{E}_i = \mathcal{E}_{\text{M}}(E_i)$, and $\tilde{M} = M\mathcal{E}_{\text{M}}$ the noisy versions of the initial state and measurement. Here, we assume that $\mathcal{E}_{\text{M}}^\dagger$ and \mathcal{E}_{SP} are trace non-increasing quantum channels.

5.2 The effective measurement frame

Besides the projection to a specific irrep, the only non-trivial ingredient to the filter function (2) is the pseudo-inverse of the superoperator S . Therefore, it is instructive to first analyze the structure of S in the following.

In filtered randomized benchmarking, one effectively approximates measurements of the POVM

given by $(i, g) \mapsto \omega(g)^\dagger |E_i\rangle \langle E_i| d\mu(g)$. In Eq. (1) we defined an associated superoperator

$$S := \sum_{i \in [d]} \int_G \omega(g)^\dagger |E_i\rangle \langle E_i| \omega(g) d\mu(g) = \int_G \omega(g)^\dagger M \omega(g) d\mu(g). \quad (22)$$

Recall that M is defined as $M = \sum_{i \in [d]} |E_i\rangle \langle E_i|$. From the definition, it is evident that S is a quantum channel. Moreover, it is easy to see that S is a positive semidefinite operator.

In frame theory, the superoperator S is called the *frame operator* associated with the set of operators $\{\omega(g)^\dagger |E_i\rangle \langle E_i|\}_{i \in [d], g \in G}$ [80]. Strictly speaking, these might fail to form a proper *frame* since their span might not be all of $\text{End}(\mathcal{H})$ (i.e. the POVM might not be *informationally complete*). Since the range of S is the span of $\omega(g)^\dagger |E_i\rangle$, S would then not be of full rank. Despite the possible lack of invertibility, we still call S a *frame operator*. A full rank is guaranteed if G and its representation ω fulfill certain properties [80, Ch. 10]. For instance, this is the case if G forms a unitary 2-design. However, one can readily check that this is not always the case: Take $d = 2^n$, measurements in the computational basis, and G the n -qubit Pauli group. Then, S is not of full rank, as shown explicitly below.

Recall that ω acts on the vector space of linear operators $V = \text{End}(\mathcal{H})$. Let us consider an irreducible subrepresentation τ_λ of ω and denote the τ_λ -isotypic subrepresentation of ω by $\omega_\lambda \simeq \tau_\lambda^{\oplus n_\lambda}$, where n_λ is its multiplicity. Let P_λ be the orthogonal projection onto the associated isotypic component $V(\lambda) \subset V$, c.f. Eq. (10). We can write P_λ using a suitable isometric embedding $X_\lambda : V(\lambda) \rightarrow V$ as

$$P_\lambda = X_\lambda X_\lambda^\dagger.$$

In representation-theoretic terms, the frame operator (22) is exactly the projection of the quantum channel M onto the commutant of ω . In particular, Schur's lemma implies that

$$S = \bigoplus_{\lambda \in \text{Irr } \omega} S_\lambda \simeq \bigoplus_{\lambda \in \text{Irr } \omega} \text{id}_\lambda \otimes s_\lambda,$$

where $S_\lambda = X_\lambda^\dagger S X_\lambda$ and $s_\lambda \in \mathbb{C}^{n_\lambda \times n_\lambda}$ is a positive semidefinite matrix acting on the multiplicity space of τ_λ in ω . Alternatively, we can deduce this from the Fourier theory introduced in Sec. 4.3 by noting that $S = \widehat{\omega}[\omega](M)$. Then, Eq. (14) implies $S = \bigoplus_{\lambda \in \text{Irr } \omega} \widehat{\omega}[\omega_\lambda](M)$ and Prop. 2 gives the form of $\widehat{\omega}[\omega_\lambda](M)$. In particular, we have $S_\lambda = \widehat{\omega}[\omega_\lambda](M) X_\lambda$.

In the case that τ_λ is multiplicity-free, we find $S_\lambda = s_\lambda \text{id}_\lambda$ for a scalar $s_\lambda = \text{tr}(P_\lambda M)/d_\lambda \geq 0$. In the language of frame theory, $\{\tau_\lambda(g)^\dagger X_\lambda^\dagger |E_i\rangle \langle E_i|\}_{i \in [d], g \in G}$ then constitute a tight-frame for V_λ if $s_\lambda \neq 0$. In the case of multiplicities, $n_\lambda > 1$, we have the relation $\text{tr}(s_\lambda) = \text{tr}(P_\lambda M)/d_\lambda$ instead. For some choice of irrep decomposition of $V(\lambda)$, let $P_\lambda^{(i)} = X_\lambda^{(i)} X_\lambda^{(i)\dagger}$ be the projection onto the i -th copy of the irrep τ_λ ; then we can write the matrix s_λ explicitly as

$$s_\lambda = d_\lambda^{-1} \sum_{i,j=1}^{n_\lambda} \text{tr}(X_\lambda^{(i)\dagger} M X_\lambda^{(j)}) |i\rangle \langle j|. \quad (23)$$

Note that since s_λ is positive semi-definite, it can always be unitarily diagonalized. The corresponding diagonalizing transformation can be understood as a change of the irrep decomposition of $V(\lambda)$ such that $\text{tr}(X_\lambda^{(i)\dagger} M X_\lambda^{(j)}) = 0$ for all $i \neq j$. In particular, $\{\tau_\lambda(g)^{(j)\dagger} X_\lambda^{(j)\dagger} |E_i\rangle \langle E_i|\}_{i \in [d], g \in G}$ is a tight-frame for $V_\lambda^{(j)}$ if $s_\lambda^{(j)} = \text{tr}(P_\lambda^{(j)} M) \neq 0$.

Examples For concreteness, let us discuss a few important examples. We take G to be a subgroup of the unitary group $U(d)$, and the representation $\omega(g) = U_g(\cdot) U_g^\dagger$. First, for $G = U(d)$, we have the multiplicity-free trivial and adjoint irrep which we label by 1 and ad, respectively. The associated blocks of the frame operator are proportional to the scalars

$$s_1 = \text{tr}(P_1 M) = \sum_{j \in [d]} d^{-1} (E_j | \mathbb{1}) (\mathbb{1} | E_j) = 1,$$

$$s_{\text{ad}} = \frac{1}{d^2 - 1} \text{tr}(P_{\text{ad}} M) = \frac{1}{d^2 - 1} \left(\sum_{j \in [d]} (E_j | E_j) - s_1 \right) = \frac{1}{d + 1},$$

where we have used that $P_1 = \frac{1}{d}|\mathbb{1}\rangle\langle\mathbb{1}|$ ($\mathbb{1}$ is the projector onto the trivial irrep, $P_{\text{ad}} = \text{id} - P_1$ and $d_\lambda = \text{tr}[P_\lambda]$). We can use this information to write the frame operator in a more recognizable form, namely as a convex combination of the identity and the *completely depolarizing channel* $\mathcal{D} = P_1$:

$$S = P_1 + \frac{1}{d+1}P_{\text{ad}} = \left(1 - \frac{1}{d+1}\right) \frac{1}{d}|\mathbb{1}\rangle\langle\mathbb{1}| + \frac{1}{d+1}\text{id} = \frac{1}{d+1}(d\mathcal{D} + \text{id}) =: \mathcal{D}_{\frac{1}{d+1}}. \quad (24)$$

In other words, $1/(d+1)$ is the *effective depolarizing parameter* of the dephasing channel M . The same result holds for the multi-qudit Clifford group $\text{Cl}_n(p)$ with $d = p^n$ where p is prime, and more generally, for any unitary 2-group since it has the same irreps as $\text{U}(d)$.

Next, let us consider the *local Clifford group* $G = \text{Cl}_1(p)^{\otimes n}$ (for p prime). Its irreps are multiplicity-free and given as all possible tensor products of the single-qudit trivial and adjoint irreps, i.e. there are 2^n many. Let us label such an irrep by a binary string $b \in \{0,1\}^n$ where the ‘0’ corresponds to an adjoint irrep on the respective system, and ‘1’ to the trivial irrep. It is straightforward to see that s_b is then the product

$$s_b = s_1^{|b|} s_{\text{ad}}^{n-|b|} = (p+1)^{-(n-|b|)}$$

where $|b|$ denotes the Hamming weight of b . Indeed, we have

$$\begin{aligned} s_b &= \left(\frac{1}{p^2-1}\right)^{n-|b|} \sum_{y \in \mathbb{F}_p^n} \prod_{i=1}^n (E_{y_i} | P_{b_i} | E_{y_i}) \\ &= p^n \left(\frac{1}{p^2-1}\right)^{n-|b|} \left(\frac{1}{p}\right)^{|b|} \left(1 - \frac{1}{p}\right)^{n-|b|} = \left(\frac{1}{p+1}\right)^{n-|b|}. \end{aligned}$$

The same argument holds more generally for a locally acting group $G = G_1 \otimes \dots \otimes G_k$ when every factor G_i is a unitary 2-design, possibly of different local dimension.

As a final example, consider the *Heisenberg-Weyl* (or generalized Pauli) group $G = \text{HW}_n(p)$. Its irreps are one-dimensional and given as the span of the Weyl operators $w(z, x)$ for $(z, x) \in \mathbb{F}_p^{2n}$, see Eq. (19) and (21). Let us label the elements of the measurement basis by $|y\rangle$ with $y \in \mathbb{F}_p^n$. We find that

$$s_{x,z} = \sum_{y \in \mathbb{F}_p^n} d^{-1} |\langle y | w(z, x) | y \rangle|^2 = \sum_{y \in \mathbb{F}_p^n} d^{-1} |\langle y | y + x \rangle|^2 = \delta_{x,0}.$$

Hence, the frame operator vanishes on every irrep with $x \neq 0$.

Eigenvalues of the frame operator. For our analysis of the filtered RB protocol for arbitrary compact groups G in Secs. 5.3 and 5.4, the properties of the associated frame operator S and, in particular, $\|S_\lambda^+\|_\infty = \|s_\lambda^+\|_\infty$ will be of some importance. This is exactly the inverse of the smallest non-zero eigenvalue of s_λ , as s_λ is positive semidefinite. By Eq. (23), the eigenvalues of s_λ are of the form $\text{tr}(P_\lambda^{(i)} M)/d_\lambda$ where $P_\lambda^{(i)}$ are the projections associated to an irrep decomposition of $V(\lambda)$ which diagonalizes s_λ . Using Hölder’s inequality, we can bound these eigenvalues as follows:

$$\frac{\text{tr}(P_\lambda^{(i)} M)}{d_\lambda} \leq \frac{\min\{d_\lambda, d-1\}}{d_\lambda} = \min\left\{1, \frac{d-1}{d_\lambda}\right\}.$$

Here, we have used the bound $d-1$ since, if λ is not the trivial irrep, P_λ is supported on the traceless subspace, and thus we can consider the corresponding restriction of M of rank $d-1$. Hence, if $\|S_\lambda^+\|_\infty \neq 0$, we have the lower bound

$$\|S_\lambda^+\|_\infty \geq \max\left\{1, \frac{d_\lambda}{d-1}\right\}. \quad (25)$$

This lower bound is tight, e.g. for unitary 2-designs.

In the following discussion, we often restrict to the case where $[P_\lambda, M] = 0$. We refer to this condition as the measurement M *being aligned with the irrep* λ . Moreover, many calculations are simplified by the assumption that λ is multiplicity-free in ω . Both restrictions are met by the

Clifford group, the local Clifford group and the Heisenberg-Weyl group together with the basis measurement in the associated Z -basis.

For any irrep λ aligned with M we can also give an upper bound on the spectral norm $\|S_\lambda^+\|_\infty$. Let $P_\lambda^{(i)}$ be as above. Then, we have $[P_\lambda, M] = 0$ if and only if $[P_\lambda^{(i)}, M] = 0$ for all $i = 1, \dots, n_\lambda$. Assuming that $s_\lambda \neq 0$, the smallest non-zero eigenvalue is thus given as $\text{tr}(P_\lambda^{(i)} M)/d_\lambda = \text{rank}(P_\lambda^{(i)} M)/d_\lambda \geq 1/d_\lambda$ for some i . Thus, we obtain the bound:

$$\|S_\lambda^+\|_\infty \leq d_\lambda \quad (\text{for } \lambda \text{ aligned with } M). \quad (26)$$

This bound is tight, for instance for the Heisenberg-Weyl group. Note however, that the bound is overestimating $\|S_\lambda^+\|_\infty$ for large irreps, and it is possible to give tighter bounds under additional assumptions.

5.3 Signal guarantees for filtered randomized benchmarking

We now derive a general guarantee for the expected signal $F_\lambda(m)$ of filtered RB that is then discussed and analyzed in detail in the remainder of this work.

With the notation introduced in the preliminaries, we can, as a first step, very compactly write the expected signal for a general implementation function ϕ . Recall that to isolate the decay parameter associated with a given irreducible representation τ_λ we have introduced the filter function f_λ in Eq. (2). In the notation of Sec. 4.1, it reads:

$$f_\lambda(i, g_1, \dots, g_m) = (E_i | \omega(g_1 \cdots g_m) S^+ P_\lambda | \rho).$$

Note that f_λ is real-valued, as all involved superoperators are in fact Hermiticity-preserving: For the projector P_λ , this follows from the definition (10) and the fact that real representations have real characters. Moreover, S is a quantum channel, hence S^+ is Hermiticity-preserving as argued in Sec. 4.1. Thus, we can omit the complex conjugation in the computation of the estimator $\hat{F}_\lambda(m)$.

Let us define the noisy quantum channel $\tilde{M} := \sum_{i \in [d]} |E_i\rangle\langle \tilde{E}_i|$. Then, by linearity of the expected value and the assumption of i.i.d. experiments in the data acquisition, the filtered RB signal becomes

$$\begin{aligned} F_\lambda(m) &= \sum_{i \in [d]} \int_{G^m} f_\lambda(i, g_1, \dots, g_m) p(i|g_1, \dots, g_m) d\nu(g_1) \cdots d\nu(g_m) \\ &= \sum_{i \in [d]} (\rho | P_\lambda S^+ \int \omega(g_1)^\dagger \cdots \omega(g_m)^\dagger | E_i \rangle \langle \tilde{E}_i | d(\phi\nu)(g_m) \cdots d(\phi\nu)(g_1) | \tilde{\rho}) \\ &= (\rho | P_\lambda S^+ \left(\int \omega(g)^\dagger(\cdot) d(\phi\nu)(g) \right)^m (\tilde{M}) | \tilde{\rho}) \\ &= (\rho | X_\lambda S_\lambda^+ \widehat{\phi\nu}[\omega_\lambda]^m (X_\lambda^\dagger \tilde{M}) | \tilde{\rho}). \end{aligned} \quad (27)$$

We use in the last line that S^+ and $\omega(g)$ are block-diagonal, hence $X_\lambda^\dagger S^+ = S_\lambda^+ X_\lambda^\dagger$ and $X_\lambda^\dagger \omega(g) = \omega_\lambda(g) X_\lambda^\dagger$.

We observe that filtered randomized benchmarking explicitly exposes the m th power of the Fourier transform of the implementation map ϕ and the measure ν restricted to the irreducible representation τ_λ . This observation already justifies the name *filtered* RB. It is interesting to note that the general structure of a filtered RB signal is even slightly simpler than the signal form of RB protocols that include an inversion, c.f. [9, Eq. (75)]: The latter additionally involves an inverse Fourier transformation.

Without further assumption on in the implementation map ϕ , the form of Eq. (27) is far from describing a simple functional dependence. For sufficiently large m , we can, however, hope that the signal is mostly governed by the dominant eigenvalue of $\widehat{\phi\nu}[\omega_\lambda]$, giving rise to a simpler signal model that can be fitted. This approximation constitutes the core of RB. And the following theorem formulates a precise statement aligned with this expectation.

To show that the filtered RB signal (27) indeed follows a ‘simple’ exponential decay, we use that $\widehat{\phi\nu}[\omega_\lambda]$ is close to $\widehat{\omega\nu}[\omega_\lambda]$ if the implementation is sufficiently good. Recall from Sec. 4.4 that $\widehat{\omega\nu}[\omega_\lambda]$ has the interpretation as a moment operator for the probability measure ν and, thus, its subdominant eigenvalues are controlled by the spectral gap Δ_λ of the moment operator. If the deviation of $\widehat{\phi\nu}[\omega_\lambda]$ from $\widehat{\omega\nu}[\omega_\lambda]$ is small compared to Δ_λ , the perturbation theory of invariant subspaces [81] ensures that $\widehat{\phi\nu}[\omega_\lambda]$ has a similar decomposition as the moment operator. This gives rise to a simple explicit formula for the RB signal. Formally, we arrive at the following result:

Theorem 8 (Signal guarantee for filtered RB with random circuits). *Fix a non-trivial irrep λ of ω and let $\omega_\lambda \subset \omega$ be its isotypic subrepresentation with multiplicity n_λ . Suppose the spectral gap of $\widehat{\omega\nu}[\omega_\lambda]$ is larger than $\Delta_\lambda > 0$ and there is $\delta_\lambda > 0$ such that*

$$\|\widehat{\phi\nu}[\omega_\lambda] - \widehat{\omega\nu}[\omega_\lambda]\|_\infty \leq \delta_\lambda < \frac{\Delta_\lambda}{4}. \quad (\text{A})$$

Then, the λ -filtered RB signal given in Eq. (27) obeys

$$F_\lambda(m) = \text{tr}(A_\lambda I_\lambda^m) + \text{tr}(B_\lambda O_\lambda^m), \quad (\text{S})$$

where $A_\lambda, I_\lambda \in \mathbb{R}^{n_\lambda \times n_\lambda}$, and $B_\lambda, O_\lambda \in \mathbb{R}^{k_\lambda \times k_\lambda}$ for $k_\lambda := d_\lambda d^2 - n_\lambda$. Moreover, I_λ and O_λ do not depend on the initial state and measurement and we have

$$\text{spec}_{\mathbb{R}}(I_\lambda) \subset (1 - 2\delta_\lambda, 1], \quad \|O_\lambda\|_\infty \leq 1 - \Delta_\lambda + 2\delta_\lambda.$$

The magnitude of the second matrix exponential decay is suppressed as

$$|\text{tr}(B_\lambda O_\lambda^m)| \leq c_\lambda \sqrt{(\rho|P_\lambda|\rho)} g(\delta_\lambda/\Delta_\lambda)(1 - \Delta_\lambda + 2\delta_\lambda)^m. \quad (\text{B})$$

Here, c_λ is a frame- and SPAM-dependent constant, defined as

$$c_\lambda := \begin{cases} \sqrt{\text{tr } S_\lambda} \|S_\lambda^+\|_\infty & \text{if } [P_\lambda, M] = 0, \\ \min\{\sqrt{d_\lambda}, \sqrt{d}\} \|S_\lambda^+\|_\infty & \text{else.} \end{cases}$$

The function given by $g(x) := (1 - 4x)x + \frac{1+x}{1-4x}$ is monotonically increasing and diverges for $x \rightarrow 1/4$.

Note that an important special case of Theorem 8 is given by $\Delta_\lambda = 1$, i.e. when filtered RB is performed with an *exact* $\omega_\lambda \otimes \omega$ -design. The theorem only applies to non-trivial irreps of ω . The case of the trivial irrep can be derived analogously, but differs in the specific bounds. We provide the statement for the trivial irrep in Subsection 5.3.5 at the end of this section.

Before presenting the proof of the theorem, it is instructive to take a closer look on the structure of the theorem. The theorem consists of three central parts: First, the precise *assumption* (A) on the quality of the implementation. The assumption quantifies an initial belief that is sufficient to ensure the correct functioning of the RB protocol. Second, a statement for the *expected signal form* (S). Here, the first summand is the dominant contribution that constitutes the model for fitting the signal. In particular, after performing the fit, the RB protocol outputs the eigenvalues of I_λ as the RB decay parameters. The second summand in Eq. (S) describes a sub-dominant contribution to the expected RB signal that we want to be small in order to fit the dominant exponential decay. To this end, the third part of the theorem, provides a *bound on the sub-dominant contribution* (B). Since by assumption $1 - \Delta_\lambda + 2\delta_\lambda < 1$, the bound decays exponentially in m and becomes small for sufficiently large m . We derive more explicit sufficient conditions on the sequence length as corollaries of Theorem 8 in Section 5.5.

We will now discuss the parts in more detail.

5.3.1 Assumptions on the quality of the implementation function

The central assumption of Theorem 8 reads

$$\|\widehat{\phi\nu}[\omega_\lambda] - \widehat{\omega\nu}[\omega_\lambda]\|_\infty \leq \delta_\lambda < \frac{\Delta_\lambda}{4}. \quad (\text{A})$$

Although our analysis works in the full perturbative regime $\delta_\lambda < \Delta_\lambda/4$, there are certain quantities like $g(\delta_\lambda/\Delta_\lambda)$ that diverge for $\delta_\lambda/\Delta_\lambda \rightarrow 1/4$. In practice, this means that the implementation error should be bounded away from $1/4$, for instance $\delta_\lambda/\Delta_\lambda \leq 1/5$ such that $g(1/5) \approx 6$ can be considered constant.

Intuitively, the assumption $\|\widehat{\phi\nu}[\omega_\lambda] - \widehat{\omega\nu}[\omega_\lambda]\|_\infty < \Delta_\lambda/4$ can be phrased as the assumption that the implementation function ϕ is sufficiently close to the reference representation ω *on average w.r.t. the measure ν* . Since we do typically not know the implementation function ϕ , there is a priori no way of determining this error measure and verifying assumption (A). Hence, the assumption that the implementation error $\|\widehat{\phi\nu}[\omega_\lambda] - \widehat{\omega\nu}[\omega_\lambda]\|_\infty$ is small should be seen as an initial belief on the quality of the experiment. An advantage of the approach taken here is that this initial belief only ever involves the quality of gates in $\text{supp}(\nu)$. Typically, these are gates native to the platform. Experimentally motivated noise models might then be used to approximate the implementation error $\|\widehat{\phi\nu}[\omega_\lambda] - \widehat{\omega\nu}[\omega_\lambda]\|_\infty$, or trust can be build in independent experiments.

Since this implementation error does not bear an obvious operational meaning, we attempt to relate this quantity to more familiar ones in the following. As a starting point, we may use the bound

$$\|\widehat{\phi\nu}[\omega_\lambda] - \widehat{\omega\nu}[\omega_\lambda]\|_\infty \leq \int_G \|\bar{\omega}_\lambda(g) \otimes (\phi(g) - \omega(g))\|_\infty d\nu(g) = \int_G \|\phi(g) - \omega(g)\|_\infty d\nu(g), \quad (28)$$

where we first used Eq. (13) and the triangle inequality, and then that unitaries have unit spectral norm. Eq. (28) is probably a crude bound as averaging inside the norm might significantly reduce the error. Moreover, we discard the irrep-specific component. Nevertheless, the RHS of Eq. (13) has a clear meaning as the average error of the gates that are primitives in the experiment, although the spectral distance of quantum channels lacks an operational interpretation.

Furthermore, recall that the *average gate fidelity* between a quantum channel \mathcal{E} and a unitary gate U is defined as

$$F_{\text{avg}}(U, \mathcal{E}) := \int \langle \psi | U^\dagger \mathcal{E}(|\psi\rangle\langle\psi|) U | \psi \rangle d\psi.$$

Hence, the average gate infidelity between $\phi(g)$ and $\omega(g)$ is

$$\begin{aligned} 1 - F_{\text{avg}}(\omega(g), \phi(g)) &= \int \langle \psi | (\text{id} - \omega(g)^\dagger \phi(g)) (|\psi\rangle\langle\psi|) | \psi \rangle d\psi \\ &\leq \|\text{id} - \omega(g)^\dagger \phi(g)\|_\infty = \|\omega(g) - \phi(g)\|_\infty. \end{aligned}$$

In the last step, we used that the spectral norm is unitarily invariant so we can multiply with the unitary superoperator $\omega(g)$ from the left. Hence, if we assume that the ν -average of $\|\phi(g) - \omega(g)\|_\infty$ is small, this implies that the ν -averaged infidelity between ϕ and ω is small, too. On a superficial level, this is exactly the quantity which randomized benchmarking claims to measure.⁵ Thus, one can understand the assumption that the implementation is reasonable good in spectral distance as a consistency condition for RB. That is, if the implementation is sufficiently good, we are in a regime where RB can estimate how good it precisely is.

Finally, let us comment on the condition $\|\widehat{\phi\nu}[\omega_\lambda] - \widehat{\omega\nu}[\omega_\lambda]\|_\infty \leq \Delta_\lambda/4$. If ν is a poor approximation to a design, then the spectral gap is small and hence the implementation has to be rather good. In contrast, if ν is an exact design, then $\Delta_\lambda = 1$, and more noise can be tolerated. Hence, there is a trade-off between the quality of gates and the quality of random circuits. In particular, if the gate errors become too large, the scrambling is no longer controlled by the random circuit. More concretely, typical random circuits have spectral gaps that scale as $O(1/n)$ (cf. Sec. 5.7), thus *the implementation of gates has to improve with the number of qubits*, at least for a general perturbative argument to hold. Similar findings have been reported by Liu et al. [26] and Dalzell, Hunter-Jones, and Brandão [27] who require gate error rates which are $O(1/n)$ and $O(1/n \log(n))$, respectively. However, note that our notion of ‘implementation error’ is distinct from their use of ‘gate error’.

⁵The difficulties in this interpretation of RB coming from the intrinsic gauge freedom of the protocol have been intensively discussed in the literature [9, 12–14]. We do not intend to contribute to this discussion in this work.

5.3.2 The dominant signal

In the perturbative regime, Theorem 8 ensures that the RB signal is the sum of two (matrix) exponential decays, Eq. (S). In particular, if the irrep τ_λ appears in ω without multiplicities the signal becomes a scalar decay governed by a single decay parameter $I_\lambda \in (1 - 2\delta_\lambda, 1] \subset \mathbb{R}$. If τ_λ has multiplicity n_λ the matrix I_λ has the corresponding dimension. If I_λ is diagonalizable (over \mathbb{C}) the RB signal is a linear combination of exponentials in the (up-to n_λ) inequivalent and potentially complex eigenvalues of I_λ . As a consequence the signal can decay and oscillate with the sequence length. The decay parameter I_λ does not depend on SPAM errors, these only affect the linear coefficients A_λ and B_λ . This behavior provides the desired SPAM robustness of extracting the decay parameters.

Even though not included in the statement of the theorem, the trace of the matrix coefficients A_λ (the SPAM constants) coincides with the filtered RB signal which we would obtain for an ideal implementation map $\phi = \omega$ and the Haar measure $\nu = \mu$ but with the *same SPAM errors*. From the expression (32) for the trace of A_λ given in Sec. 5.3.4 below, we obtain the *signal under only SPAM errors*:

$$\text{tr}(A_\lambda) = (\rho | P_\lambda S^+ \hat{\omega}[\omega](\tilde{M}) | \tilde{\rho}) = F_\lambda(m)_{\text{SPAM}}. \quad (29)$$

Furthermore, if λ is multiplicity-free and aligned with M , then $\hat{\omega}[\tau_\lambda](X_\lambda^\dagger \tilde{M})$ is proportional to X_λ^\dagger with proportionality factor given as $\text{tr}(P_\lambda \tilde{M})/d_\lambda$ (cf. Sec. 5.2). In this case, we have

$$F_\lambda(m)_{\text{SPAM}} = d_\lambda^{-1} s_\lambda^{-1} \text{tr}(P_\lambda \tilde{M}) (\rho | P_\lambda | \tilde{\rho}) = \frac{\text{tr}(P_\lambda \tilde{M})}{\text{tr}(P_\lambda M)} (\rho | P_\lambda | \tilde{\rho}),$$

where we used that $\text{tr}(P_\lambda M) = d_\lambda s_\lambda$. In the absence of SPAM noise, we thus recover the ideal, noiseless signal (5) from Sec. 2:

$$F_\lambda(m)_{\text{ideal}} = (\rho | P_\lambda | \rho).$$

We can, thus, measure the deviation from the ideal signal due to SPAM in terms of the two relative quantities that we call the *SPAM visibilities*:

$$v_{\text{SP}} := \frac{|\text{tr}(P_\lambda \tilde{\rho})|}{|\text{tr}(P_\lambda \rho)|}, \quad v_{\text{M}} := \frac{|\text{tr}(P_\lambda \tilde{M})|}{|\text{tr}(P_\lambda M)|}.$$

In terms of the visibilities, we can rewrite the absolute value of the signal affected only by SPAM for λ multiplicity-free and aligned with M as $|F_\lambda(m)_{\text{SPAM}}| = v_{\text{SP}} v_{\text{M}} (\rho | P_\lambda | \rho)$. SPAM errors can decrease the signal-to-noise ratio as well as the ratio between the dominant and sub-dominant signals. As a result the number of samples and required sequence length to accurately estimate the dominant RB signal and extract the decay parameter also depends on the strength of the SPAM noise. This situation should not come as a surprise as the ability to extract information depends crucially on the quality of state preparation and measurement. We will make use of the visibilities to formulate explicit bounds in the following section, and will eventually assume that they are lower bounded by a constant.

Note that similar assumptions about the SPAM constants were made in Refs. [31, 82]. In contrast to *stability* condition in Ref. [31], which requires that SPAM constants are within additive error of their ideal value, the here introduced *visibilities* capture relative deviations.

Examples. As an instructive example, we consider depolarizing SPAM noise. Recall that $\tilde{\rho} = \mathcal{E}_{\text{SP}}(\rho)$ and $\tilde{M} = M \mathcal{E}_{\text{M}}$ with state preparation and measurement noise channels \mathcal{E}_{SP} and \mathcal{E}_{M} , respectively. Assuming that $\mathcal{E}_{\text{SP}} = \mathcal{E}_{\text{M}} = p \text{id} + (1 - p)(\mathbb{1}/d)$ is a depolarizing channel, we have

$$v_{\text{SP}} = p + \frac{1 - p}{d} \frac{(\rho | P_\lambda | \mathbb{1})}{(\rho | P_\lambda | \rho)} = p, \quad v_{\text{M}} = p + \frac{1 - p}{d} \frac{(\mathbb{1} | P_\lambda M | \mathbb{1})}{d_\lambda s_\lambda} = p,$$

where we use twice that $P_\lambda(\mathbb{1}) = 0$ since λ is, by assumption, not the trivial irrep. Hence, $F_\lambda(m)_{\text{SPAM}}$ is suppressed by p^2 compared to the SPAM-free situation.

In principle and without further assumptions, the state-preparation errors could increase the visibility and can change the sign of the filtered RB signal. For example, consider the representation $b = 00$ of $\text{Cl}_1(2)^{\otimes 2}$.

Then, for $\rho = |00\rangle\langle 00|$ and the maximally entangled Bell-state $\tilde{\rho} = |\Psi_+\rangle\langle \Psi_+|$, we have $(\rho|P_{00}|\tilde{\rho}) = -(\rho|P_{00}|\rho)$.

If $\text{HW}_n(p) < G$ and ρ is a pure stabilizer state, e.g. $\rho = |0\rangle\langle 0|$, we can establish that $v_{\text{SP}} \leq 1$. To see this, recall that $w(a)$ denote the Weyl operators for $a \in \mathbb{F}_p^n$. Any stabilizer state can be written as $\rho = \frac{1}{d} \sum_{a \in L} \xi^{f(a)} w(a)$, where L is a suitable subspace of \mathbb{F}_p^n , $f : L \rightarrow \mathbb{F}_p$ is a suitable function on L , and $\xi = \exp(2\pi i/p)$ is a primitive p -th root of unity. Furthermore, if $\text{HW}_n(p) < G$, P_λ is diagonal in the Weyl basis and can be written as $P_\lambda = \frac{1}{d} \sum_{a \in \Omega} |w(a)\rangle\langle w(a)|$ for some set $\Omega \subset \mathbb{F}_p^n$. Using $\|w(a)\|_\infty \leq 1$ for all a , we then have $|(\rho|P_\lambda|\tilde{\rho})| = \frac{1}{d} \sum_{a \in L \cap \Omega} |(w(a)|\tilde{\rho})| \leq \frac{1}{d} \sum_{a \in L \cap \Omega} 1 = (\rho|P_\lambda|\rho)$. Hence, we have shown that $v_{\text{SP}} \leq 1$.

Next, we show a similar statement for the measurement visibility v_{M} : Here, we only need that $[P_\lambda, M] = 0$, which is in particular the case if $\text{HW}_n(p) < G$. Then, $P_\lambda M$ is a projector with range in the traceless subspace (since λ is non-trivial by assumption). Hence, $\text{tr}(P_\lambda M) = \text{tr}(P_\lambda M \mathcal{E}_{\text{M}})$ depends only on the unital and trace-preserving part of \mathcal{E}_{M} and we can thus replace \mathcal{E}_{M} with its projection onto unital and trace-preserving channels. Since these channels have spectral norm one [83, Thm. 4.27], we finally find that $|\text{tr}(P_\lambda \tilde{M})| \leq \|P_\lambda M\|_1 \|\mathcal{E}_{\text{M}}\|_\infty = \text{tr}(P_\lambda M)$, and thus $v_{\text{M}} \leq 1$.

Although our assumptions do not explicitly exclude examples of ‘malicious noise’, we generally expect physical noise processes in state preparation and measurement to be less targeted and unable to change the sign of the RB signal (as this would lead to clearly observable negative decay curves).

5.3.3 The bound on the sub-dominant signal

For both gate-dependent noise and when using a non-uniform measure ν , there exist a sub-dominant decay in the expected RB signal, the second summand in Eq. (S). The third part of Theorem 8 provides the bound (B) on sub-dominant decay. The constant c_λ can introduce a prefactor to the bound scaling polynomially in the dimension of the irrep λ . Note that this prefactor stems from the inverse of the effective measurement frame in the filter function. It is a direct consequence of not implementing an inverse gate at the end of the sequences and can be seen as the price to pay for inversionless RB compared to standard RB.

To be more concrete, let us again assume that λ is aligned with M . For ω_λ multiplicity-free, $S_\lambda = s_\lambda \text{id}_\lambda$, cp. Eq. (23). If $s_\lambda \neq 0$ (otherwise we have $F_\lambda(m) = 0$), we find the simple expressions $\|S_\lambda^+\|_\infty = s_\lambda^{-1}$ and $\text{tr} S_\lambda = d_\lambda s_\lambda$. Since $[P_\lambda, M] = 0$, Theorem 8 then states that $c_\lambda = \sqrt{d_\lambda/s_\lambda}$. By Eqs. (25) and (26), $d_\lambda \leq d_\lambda/s_\lambda \leq d_\lambda^2$, hence the λ -dependent prefactor cannot exceed d_λ . In the case of multiplicities, we have to adapt our argument slightly to use Eqs. (25) and (26) for bounds on $c_\lambda = \sqrt{\text{tr}(P_\lambda M) \|S_\lambda^+\|_\infty}$. Recall from Sec. 5.2 that $\text{tr}(P_\lambda M) = \text{tr}(S_\lambda) \geq d_\lambda \|S_\lambda^+\|_\infty^{-1}$, since $\|S_\lambda^+\|_\infty^{-1}$ is exactly the smallest non-zero eigenvalue of S_λ and each eigenvalue occurs at least d_λ times. On the other hand, $\text{tr}(P_\lambda M) \leq \text{tr}(P_\lambda) = n_\lambda d_\lambda$ by Hölder’s inequality. Using the bounds (25) and (26) on $\|S_\lambda^+\|_\infty$, we then obtain the following inequalities:

$$\sqrt{d_\lambda} \leq c_\lambda \leq d_\lambda \sqrt{n_\lambda d_\lambda}.$$

For our examples from Sec. 5.2, namely unitary 2-groups, local products of unitary 2-groups, and the Heisenberg-Weyl group, all irreps are multiplicity-free and $\text{HW}_n(p) < G$.⁶ The latter fact implies that the projectors P_λ are diagonal in the Weyl basis and in particular $[P_\lambda, M] = 0$. Thus, we can use $c_\lambda = \sqrt{d_\lambda/s_\lambda}$, and the s_λ which have been computed in Sec. 5.2:

$$\begin{aligned} \sqrt{d_{\text{ad}}/s_{\text{ad}}} &= (d+1)\sqrt{d-1} && \text{for unitary 2-groups,} \\ \sqrt{d_b/s_b} &= \left[(p+1)\sqrt{p-1}\right]^{n-|b|} && \text{for local unitary 2-groups,} \\ \sqrt{d_{0,z}/s_{0,z}} &= 1 && \text{for the Heisenberg-Weyl group.} \end{aligned}$$

⁶Scalable unitary 2-groups are either dense in the unitary group or a suitable subgroup of the Clifford group containing $\text{HW}_n(p)$ [76, 77], see also Ref. [37, Sec. V] for a comprehensive summary.

Besides c_λ , the additional factors $\sqrt{(\rho|P_\lambda|\rho)}$ and $g(\delta_\lambda/\Delta_\lambda)$ appear in the bound (B). Here, $\sqrt{(\rho|P_\lambda|\rho)} \leq 1$ is bounded and can, in fact, be very small for small irreps. If the implementation error $\delta_\lambda/\Delta_\lambda$ is bounded away from $1/4$, $g(\delta_\lambda/\Delta_\lambda)$ can be considered constant for all practical purposes. We comment on this in more detail in Sec. 5.5.

5.3.4 Proof of Theorem 8

We now provide the proof of Theorem 8. At the core of our argument is a statement from matrix perturbation theory. In Appendix B, we collect relevant results from the perturbation theory of invariant subspace given in Ref. [81], and derive a corollary, Theorem 26, that specifically applies to moment operators.

As a first step, we use the identity (27) for the expected RB signal in terms of the Fourier transform of $\phi\nu$ restricted to the isotype τ_λ :

$$F_\lambda(m) = (\rho|X_\lambda S_\lambda^+ \widehat{\phi\nu}[\omega_\lambda]^m (X_\lambda^\dagger \tilde{M})|\tilde{\rho}). \quad (30)$$

Before we proceed, we argue that the involved operators are, in fact, real since they act on the real vector space of Hermitian matrices. Indeed, τ_λ is by assumption real and, thus, the isotypic component $V(\lambda)$ splits as $V(\lambda) = H(\lambda) \oplus iH(\lambda)$ where $H(\lambda) \subset \text{Herm}(\mathcal{H}) =: H$, c.f. Sec. 5.1. Since real representations have real characters, we find that the projector P_λ is Hermiticity-preserving and we can choose a basis such that X_λ and X_λ^\dagger are too. As \tilde{M} is a quantum channel, we thus find that $X_\lambda^\dagger \tilde{M}$ is Hermiticity-preserving. Next, it is immediate from its definition that $\widehat{\phi\nu}[\omega_\lambda]$ preserves the set of Hermiticity-preserving maps $V \rightarrow V(\lambda)$. Recall that S is a quantum channel, hence S_λ has to be Hermiticity-preserving and thus S_λ^+ is Hermiticity-preserving, too (c.f. Sec. 4.1). Finally, this shows that all objects in Eq. (30) can be treated as (super-)operators on the real vector space of Hermitian matrices, in particular they can be described by real matrices. Thus, we only consider the restriction to $\text{Herm}(\mathcal{H})$ in the following.

We can write $\omega_\lambda = T^\dagger(\tau_\lambda \otimes \text{id}_{n_\lambda})T$ and $H(\lambda) = T^\dagger(H_\lambda \otimes \mathbb{R}^{n_\lambda})$, for a suitable real orthogonal matrix T and irreducible subspace H_λ . As in Eq. (14), we then find $\widehat{\phi\nu}[\omega_\lambda]^m (X_\lambda^\dagger \tilde{M}) = T^\dagger(\widehat{\phi\nu}[\tau_\lambda]^m \otimes \text{id}_{n_\lambda})(TX_\lambda^\dagger \tilde{M})$. For the sake of notation, let us define the superoperators $\tilde{M}_\lambda := TX_\lambda^\dagger \tilde{M} \in \text{Hom}(H, H_\lambda \otimes \mathbb{R}^{n_\lambda})$ and $Q_\lambda^\dagger := |\tilde{\rho})(\rho|X_\lambda S_\lambda^+ T^\dagger \in \text{Hom}(H_\lambda \otimes \mathbb{R}^{n_\lambda}, H)$. Note that $|\tilde{M}_\lambda)(Q_\lambda|$ is a linear operator on $\text{Hom}(H, H_\lambda \otimes \mathbb{R}^{n_\lambda})$. With this, we find

$$\begin{aligned} F_\lambda(m) &= (\rho|X_\lambda S_\lambda^+ \widehat{\phi\nu}[\omega_\lambda]^m (X_\lambda^\dagger \tilde{M})|\tilde{\rho}) \\ &= \text{tr} \left[Q_\lambda^\dagger \left(\widehat{\phi\nu}[\tau_\lambda]^m \otimes \text{id}_{n_\lambda} \right) (\tilde{M}_\lambda) \right] \\ &= \text{tr} \left[\left(\widehat{\phi\nu}[\tau_\lambda]^m \otimes \text{id}_{n_\lambda} \right) |\tilde{M}_\lambda)(Q_\lambda| \right]. \end{aligned} \quad (31)$$

We treat $\widehat{\phi\nu}[\tau_\lambda] = \widehat{\omega\nu}[\tau_\lambda] + E$ as a perturbation of the moment operator $\widehat{\omega\nu}[\tau_\lambda]$. Recall from Sec. 4.4, Eq. (15), that $\widehat{\omega\nu}[\tau_\lambda]$ is block-diagonal where the upper block corresponds to the range of the projector $\widehat{\omega}[\tau_\lambda]$. By assumption (A), $\|E\|_\infty \leq \delta_\lambda < \Delta_\lambda/4$, hence we can invoke Thm. 26 to write

$$\widehat{\phi\nu}[\tau_\lambda] = R_{\lambda,1} I_\lambda L_{\lambda,1}^\dagger + R_{\lambda,2} O_\lambda L_{\lambda,2}^\dagger,$$

for suitable real operators $R_\lambda = [R_{\lambda,1}, R_{\lambda,2}]$ and $L_\lambda = [L_{\lambda,1}, L_{\lambda,2}]$ with $L_\lambda^\dagger R_\lambda = \text{id}$. Moreover, I_λ is a real linear operator on the n_λ -dimensional perturbed range of $\widehat{\omega}[\tau_\lambda] = R_{\lambda,1} L_{\lambda,1}^\dagger$. Likewise, O_λ is a real linear operator on the $(d_\lambda d^2 - n_\lambda)$ -dimensional perturbation of the kernel. We arrive at the following expression:

$$\begin{aligned} F_\lambda(m) &= \text{tr} \left[\left((L_{\lambda,1}^\dagger \otimes \text{id}_{n_\lambda}) |\tilde{M}_\lambda)(Q_\lambda| (R_{\lambda,1} \otimes \text{id}_{n_\lambda}) \right) (I_\lambda^m \otimes \text{id}_{n_\lambda}) \right] \\ &\quad + \text{tr} \left[\left((L_{\lambda,2}^\dagger \otimes \text{id}_{n_\lambda}) |\tilde{M}_\lambda)(Q_\lambda| (R_{\lambda,2} \otimes \text{id}_{n_\lambda}) \right) (O_\lambda^m \otimes \text{id}_{n_\lambda}) \right] \\ &= \text{tr} [A_\lambda I_\lambda^m] + \text{tr} [B_\lambda O_\lambda^m], \end{aligned}$$

with $A_\lambda := L_{\lambda,1}^\dagger \text{tr}_{n_\lambda} (|\tilde{M}_\lambda\rangle\langle Q_\lambda|) R_{\lambda,1}$ and $B_\lambda := L_{\lambda,2}^\dagger \text{tr}_{n_\lambda} (|\tilde{M}_\lambda\rangle\langle Q_\lambda|) R_{\lambda,2}$. In particular, we have the following expression used in Sec. 5.3.2:

$$\text{tr}(A_\lambda) = \text{tr} [\widehat{\omega}[\tau_\lambda] \otimes \text{id}_{n_\lambda}] |\tilde{M}_\lambda\rangle\langle Q_\lambda| = (\rho | X_\lambda S_\lambda^+ \widehat{\omega}[\omega_\lambda] (X_\lambda^\dagger \tilde{M}) | \bar{\rho}). \quad (32)$$

Here, we used that $R_{\lambda,1} L_{\lambda,1}^\dagger = \widehat{\omega}[\tau_\lambda]$ and then traced the steps leading to Eq. (31) backwards.

The claimed spectral bound on O_λ follows directly from Thm. 26, as well as $\|I_\lambda - \text{Id}\|_\infty < 1 - 2\delta_\lambda$. The latter statement already shows that $\text{spec}(I_\lambda) \subset (1 - 2\delta_\lambda, 1 + 2\delta_\lambda)$. Note that $\widehat{\phi\nu}[\omega]$ maps quantum channels to quantum channels and thus has unit $\diamond \rightarrow \diamond$ norm. Hence, its eigenvalues lie in $[-1, 1]$ and the same holds for $\widehat{\phi\nu}[\tau_\lambda]$ as it corresponds to a block in the block diagonalization of $\widehat{\phi\nu}[\omega]$ by the irreps of ω . Since every eigenvalue of I_λ is also an eigenvalue of $\widehat{\phi\nu}[\tau_\lambda]$, we conclude that $\text{spec}(I_\lambda) \subset (1 - 2\delta_\lambda, 1]$. This establishes the signal form (S).

Next, we can bound the subdominant decays as follows

$$\begin{aligned} |\text{tr}[B_\lambda O_\lambda^m]| &\leq \|B_\lambda\|_1 \|O_\lambda\|_\infty^m \\ &\leq \|(L_{\lambda,2}^\dagger \otimes \text{id}_{n_\lambda}) |\tilde{M}_\lambda\rangle\langle Q_\lambda| (R_{\lambda,2} \otimes \text{id}_{n_\lambda})\|_1 \|O_\lambda\|_\infty^m \\ &= \|(L_{\lambda,2}^\dagger \otimes \text{id}_{n_\lambda}) (\tilde{M}_\lambda)\|_2 \|(R_{\lambda,2} \otimes \text{id}_{n_\lambda}) (Q_\lambda)\|_2 \|O_\lambda\|_\infty^m \\ &\leq \|L_{\lambda,2}\|_\infty \|R_{\lambda,2}\|_\infty \|X_\lambda^\dagger \tilde{M}\|_2 \|S_\lambda^+ X_\lambda |\rho\rangle\langle \bar{\rho}|\|_2 \|O_\lambda\|_\infty^m. \end{aligned}$$

Here, we have used that the partial trace is a contraction w.r.t. to trace norm and that we have $\|AB\|_2 \leq \|A\|_2 \|B\|_\infty$. To proceed, recall that $\tilde{M} = M \mathcal{E}_M$ and $M = \sum_i |E_i\rangle\langle E_i|$ is a projection i.e. $M^2 = M$. We have $\|X_\lambda^\dagger \tilde{M}\|_2^2 = \text{tr}(P_\lambda M \mathcal{E}_M \mathcal{E}_M^\dagger M)$. The superoperator $M \mathcal{E}_M \mathcal{E}_M^\dagger M$ is completely positive and self-adjoint, however, it is generally not trace-preserving. The range of P_λ for λ non-trivial has to lie within the traceless subspace of $\text{End}(\mathcal{H})$. Thus, for the trace inner product of P_λ and $M \mathcal{E}_M \mathcal{E}_M^\dagger M$, only the part of $M \mathcal{E}_M \mathcal{E}_M^\dagger M$ restricted to the traceless subspace plays a role. In particular, we can without loss of generality replace $M \mathcal{E}_M \mathcal{E}_M^\dagger M$ by its projection onto unital and trace-preserving quantum channels, since it only changes $M \mathcal{E}_M \mathcal{E}_M^\dagger M$ outside of the traceless subspace. However, M is already unital and trace-preserving, thus the projection of $M \mathcal{E}_M \mathcal{E}_M^\dagger M$ is in fact the projection of $\mathcal{E}_M \mathcal{E}_M^\dagger$, conjugated by M . Since unital and trace-preserving quantum channels have spectral norm 1, we have $\|\mathcal{E}_M \mathcal{E}_M^\dagger\|_\infty = 1$, cf. Ref. [83, Thm. 4.27], and thus we find using Hölder's inequality:

$$\|X_\lambda^\dagger \tilde{M}\|_2^2 = \text{tr}(P_\lambda M \mathcal{E}_M \mathcal{E}_M^\dagger M) \leq \|P_\lambda M\|_1 \|\mathcal{E}_M \mathcal{E}_M^\dagger\|_\infty \leq \min\{d_\lambda, d\}. \quad (33)$$

In particular, if $[P_\lambda, M] = 0$, we obtain the refined upper bound:

$$\|X_\lambda^\dagger \tilde{M}\|_2^2 = \text{tr}(P_\lambda M \mathcal{E}_M \mathcal{E}_M^\dagger M) \leq \|P_\lambda M\|_1 \|\mathcal{E}_M \mathcal{E}_M^\dagger\|_\infty = \text{tr}(P_\lambda M) = \text{tr}(S_\lambda). \quad (34)$$

Finally, the state-dependent part can be written as

$$\|S_\lambda^+ X_\lambda |\rho\rangle\langle \bar{\rho}|\|_2 \leq \|S_\lambda^+\|_\infty \sqrt{(\rho | P_\lambda | \rho)} \|\bar{\rho}\|_2 \leq \|S_\lambda^+\|_\infty \sqrt{(\rho | P_\lambda | \rho)}.$$

Combining the above bounds, we define

$$c_\lambda := \begin{cases} \sqrt{\text{tr } S_\lambda} \|S_\lambda^+\|_\infty & \text{if } [P_\lambda, M] = 0 \\ \min\{\sqrt{d_\lambda}, \sqrt{d}\} \|S_\lambda^+\|_\infty & \text{else} \end{cases}.$$

To obtain the final bound, we use the following result from Thm. 26:

$$\|L_{\lambda,2}\|_\infty \|R_{\lambda,2}\|_\infty \leq g(\delta_\lambda / \Delta_\lambda), \quad g(x) := (1 - 4x)x + \frac{1 + x}{1 - 4x}.$$

Combining the above results, we then find

$$\begin{aligned} |F_\lambda(m) - \text{tr}[A_\lambda I_\lambda^m]| &\leq c_\lambda \sqrt{(\rho | P_\lambda | \rho)} \|L_{\lambda,2}\|_\infty \|R_{\lambda,2}\|_\infty \|O_\lambda\|_\infty^m \\ &< c_\lambda \sqrt{(\rho | P_\lambda | \rho)} g(\delta_\lambda / \Delta_\lambda) (1 - \Delta_\lambda + 2\delta_\lambda)^m. \end{aligned}$$

5.3.5 Filtering onto trivial irrep: Measuring average trace-preservation

In the proof of Theorem 8, we assumed that the irrep λ is not trivial. We treat this case separately in this section, as the arguments simplify considerably. The filtered RB protocol for the trivial irrep and with G an exact unitary 1-design has been proposed as a protocol to detect “incoherent” leakage errors in Ref. [84]. See also Ref. [18] in this context. Going beyond simply aiming at completeness, this section, thus provides guarantees for incoherent leakage benchmarking for non-uniform measures and gate-dependent noise. We think that our framework can be extended to also capture more general (coherent) leakage errors, we however leave this for future work.

In the following, we assume that the only trivial irrep in ω is spanned by the identity operator $\mathbb{1}$. If this is not the case, the following still holds if one filters onto the copy of the trivial irrep spanned by $\mathbb{1}$ instead of filtering onto the whole trivial subrepresentation. Using that $P_1 = |\mathbb{1}\rangle(\mathbb{1}|/d$ and $S_1 = P_1$, we find that

$$\begin{aligned} F_1(m) &= \frac{1}{d}(\rho|\mathbb{1})(\mathbb{1}|S_1^\dagger\widehat{\phi\nu}[\omega](\tilde{M})|\tilde{\rho}) \\ &= \frac{1}{d}\sum_{i\in[d]}\int_G(\tilde{E}_i|\phi(g_m)\dots\phi(g_1)|\tilde{\rho})d\nu(g_1)\dots d\nu(g_m) \\ &= \frac{1}{d}\int_G(\tilde{\mathbb{1}}|\phi(g_m)\dots\phi(g_1)|\tilde{\rho})d\nu(g_1)\dots d\nu(g_m). \end{aligned}$$

Here, we set $\tilde{\mathbb{1}} := \mathcal{E}_M^\dagger(\mathbb{1})$ which is simply $\mathbb{1}$ if the measurement noise is trace-preserving. In this case, $F_1(m)$ can be interpreted as the average trace-preservation of a sequence of length m . In particular, if ϕ (and \mathcal{E}_M) is trace-preserving, $F_1(m) = 1/d$ for all m .

Note that the Fourier transform evaluated at the trivial irrep $\tau_1(g) \equiv 1$ can be identified with the integral over ϕ :

$$\widehat{\phi\nu}[\tau_1] = \int_G 1(\cdot)\phi(g)d\nu(g) \simeq \int_G \phi(g)d\nu(g)$$

Thus, we indeed recover a formula similar to the non-trivial case:

$$F_1(m) = \frac{1}{d}(\tilde{\mathbb{1}}|\widehat{\phi\nu}[\tau_1]^m|\tilde{\rho}). \quad (35)$$

We can then show that $F_1(m)$ has the form of an exponential decay by treating $\widehat{\phi\nu}[\tau_1]$ as a perturbation of $\widehat{\omega\nu}[\tau_1]$.

Theorem 9 (Filtering onto trivial irrep). *Suppose that the trivial irrep is multiplicity-free and $\widehat{\omega\nu}[\tau_1] \simeq \int_G \omega(g)d\nu(g)$ has a spectral gap $\Delta_1 > 0$. If there is $\delta_1 > 0$ such that*

$$\left\| \int_G (\phi(g) - \omega(g))d\nu(g) \right\|_\infty \leq \delta_1 < \frac{\Delta_1}{4}$$

then the filtered RB signal (27) is given by

$$F_1(m) = \frac{1}{d} \left(\frac{1}{d} \text{tr} \mathcal{E}_M(\mathbb{1}) I_1^m + \text{tr}(B_1 O_1^m) \right),$$

where \mathcal{E}_M is the trace non-increasing measurement noise channel, $1 - 2\delta_1 < I_1 \leq 1$ and B_1 and O_1 are real operators on the traceless subspace of $\text{Herm}(\mathbb{C}^d)$. Moreover, I_1 and O_1 do not depend on the initial state and measurement, and we have $I_1 = 1$ if $\phi(g)$ is trace-preserving ν -almost everywhere. Finally, we have the bounds $\|O_1\|_\infty \leq 1 + \Delta_1 - 2\delta_1$ and

$$\frac{1}{d}|\text{tr}(B_1 O_1^m)| \leq \left[\frac{1 + 2\sqrt{d}}{\Delta_1/\delta_1 - 4} + 2\|\mathcal{E}_M(\mathbb{1})_0\|_2 \left(1 + \frac{1}{\Delta_1/\delta_1 - 4} \right) \right] (1 + \Delta_1 - 2\delta_1)^m,$$

where $\mathcal{E}_M(\mathbb{1})_0 = \mathcal{E}_M(\mathbb{1}) - \text{tr}(\mathcal{E}_M(\mathbb{1}))\mathbb{1}/d$ is the traceless part of $\mathcal{E}_M(\mathbb{1})$.

Proof. We start from Eq. (35) and apply perturbation theory to the block diagonalization of $\widehat{\omega\nu}[\tau_1] \simeq \int_G \omega(g) d\nu(g)$ as in the proof of Thm. 8, c.f. Sec. 5.3.4. Moreover, we can again restrict to the action on the real vector space of Hermitian matrices $\text{Herm}(\mathbb{C}^d)$. We then obtain from Thm. 26 in App. B that

$$\widehat{\phi\nu}[\tau_1] = R_1 I_1 L_1^\dagger + R_2 O_1 L_2^\dagger = I_1 P_1 + R_2 O_1 L_2^\dagger.$$

Here, we used that the first block is 1×1 , thus the first term becomes $I_1 R_1 L_1^\dagger$, and $R_1 L_1^\dagger = P_1 = |\mathbb{1}\rangle\langle\mathbb{1}|/d$ is the projection onto the first block, i.e. onto the trivial irrep of ω . The other block corresponds to the traceless subspace. We then obtain

$$F_1(m) = \frac{1}{d}(\tilde{\mathbb{1}}|P_1|\tilde{\rho})I_1^m + \frac{1}{d}(\tilde{\mathbb{1}}|R_2 O_1^m L_2^\dagger|\tilde{\rho}) = \frac{\text{tr } \tilde{\mathbb{1}}}{d^2}I_1^m + \frac{1}{d}(\tilde{\mathbb{1}}|R_2 O_1^m L_2^\dagger|\tilde{\rho}).$$

Let $E = \widehat{\phi\nu}[\tau_1] - \widehat{\omega\nu}[\tau_1]$ be the perturbation error, then we can use the formula $I_1 = 1 + E_{11} + E_{12}Q_1$ from Thm. 26, where $E_{ij} = X_i^\dagger E X_j$ are the blocks of perturbation (here we rename the operators P_i in Thm. 26 to Q_i to avoid confusion). Since the first block is one-dimensional, we can make the identification $X_1 \equiv |\mathbb{1}\rangle\langle\mathbb{1}|/\sqrt{d}$. Note that if ϕ is trace-preserving ν -almost everywhere, then

$$X_1^\dagger E = \frac{1}{\sqrt{d}} \int_G (\mathbb{1}|\phi(g) - \omega(g)) = \frac{1}{\sqrt{d}} \int_G [(\mathbb{1}| - (\mathbb{1}|)] = 0.$$

Thus, $E_{11} = 0$ and $E_{12} = 0$ which shows that $I_1 = 1$ in this case.

Next, we use the formulae $R_2 = X_1 Q_2 + X_2(Q_1 Q_2 + \text{id}_2)$ and $L_2 = X_2 - X_1 Q_1^\dagger$. Recall that Q_1 maps from the first block to the second block and vice versa for Q_2 . Since the second block corresponds to the traceless subspace, we can make the further identifications $Q_1 = |q_1\rangle\langle q_2|$ for suitable traceless operators q_1, q_2 on $\text{Herm}(\mathbb{C}^d)$. Note that we then have $\|Q_i\|_\infty = \|q_i\|_2$ for $i = 1, 2$. Let $\tilde{\rho}_0 \simeq \tilde{\rho} - \mathbb{1}/d$ and $\tilde{\mathbb{1}}_0 \simeq \tilde{\mathbb{1}} - \text{tr}(\tilde{\mathbb{1}})\mathbb{1}/d$ be the traceless part of $\tilde{\rho}$ and $\tilde{\mathbb{1}}$, respectively. We then find that

$$\begin{aligned} R_2^\dagger(\tilde{\mathbb{1}}) &= (\text{id}_2 + Q_2^\dagger Q_1^\dagger)X_2^\dagger(\tilde{\mathbb{1}}) + Q_2^\dagger X_1^\dagger(\tilde{\mathbb{1}}) = \left((q_1|\tilde{\mathbb{1}}_0) + \frac{\text{tr } \tilde{\mathbb{1}}}{\sqrt{d}}\right) q_2 + \tilde{\mathbb{1}}_0, \\ L_2^\dagger(\tilde{\rho}) &= X_2^\dagger(\tilde{\rho}) - \frac{\text{tr } \tilde{\rho}}{\sqrt{d}} q_1 = \tilde{\rho}_0 - \frac{1}{\sqrt{d}} q_1. \end{aligned}$$

Next, we use the bounds (90), (92), and (93) on Q_1 and Q_2 , namely

$$\|Q_1\|_\infty < 4 \frac{\delta_1}{\Delta_1} < 1, \quad \|Q_2\|_\infty \leq \frac{2}{\Delta_1/\delta_1 - 4}, \quad \|Q_1\|_\infty \|Q_2\|_\infty \leq \frac{4\delta_1/\Delta_1}{\Delta_1/\delta_1 - 4} \leq \frac{1}{\Delta_1/\delta_1 - 4}.$$

Moreover, we use $\text{tr } \tilde{\mathbb{1}} = \text{tr}(\mathcal{E}_M(\mathbb{1})) \leq \text{tr } \mathbb{1} = d$ and $\|\tilde{\rho}_0\|_2 \leq 1$ to obtain

$$\begin{aligned} (\tilde{\mathbb{1}}|R_2 O_1^m L_2^\dagger|\tilde{\rho}) &= \left(\frac{\text{tr } \tilde{\mathbb{1}}}{\sqrt{d}} + (\tilde{\mathbb{1}}_0|q_1)\right) (q_2|O_1^m|\tilde{\rho}_0 - q_1/\sqrt{d}) + (\tilde{\mathbb{1}}_0|O_1^m|\tilde{\rho}_0 - q_1/\sqrt{d}) \\ &\leq \left(\frac{\text{tr } \tilde{\mathbb{1}}}{\sqrt{d}} + \|\tilde{\mathbb{1}}_0\|_2 \|Q_1\|_\infty\right) \left(\|Q_2\|_\infty \|\tilde{\rho}_0\|_2 + \frac{1}{\sqrt{d}} \|Q_1\|_\infty \|Q_2\|_\infty\right) \|O_1\|_\infty^m \\ &\quad + \|\tilde{\mathbb{1}}_0\|_2 \left(\|\tilde{\rho}_0\|_2 + \frac{1}{\sqrt{d}} \|Q_1\|_\infty\right) \|O_1\|_\infty^m \\ &\leq \left(\sqrt{d} \|Q_2\|_\infty + \|Q_1\|_\infty \|Q_2\|_\infty\right) \|O_1\|_\infty^m \\ &\quad + \|\tilde{\mathbb{1}}_0\|_2 \left(1 + \frac{1}{\sqrt{d}} \|Q_1\|_\infty\right) \left(1 + \|Q_1\|_\infty \|Q_2\|_\infty\right) \|O_1\|_\infty^m \\ &\leq \left[\frac{1 + 2\sqrt{d}}{\Delta_1/\delta_1 - 4} + 2 \|\tilde{\mathbb{1}}_0\|_2 \left(1 + \frac{1}{\Delta_1/\delta_1 - 4}\right)\right] \|O_1\|_\infty^m. \end{aligned}$$

The remaining claims follow from Thm. 26 as in Thm. 8. \square

5.4 Sampling complexity of filtered randomized benchmarking

The expression for the filtered RB signal $F_\lambda(m)$ from Eq. (4) has the form of an expected value for the random variable $f_\lambda(i, g_1, \dots, g_m)$ where $(i, g_1, \dots, g_m) \sim p(i|g_1, \dots, g_m) d\nu(g_1) \dots d\nu(g_m)$. In the following, we consider the unbiased estimator $\hat{F}_\lambda(m)$, given as the mean of N iid samples $(i^{(l)}, g_1^{(l)}, \dots, g_m^{(l)})$:

$$\hat{F}_\lambda(m) = \frac{1}{N} \sum_{l=1}^N f_\lambda(i^{(l)}, g_1^{(l)}, \dots, g_m^{(l)}). \quad (36)$$

In this section, we derive bounds on the number of samples N needed to guarantee that $\hat{F}_\lambda(m)$ is, with high probability, close to $F_\lambda(m)$. We base our analysis on the variance of $\hat{F}_\lambda(m)$ because the function f_λ may take on values as large as the Hilbert space dimension d . We have $\text{Var}[\hat{F}_\lambda(m)] = \text{Var}[f_\lambda]/N$, thus the second moment of f_λ is key for our sampling complexity bounds. To this end, we show that the second moment of f_λ is close to the second moment in the idealized situation where all gates are noiseless and sampled from the Haar measure on G , provided that the sequence length m is sufficiently large. Hence, the noisy implementation and the non-uniform sampling cannot disturb the efficiency of filtered randomized benchmarking.

The proof strategy is as follows: First, we show that the second moment $\mathbb{E}[f_\lambda^2]$ has a similar form as the first moment $\mathbb{E}[f_\lambda] = F_\lambda(m)$ and thus admits an analogous perturbative expansion as in Thm. 8. Then, we proceed by deriving appropriate bounds on the subdominant terms, in analogy to Sec. 5.5.1. Finally, we combine these results to relate $\mathbb{E}[f_\lambda^2]$ to its value in the idealized situation, and derive additive and relative-precision guarantees for the estimator $\hat{F}_\lambda(m)$. For additive precision, we find that the sampling complexity is essentially the same as in the idealized situation. In contrast, relative precision requires that the number of sampling increases with the sequence length as $1/I_\lambda^{2m}$ where I_λ is the decay parameter from Thm. 8. This is however unavoidable since the signal $F_\lambda(m)$ decays as I_λ^m .

In analogy to Eq. (27) for the first moment $F_\lambda(m)$, the perturbative expansion of the second moment $\mathbb{E}[f_\lambda^2]$ is based on the following observation:

$$\begin{aligned} \mathbb{E}[f_\lambda^2] &= \sum_{i \in [d]} \int_{G^m} f_\lambda(i, g_1, \dots, g_m)^2 p(i|g_1, \dots, g_m) d\nu(g_1) \dots d\nu(g_m) \\ &= \sum_{i \in [d]} \int [(\rho | P_\lambda S^+ \omega(g_1)^\dagger \dots \omega(g_m)^\dagger | E_i)]^2 (\tilde{E}_i | d(\phi\nu)(g_m) \dots d(\phi\nu)(g_1) | \tilde{\rho}) \\ &= (\rho^{\otimes 2} | (P_\lambda S^+)^{\otimes 2} \left(\int \omega(g)^\dagger \otimes 2(\cdot) d(\phi\nu)(g) \right)^m (\tilde{M}_3) | \tilde{\rho}) \\ &= (\rho^{\otimes 2} | (X_\lambda S_\lambda^+)^{\otimes 2} \widehat{\phi\nu}[\omega_\lambda^{\otimes 2}]^m (X_\lambda^{\dagger \otimes 2} \tilde{M}_3) | \tilde{\rho}), \end{aligned}$$

where we have defined

$$\tilde{M}_3 := \sum_{i \in [d]} |E_i \otimes E_i\rangle \langle \tilde{E}_i|.$$

Note that $\omega_\lambda^{\otimes 2}$ is generally reducible and can thus be decomposed into isotypic representations $\omega_\sigma^{(2)}$. Moreover, $S_\lambda^{\otimes 2}$ commutes with $\omega_\lambda^{\otimes 2}$ and is thus block-diagonal in this decomposition. Finally, we can write the partial isometry $X_\lambda^{\otimes 2}$ as a concatenation of partial isometries on the isotypic components. In summary, we have:

$$\omega_\lambda^{\otimes 2} = \bigoplus_{\sigma \in \text{Irr}(\omega_\lambda^{\otimes 2})} \omega_\sigma^{(2)}, \quad (S_\lambda^+)^{\otimes 2} = \bigoplus_{\sigma \in \text{Irr}(\omega_\lambda^{\otimes 2})} T_\sigma^+, \quad X_\lambda^{\otimes 2} = \bigoplus_{\sigma \in \text{Irr}(\omega_\lambda^{\otimes 2})} Y_\sigma.$$

Hence, the second moment can be written as

$$\mathbb{E}[f_\lambda^2] = \sum_{\sigma \in \text{Irr}(\omega_\lambda^{\otimes 2})} (\rho^{\otimes 2} | Y_\sigma T_\sigma^+ \widehat{\phi\nu}[\omega_\sigma^{(2)}]^m (Y_\sigma^\dagger \tilde{M}_3) | \tilde{\rho}). \quad (37)$$

The expressions on the right-hand side have the same form as the filtered RB signal itself. Thus, we can argue as in the proof of Theorem 8 to compute the RHS of Eq. (37), provided that the appropriate assumptions are fulfilled for every $\sigma \in \text{Irr}(\omega_\lambda^{\otimes 2})$. As it turns out, the multiplicity of σ in $\omega_\lambda^{\otimes 2}$ does not affect the form of Eq. (37).

Theorem 10 (Data guarantees for second moment of filtered RB with random circuits). *Fix a non-trivial irrep τ_λ appearing in ω . Suppose that for all $\sigma \in \text{Irr}(\tau_\lambda^{\otimes 2})$ the spectral gap of $\widehat{\omega\nu}[\tau_\sigma]$ is lower bounded by $\Delta_\sigma > 0$, and there are $\delta_\sigma > 0$ such that*

$$\|\widehat{\phi\nu}[\tau_\sigma] - \widehat{\omega\nu}[\tau_\sigma]\|_\infty \leq \delta_\sigma < \frac{\Delta_\sigma}{4}.$$

Then, the second moment of the λ -filtered RB signal estimator obeys

$$\mathbb{E}[f_\lambda^2] = \sum_{\sigma \in \text{Irr}(\omega) \cap \text{Irr}(\tau_\lambda^{\otimes 2})} \text{tr}(C_\sigma I_\sigma^m) + \sum_{\sigma \in \text{Irr}(\tau_\lambda^{\otimes 2})} \text{tr}(D_\sigma O_\sigma^m). \quad (38)$$

Here, $C_\sigma, I_\sigma \in \mathbb{R}^{n_\sigma \times n_\sigma}$, where n_σ is the multiplicity of τ_σ in ω . The matrices I_σ and O_σ do not depend on the initial state and measurement. For $\sigma \in \text{Irr}(\omega) \cap \text{Irr}(\tau_\lambda^{\otimes 2})$, I_σ and O_σ are the same as in Thm. 8. We have the bounds

$$\text{spec}(I_\sigma) \subset (1 - 2\delta_\sigma, 1] \quad \|O_\sigma\|_\infty \leq \begin{cases} 1 - \Delta_\sigma + 2\delta_\sigma, & \text{if } \sigma \in \text{Irr}(\omega), \\ 1 - \Delta_\sigma + \delta_\sigma, & \text{else.} \end{cases}$$

Define the quantities

$$\Delta_\lambda^{(3)} := \min_{\sigma \in \text{Irr}(\tau_\lambda^{\otimes 2})} \Delta_\sigma, \quad r_\lambda^{(3)} := \max_{\sigma \in \text{Irr}(\tau_\lambda^{\otimes 2})} \delta_\sigma / \Delta_\sigma,$$

Then, we can bound the second sum of matrix exponentials as follows:

$$\left| \sum_{\sigma \in \text{Irr}(\tau_\lambda^{\otimes 2})} \text{tr}(D_\sigma O_\sigma^m) \right| \leq c_\lambda \|S_\lambda^+\|_\infty (\rho | P_\lambda | \rho) g(r_\lambda^{(3)}) \left(1 - \Delta_\lambda^{(3)} (1 - 2r_\lambda^{(3)})\right)^m,$$

where c_λ is given in Thm. 8 and $g(x) := (1 - 4x)x + \frac{1+x}{1-4x}$.

The proof of the theorem is postponed to Sec. 5.4.3 and we first proceed with its discussion.

As mentioned in the beginning of this section, it is sufficient for our choice of estimator $\hat{F}_\lambda(m)$ to consider the ‘single shot’ estimator per circuit throughout this work. Another frequently used data acquisition scheme that also yields an estimator for $F_\lambda(m)$ is the following: Instead of only taking a single sample per circuit, we sample N_C different random circuits according to ν , and then take N_M samples from the outcome distribution for each circuit. We discuss the resulting estimator in App. A, and show that its variance involves an additional term compared to the one of $\hat{F}_\lambda(m)$, which is a fourth moment of ν w.r.t. ω . As explained in App. A, we expect the sampling complexity of such a scheme to be higher than for our approach. This difference makes using the single shot estimator particularly important for small Hilbert space dimensions. When the Hilbert space dimension is large compared to the inverse desired precision, using less sequences and more shots per sequence yields essentially the same sampling complexity. The techniques in this section can be adapted for this estimator, but would become more involved.

5.4.1 Discussion of assumptions and dominant signal

The similarities to Thm. 8 are imminent, hence we concentrate on the differences between the theorems for the first and second moment of f_λ .

Simplified assumptions. Instead of involving only a single irrep λ , Thm. 10 involves all irreps appearing in the tensor square $\tau_\lambda^{\otimes 2}$. Note that we would find a similar situation in Thm. 8, if we would not filter on irreps, but on reducible subrepresentations instead. However, the perturbative

expansion is done independently for every irrep $\sigma \in \text{Irr}(\tau_\lambda^{\otimes 2})$, and thus Thm. 10 makes only irrep-specific assumptions.

Nevertheless, it might be simpler to use σ -independent bounds in practice. To this end, the quantity $\Delta_\lambda^{(3)}$ introduced in Thm. 10 is helpful since it bounds the spectral gap of the third moment operator $\widehat{\omega\nu}[\tau_\lambda^{\otimes 2}]$:

$$1 - \Delta_\lambda^{(3)} \geq \max_{\sigma \in \text{Irr}(\tau_\lambda^{\otimes 2})} \|\widehat{\omega\nu}[\tau_\sigma] - \widehat{\omega}[\tau_\sigma]\|_\infty = \|\widehat{\omega\nu}[\tau_\lambda^{\otimes 2}] - \widehat{\omega}[\tau_\lambda^{\otimes 2}]\|_\infty.$$

A sufficient condition for the assumptions of Thm. 10 is then $\delta_\lambda^{(3)} \leq \Delta_\lambda^{(3)}/4$, where

$$\delta_\lambda^{(3)} \geq \|\widehat{\phi\nu}[\tau_\lambda^{\otimes 2}] - \widehat{\omega\nu}[\tau_\lambda^{\otimes 2}]\|_\infty = \max_{\sigma \in \text{Irr}(\tau_\lambda^{\otimes 2})} \|\widehat{\phi\nu}[\tau_\sigma] - \widehat{\omega\nu}[\tau_\sigma]\|_\infty.$$

In this case, we have $r_\lambda^{(3)} \leq \delta_\lambda^{(3)}/\Delta_\lambda^{(3)}$ and $g(r_\lambda^{(3)}) \leq g(\delta_\lambda^{(3)}/\Delta_\lambda^{(3)})$ since g is monotonic.

Form of the dominant signal. In the following, we discuss the role of the matrix coefficients appearing in the dominant terms of the second moment (38). Analogously to the SPAM constants $\text{tr}(A_\lambda)$ discussed in Sec. 5.3.2, we derive in Sec. 5.4.3, Eq. (46) that

$$\text{tr}(C_\sigma) = (\rho^{\otimes 2} | Y_\sigma T_\sigma^+ \widehat{\omega}[\omega_\sigma^{(2)}] (Y_\sigma^\dagger \tilde{M}_3) | \tilde{\rho}).$$

Hence, $\text{tr}(C_\sigma)$ is the σ -contribution to the *second moment of the ideal, noiseless implementation* $\phi = \omega$ with unitaries sampled from the Haar measure $\nu = \mu$, but subject to the same SPAM noise. Consequently, the sum over σ yields the total second moment:

$$\sum_{\sigma \in \text{Irr}(\omega^{\otimes 2})} \text{tr}(C_\sigma) = (\rho^{\otimes 2} | (X_\lambda S_\lambda^+)^{\otimes 2} \widehat{\omega}[\tau_\lambda^{\otimes 2}] (X_\lambda^{\dagger \otimes 2} \tilde{M}_3) | \tilde{\rho}) =: \mathbb{E}[f_\lambda^2]_{\text{SPAM}}. \quad (39)$$

Note that irreps $\sigma \in \text{Irr}(\tau_\lambda^{\otimes 2})$ which are *not* in $\text{Irr}(\omega)$ do not contribute to the sum since $\widehat{\omega}[\omega_\sigma^{(2)}] = 0$ in this case.

As in Sec. 5.3, we would like to compare the second moment under only SPAM noise $\mathbb{E}[f_\lambda^2]_{\text{SPAM}}$ to the ideal, noiseless second moment $\mathbb{E}[f_\lambda^2]_{\text{ideal}}$. The discussion is made somewhat more complicated by the presence of multiplicities in $\tau_\lambda^{\otimes 2}$ even if all irreps in ω are multiplicity-free. Consequently, the rank of the projector $\widehat{\omega}[\tau_\lambda^{\otimes 2}]$ is generally much larger than the rank of $\widehat{\omega}[\tau_\lambda]$ and given by the summed multiplicities of the irreps $\sigma \in \text{Irr}(\tau_\lambda^{\otimes 2}) \cap \text{Irr}(\omega)$, c.f. App. C.

Similar to Sec. 5.3.2, we conjecture that for any physically relevant setting, the effect of SPAM noise is the reduction of the magnitude of the σ -contribution compared to the SPAM-free case, $|\text{tr}(C_\sigma)| \leq \text{tr}(C_\sigma)_{\text{ideal}}$. We are able to prove this under the assumption that G contains the Heisenberg-Weyl group $\text{HW}_n(p)$.

Proposition 11. *Suppose that $\text{HW}_n(p) \subset G$, the measurement is in the computational basis, and ρ is a computational basis state. Then we have*

$$|\text{tr}(C_\sigma)| \leq \text{tr}(C_\sigma)_{\text{ideal}} := (\rho^{\otimes 2} | P_\sigma^{(2)}(S^+)^{\otimes 2} \widehat{\omega}[\omega^{\otimes 2}](M_3) | \rho).$$

Proof. We consider the matrix representation of $\widehat{\omega}[\omega^{\otimes 2}]$ in the orthogonal basis $X_{a,b,c} := |w(a) \otimes w(b)\rangle\langle w(c)|$ of $\text{Hom}(V, V \otimes V)$ for $a, b, c \in \mathbb{F}_p^{2n}$. Note that $\|X_{a,b,c}\|_2 = d^{3/2}$. Let $\widehat{\omega}[\omega^{\otimes 2}]|_{\text{HW}_n(p)}$ be the restriction of the Fourier transform to the Heisenberg-Weyl group. The range of $\widehat{\omega}[\omega^{\otimes 2}]|_{\text{HW}_n(p)}$ is exactly given by the subspace of $\text{HW}_n(p)$ -equivariant maps, this is $X\mathcal{W}(a) = \mathcal{W}(a)^{\otimes 2}X$ for all $a \in \mathbb{F}_p^{2n}$, where $\mathcal{W}(a) = w(a)(\cdot)w(a)^\dagger$ is a unitary Weyl channel. It is straightforward to check that an orthonormal basis for this subspace is given by $X_{a,b,a+b}$ for $a, b \in \mathbb{F}_p^{2n}$. By the invariance of the Haar measure on G , $\widehat{\omega}[\omega^{\otimes 2}]$ is left and right invariant under the multiplication with $\widehat{\omega}[\omega^{\otimes 2}]|_{\text{HW}_n(p)}$, hence $\widehat{\omega}[\omega^{\otimes 2}]$ is diagonal in the $X_{a,b,a+b}$ basis. In particular, the diagonal entries are either 0 or 1

since $\hat{\omega}[\omega^{\otimes 2}]$ is a projector. Hence, we find

$$\begin{aligned}
\hat{\omega}[\omega^{\otimes 2}](\tilde{M}_3) &= \frac{1}{d^3} \sum_{a,b} |X_{a,b,a+b}\rangle \langle X_{a,b,a+b}| \tilde{M}_3 \\
&= \frac{1}{d^3} \sum_{a,b} \sum_{x \in \mathbb{F}_p^n} |X_{a,b,a+b}\rangle (w(a) \otimes w(b) | E_x \otimes E_x) (\tilde{E}_x | w(a+b)) \\
&= \frac{1}{d^3} \sum_{a,b} \delta_{a_x,0} \delta_{b_x,0} |X_{a,b,a+b}\rangle \sum_{x \in \mathbb{F}_p^n} \xi^{-(a_z+b_z) \cdot x} (E_x | \mathcal{E}_M | Z(a_z+b_z)) \\
&= \frac{1}{d^3} \sum_{z,z'} |X_{z,z',z+z'}\rangle \langle Z(z+z') | \mathcal{E}_M | Z(z+z') \rangle;
\end{aligned}$$

here the sums are over suitable index sets for a, b and z, z' that correspond to the support of $\hat{\omega}[\omega^{\otimes 2}]$. In the second step, we used the definition of the Weyl operators, c.f. Eq. (19), and the orthonormality of the computational basis to conclude that the contribution of Weyl operators with a non-vanishing X component $a_x \neq 0$ is zero. Afterwards, we use of the definition $Z(z) = \sum_x \xi^{z \cdot x} |x\rangle \langle x|$. Note that we have $|(Z(z+z') | \mathcal{E}_M | Z(z+z'))| \leq d$ with equality in the noiseless case $\mathcal{E}_M = \text{id}$. Next, we consider the overlap of $X_{z,z',z+z'}$ with the remaining terms. To this end, we use $\rho = |x\rangle \langle x|$ for some x , and that $P_\sigma^{(2)}$ and $(S^+)^{\otimes 2}$ are positive semi-definite and diagonal in the Weyl basis. We find

$$\begin{aligned}
|(\rho^{\otimes 2} | P_\sigma^{(2)} (S^+)^{\otimes 2} | Z(z) \otimes Z(z')) \langle Z(z+z') | \tilde{\rho} \rangle| &= (P_\sigma^{(2)})_{z,z'} (S^+)_z (S^+)_{z'} \times \\
&\quad \times |(\rho^{\otimes 2} | Z(z) \otimes Z(z')) \rangle \langle Z(z+z') | \tilde{\rho} \rangle| \\
&\leq (P_\sigma^{(2)})_{z,z'} (S^+)_z (S^+)_{z'} \\
&= (\rho^{\otimes 2} | P_\sigma^{(2)} (S^+)^{\otimes 2} | Z(z) \otimes Z(z')) \langle Z(z+z') | \rho \rangle.
\end{aligned}$$

Here, $(P_\sigma^{(2)})_{z,z'}$ and $(S^+)_z$ are the diagonal entries of $P_\sigma^{(2)}$ and S^+ . In the last step, we use that $(\rho^{\otimes 2} | Z(z) \otimes Z(z')) \langle Z(z+z') | \tilde{\rho} \rangle = \xi^{(z+z') \cdot x} \xi^{-(z+z') \cdot x} = 1$. Finally, we obtain the desired result:

$$\begin{aligned}
|\text{tr}(C_\sigma)| &\leq \frac{1}{d^3} \sum_{z,z'} |(\rho^{\otimes 2} | P_\sigma^{(2)} (S^+)^{\otimes 2} | Z(z) \otimes Z(z')) \langle Z(z+z') | \tilde{\rho} \rangle| |(Z(z+z') | \mathcal{E}_M | Z(z+z'))| \\
&\leq \frac{1}{d^2} \sum_{z,z'} (\rho^{\otimes 2} | P_\sigma^{(2)} (S^+)^{\otimes 2} | Z(z) \otimes Z(z')) \langle Z(z+z') | \rho \rangle = \text{tr}(C_\sigma)_{\text{ideal}}.
\end{aligned} \tag{40}$$

□

Although, the contribution $\text{tr}(C_\sigma)$ per irrep σ can be split in a state preparation and a measurement term, we think that doing so does not bear the same level of insight as the treatise in Sec. 5.3.2. Thus, we simply define the *second moment SPAM visibility* as

$$v_{\text{SPAM}}^{(2)} := \frac{\mathbb{E}[f_\lambda^2]_{\text{SPAM}}}{\mathbb{E}[f_\lambda^2]_{\text{ideal}}}.$$

As a consequence of Prop. 11, we have $v_{\text{SPAM}}^{(2)} \leq 1$ for groups G that contain a Heisenberg-Weyl group.

Examples. Let us again consider depolarizing SPAM noise. That is, we assume $\tilde{\rho} = \mathcal{E}_{\text{SP}}(\rho)$ and $\tilde{M} = M\mathcal{E}_M$ with state preparation and measurement noise channels $\mathcal{E}_{\text{SP}} = \mathcal{E}_M = p \text{id} + (1 -$

$p)|\mathbb{1})(\mathbb{1}|/d$. Moreover, let us assume that S is invertible. Then, we find that

$$\begin{aligned}
\mathbb{E}[f_\lambda^2]_{\text{SPAM}} &= (\rho^{\otimes 2} | P_\lambda^{\otimes 2} (S^{-1})^{\otimes 2} \hat{\omega}[\omega^{\otimes 2}] (\tilde{M}_3) | \tilde{\rho}) \\
&= (\rho^{\otimes 2} | P_\lambda^{\otimes 2} (S^{-1})^{\otimes 2} \hat{\omega}[\omega^{\otimes 2}] (M_3) \mathcal{E}_M \mathcal{E}_{\text{SP}} | \rho) \\
&= p^2 \mathbb{E}[f_\lambda^2]_{\text{ideal}} + \frac{1-p^2}{d} (\rho^{\otimes 2} | P_\lambda^{\otimes 2} (S^{-1})^{\otimes 2} \hat{\omega}[\omega^{\otimes 2}] (M_3) | \mathbb{1})(\mathbb{1} | \rho) \\
&= p^2 \mathbb{E}[f_\lambda^2]_{\text{ideal}} + \frac{1-p^2}{d} \sum_{i \in [d]} \int_G (\rho | P_\lambda S^{-1} \omega(g) | E_i)^2 d\mu(g), \tag{41}
\end{aligned}$$

where we used $(E_i | \omega(g) | \mathbb{1}) = (E_i | \mathbb{1}) = 1$ in the last step. Using that the expressions are real-valued, we find

$$\begin{aligned}
\sum_{i \in [d]} \int_G (\rho | P_\lambda S^{-1} \omega(g) | E_i)^2 d\mu(g) &= \sum_{i \in [d]} \int_G (\rho | P_\lambda S^{-1} \omega(g)^\dagger | E_i) (E_i | \omega(g) S^{-1} P_\lambda | \rho) d\mu(g) \\
&= (\rho | P_\lambda S^{-1} S S^{-1} P_\lambda | \rho) \\
&= (\rho | P_\lambda S^{-1} | \rho),
\end{aligned}$$

where we inserted the definition of S and used that P_λ and S commute. Typically, the second term in Eq. (41) is small. To see this, let us for simplicity assume that $\text{HW}_n(p) \subset G$, the measurement is in the computational basis, and ρ is a computational basis state. Then, P_λ and M are diagonal in the Weyl basis and commute. Moreover, choose a decomposition of the λ -isotype such that $S_\lambda = \sum_i s_\lambda^{(i)} P_\lambda^{(i)}$ where $s_\lambda^{(i)} = \text{tr}(P_\lambda^{(i)} M)/d_\lambda$, see Eq. (23). We find

$$\frac{1}{d} (\rho | P_\lambda S^{-1} | \rho) = \frac{1}{d} (\rho | P_\lambda M S^{-1} | \rho) = \frac{1}{d^2} \text{tr}(P_\lambda M S^{-1}) = \frac{1}{d^2} \sum_{i=1}^{n_\lambda} \frac{d_\lambda}{\text{tr}(P_\lambda^{(i)} M)} \text{tr}(P_\lambda^{(i)} M) = \frac{n_\lambda d_\lambda}{d^2}, \tag{42}$$

where we used that $M(\rho) = \rho$ and $|(\rho | Z(z))|^2 = 1$. Hence, the SPAM visibility becomes

$$v_{\text{SPAM}}^{(2)} = p^2 + \frac{1-p^2}{\mathbb{E}[f_\lambda^2]_{\text{ideal}}} \frac{n_\lambda d_\lambda}{d^2}. \tag{43}$$

Note that Prop. 11 implies the lower bound $\mathbb{E}[f_\lambda^2]_{\text{ideal}} \geq \frac{n_\lambda d_\lambda}{d^2}$. We formulate this as a separate proposition.

Proposition 12 (Second moment bounds). *Suppose that $\text{HW}_n(p) \subset G$, the measurement is in the computational basis, and ρ is a computational basis state. Then we have the following bounds on the ideal second moment.*

$$\frac{k_\lambda d_\lambda}{d^2} \leq \mathbb{E}[f_\lambda^2]_{\text{ideal}} \leq \frac{(k_\lambda d_\lambda)^2}{d^2}.$$

Here, $k_\lambda \leq n_\lambda$ is the number of distinct non-zero eigenvalues of S_λ . In particular if S_λ is invertible, then $k_\lambda = n_\lambda$.

Proof. The first inequality follows from Prop. 11 and Eq. (43) after a straightforward modification to Eq. (42) when S_λ is not invertible. Moreover, from Eqs. (40) and (42) we find in a similar manner

$$\begin{aligned}
\mathbb{E}[f_\lambda^2]_{\text{ideal}} &= \frac{1}{d^2} \sum_{z, z'} (\rho^{\otimes 2} | (P_\lambda S^+)^{\otimes 2} | Z(z) \otimes Z(z')) (Z(z+z') | \rho) \\
&= \frac{1}{d^2} \sum_{z, z'} (Z(z) \otimes Z(z') | (P_\lambda M S^+)^{\otimes 2} | Z(z) \otimes Z(z')) \\
&\leq \frac{1}{d^2} \text{tr}(P_\lambda M S^+)^2 = \frac{(k_\lambda d_\lambda)^2}{d^2}.
\end{aligned}$$

□

For our typical examples from Sec. 5.2, we compute the exact second moments subject to SPAM noise in App. C. In particular, we give the explicit SPAM dependence for these examples. Moreover, we find $\mathbb{E}[f_\lambda^2]_{\text{SPAM}} \leq \mathbb{E}[f_\lambda^2]_{\text{ideal}}$ in agreement with Prop. 11, and that the lower bound in Prop. 12 for the ideal second moments is surprisingly tight. The results are summarized in the following Prop. 13. Interestingly, the second moment of local unitary 3-groups is bounded by a constant if the local dimension p is chosen as 2, i.e. for qubits.

Proposition 13 (Second moments of ideal implementation for typical examples). *For our typical examples from Sec. 5.2, namely unitary 3-groups, local unitary 3-groups, and the Heisenberg-Weyl group, we have $\mathbb{E}[f_\lambda^2]_{\text{SPAM}} \leq \mathbb{E}[f_\lambda^2]_{\text{ideal}}$ and the ideal second moments are given as*

$$\begin{aligned} \mathbb{E}[f_{\text{ad}}^2]_{\text{ideal}} &\leq \begin{cases} 1 - d^{-2} & d = 2, \\ 3 - d^{-2} & d \geq 3, \end{cases} && \text{for unitary 3-groups,} \\ \mathbb{E}[f_b^2]_{\text{ideal}} &\leq \begin{cases} 3^{n-|b|}/d^2 & p = 2, \\ 3^{n-|b|} & p \geq 3, \end{cases} && \text{for local unitary 3-groups,} \\ \mathbb{E}[f_{0,z}^2]_{\text{ideal}} &= d^{-2}, && \text{for Heisenberg-Weyl groups.} \end{aligned}$$

Non-malicious SPAM noise. According to Thm. 10, the matrix coefficients C_σ are modulated by the matrices I_σ in the presence of gate noise and non-uniform sampling. A central problem in analyzing the resulting sampling complexity is that – although the total second moment is non-negative – some of the contributions $\text{tr}(C_\sigma)$ per irrep might be *negative*. The explicit examples in App. C show that this can in fact happen, for instance for G being a unitary 3-design, as a consequence of malicious (i.e. fine-tuned and thus unrealistic) SPAM noise. Indeed, a negative contribution requires that either the measurement noise introduces permutations of the measurement outcomes (thus rendering the measurement useless) or that we accidentally prepare a state $\tilde{\rho}$ which has vanishing fidelity with ρ .

Proposition 11 already shows that the SPAM-free contributions $\text{tr}(C_\sigma)_{\text{ideal}}$ are non-negative under the assumptions that $\text{HW}_n(p) \subset G$. The following lemma shows the same statement in a more general setting.

Proposition 14 (Non-negativity of $\text{tr}(C_\sigma)$ in SPAM-free case). *Suppose that the measurement basis $E_i = |i\rangle\langle i|$ can be generated with gates from G acting on E_1 , and assume that the initial state is $\rho = E_1$. Then, for any irrep $\sigma \in \text{Irr}(\omega_\lambda^{\otimes 2})$, we have*

$$\text{tr}(C_\sigma)_{\text{ideal}} = (\rho^{\otimes 2} | P_\sigma^{(2)}(S^+)^{\otimes 2} \hat{\omega}[\omega^{\otimes 2}](M_3) | \rho) \geq 0.$$

Here, $P_\sigma^{(2)}$ is the projector onto the σ -isotype of $\omega_\lambda^{\otimes 2}$.

Proof. Since the measurement basis is generated by gates from G , we can write

$$\begin{aligned} (\rho^{\otimes 2} | P_\sigma^{(2)}(S^+)^{\otimes 2} \hat{\omega}[\omega^{\otimes 2}](M_3) | \rho) &= d \int_G (\rho^{\otimes 2} | P_\sigma^{(2)}(S^+)^{\otimes 2} \omega^{\otimes 2}(g)^\dagger | E_1^{\otimes 2})(E_1 | \omega(g) | \rho) d\mu(g) \\ &= d \int_G (\rho^{\otimes 3} | (P_\sigma^{(2)}(S^+)^{\otimes 2} \otimes \text{id}) \omega^{\otimes 3}(g)^\dagger | E_1^{\otimes 3}) d\mu(g) \\ &= d (\rho^{\otimes 3} | (P_\sigma^{(2)}(S^+)^{\otimes 2} \otimes \text{id}) P_1^{(3)} | E_1^{\otimes 3}), \end{aligned} \tag{44}$$

where $P_1^{(3)}$ is the projector onto the trivial isotype in $\omega^{\otimes 3}$. Recall that S^+ is in the commutant of ω , and thus $(S^+)^{\otimes 2}$ commutes with $P_\sigma^{(2)}$ as it projects onto a subrepresentation of $\omega^{\otimes 2}$. Since both commute with $\omega^{\otimes 2}(g)$ for all $g \in G$, $(P_\sigma^{(2)}(S^+)^{\otimes 2} \otimes \text{id})$ commutes with $P_1^{(3)}$, hence the product $(P_\sigma^{(2)}(S^+)^{\otimes 2} \otimes \text{id}) P_1^{(3)}$ is a positive semidefinite operator. By assumption, $\rho = E_1$, and thus Eq. (44) is non-negative as claimed. \square

Thus, negative contributions $\text{tr}(C_\sigma)$ can usually only occur as a consequence of malicious noise. In particular, if the SPAM noise is sufficiently small, it can be guaranteed that $\text{tr}(C_\sigma)$ remains non-negative. Although it is straightforward to derive sufficient bounds on the strength of the SPAM noise for this purpose, this would not add much to the discussion. Instead, we add the non-negativity of $\text{tr}(C_\sigma)$ as an assumption and define to this end:

Definition 15 (Non-malicious SPAM noise). *We call the SPAM noise non-malicious if $\text{tr}(C_\sigma) \geq 0$ for all $\sigma \in \text{Irr}(\tau_\lambda^{\otimes 2})$.*

5.4.2 Guarantees for sampling complexity

Finally, we prove guarantees for the sampling complexity of filtered randomized benchmarking. To this end, we assume that the subdominant contributions to $F_\lambda(m)$ and $\mathbb{E}[f_\lambda^2]$ are bounded and combine them with Chebyshev's inequality. Suitable error bounds that accomplish this are later derived in Sec. 5.5, and formulated as Lem. 18, 19, and 20

In the following, we assume for simplicity that all relevant irreps $\sigma \in \text{Irr}(\omega) \cap \text{Irr}(\tau_\lambda^{\otimes 2})$ are multiplicity-free in ω . Note that this is certainly fulfilled if *all* irreps of ω are multiplicity-free – which is the case for most relevant examples.

Theorem 16 (Sampling complexity of filtered RB – additive precision). *Fix a non-trivial irrep $\lambda \in \text{Irr}(\omega)$ such that λ and all $\sigma \in \text{Irr}(\omega) \cap \text{Irr}(\tau_\lambda^{\otimes 2})$ are multiplicity-free in ω . Suppose that we have non-malicious SPAM noise, and the assumptions of Thm. 10 are fulfilled. Moreover, let the sequence length m be sufficiently large such that the subdominant terms in $\mathbb{E}[f_\lambda^2]$ (see Eq. (38)) are bounded by an additive error $\alpha > 0$. Then, the mean estimator $\hat{F}_\lambda(m)$ for N samples, cf. Eq. (36), is close to the expected value with high probability,*

$$\mathbb{P} \left[\left| \hat{F}_\lambda(m) - F_\lambda(m) \right| > \epsilon \right] \leq \delta,$$

provided that

$$N \geq \frac{1}{\epsilon^2 \delta} (\mathbb{E}[f_\lambda^2]_{\text{SPAM}} + \alpha).$$

Here, $\mathbb{E}[f_\lambda^2]_{\text{SPAM}}$ is the second moment of the filter function for the ideal, noiseless implementation $\phi = \omega$ where unitaries are sampled from the Haar measure on G , but with the same SPAM noise, c.f. Eq. (39).

Proof. Chebyshev's inequality guarantees that $|\hat{F}_\lambda(m) - F_\lambda(m)| \leq \epsilon$ with probability at most $1 - \delta$, provided that the number of samples N fulfills

$$N \geq \frac{\text{Var}[f_\lambda]}{\epsilon^2 \delta} = \frac{1}{\epsilon^2 \delta} (\mathbb{E}[f_\lambda^2] - F_\lambda(m)^2)$$

Discarding $F_\lambda(m)^2$ will only make the right hand side larger, thus we can concentrate on bounding the second moment. Under the made assumptions, we find using Thm. 10 that

$$\mathbb{E}[f_\lambda^2] \leq \sum_{\sigma} \text{tr}(C_\sigma) I_\sigma^m + \alpha \leq \sum_{\sigma} \text{tr}(C_\sigma) + \alpha = \mathbb{E}[f_\lambda^2]_{\text{SPAM}} + \alpha,$$

where the sums are taken over $\sigma \in \text{Irr}(\omega) \cap \text{Irr}(\tau_\lambda^{\otimes 2})$. For the second and third step, we used that $I_\sigma \leq 1$ and $\text{tr}(C_\sigma) \geq 0$ for all σ , as well as $\sum_{\sigma} \text{tr}(C_\sigma) = \mathbb{E}[f_\lambda^2]_{\text{SPAM}}$ by Eq. (39). \square

Note that the variance $\text{Var}[f_\lambda]$, which we bounded in the proof of the sampling complexity theorem 16, is in fact decaying with m , and so is N . However, the reason for this is the simple fact that the quantity to be estimated, $F_\lambda(m)$, is decaying with m , too. Hence, we have to reduce the error ϵ with increasing m to get meaningful estimates. Therefore, we give a sampling complexity guarantee with relative error in the following.

Theorem 17 (Sampling complexity of filtered RB – relative precision). *Fix a non-trivial irrep $\lambda \in \text{Irr}(\omega)$ such that λ and all $\sigma \in \text{Irr}(\omega) \cap \text{Irr}(\tau_\lambda^{\otimes 2})$ are multiplicity-free in ω . Suppose that we have non-malicious SPAM noise, and the assumptions of Thm. 8 and Thm. 10 are fulfilled. Moreover, let the sequence length m be sufficiently large such that the subdominant terms in $F_\lambda(m)$ and $\mathbb{E}[f_\lambda^2]$ are bounded by relative errors $\gamma > 0$ and $\kappa > 0$, respectively. Then, the mean estimator $\hat{F}_\lambda(m)$ for N samples, cf. Eq. (36), is close to the expected value with high probability,*

$$\mathbb{P} \left[\left| \hat{F}_\lambda(m) - F_\lambda(m) \right| > \epsilon F_\lambda(m) \right] \leq \delta,$$

provided that

$$N \geq \frac{1}{\varepsilon^2 \delta} \left(\frac{(1 + \kappa)}{(1 - \gamma)^2} \frac{\mathbb{E}[f_\lambda^2]_{\text{SPAM}}}{F_\lambda(m)^2_{\text{SPAM}}} I_\lambda^{-2m} - 1 \right).$$

Here, $F_\lambda(m)_{\text{SPAM}}$ and $\mathbb{E}[f_\lambda^2]_{\text{SPAM}}$ are the first and second moment of the filter function, respectively, for the ideal, noiseless implementation $\phi = \omega$ where unitaries are sampled from the Haar measure on G , but with the same SPAM noise, c.f. Eqs. (29) and (39).

Proof. Chebyshev's inequality guarantees that $|\hat{F}_\lambda(m) - F_\lambda(m)| \leq \varepsilon F_\lambda(m)$ with probability at most $1 - \delta$, provided that the number of samples N fulfills

$$N \geq \frac{\text{Var}[f_\lambda]}{F_\lambda(m)^2 \varepsilon^2 \delta} = \frac{1}{\varepsilon^2 \delta} \left(\frac{\mathbb{E}[f_\lambda^2]}{F_\lambda(m)^2} - 1 \right)$$

Theorems 8 and 10 then give

$$\frac{\mathbb{E}[f_\lambda^2]}{F_\lambda(m)^2} \leq \frac{(1 + \kappa) \sum_\sigma \text{tr}(C_\sigma) I_\sigma^m}{(1 - \gamma)^2 \text{tr}(A_\lambda)^2 I_\lambda^{2m}} \leq \frac{(1 + \kappa)}{(1 - \gamma)^2} \frac{1}{F_\lambda(m)^2_{\text{SPAM}}} \sum_\sigma \text{tr}(C_\sigma) \left(\frac{I_\sigma}{I_\lambda^2} \right)^m,$$

where the sums are taken over $\sigma \in \text{Irr}(\omega) \cap \text{Irr}(\tau_\lambda^{\otimes 2})$. The claim then follows as in the proof of Thm. 16. \square

5.4.3 Proof of Theorem 10

Since ω_λ is a τ_λ -isotype, $\text{Irr}(\omega_\lambda^{\otimes 2}) = \text{Irr}(\tau_\lambda^{\otimes 2})$. For $\sigma \in \text{Irr}(\tau_\sigma^{\otimes 2})$, let m_σ denote the multiplicity of τ_σ in $\omega_\lambda^{\otimes 2}$. Starting from the decomposition given in Eq. (37), we treat the Fourier operators $\widehat{\phi\nu}[\omega_\sigma^{(2)}] \simeq \widehat{\phi\nu}[\tau_\sigma] \otimes \text{id}_{m_\sigma}$ independently. As in the proof of Thm. 8, we write

$$(\rho^{\otimes 2} | Y_\sigma T_\sigma^+ \widehat{\phi\nu}[\omega_\sigma^{(2)}]^m (Y_\sigma^\dagger \tilde{M}_3) | \tilde{\rho}) = \text{tr} \left[\left(\widehat{\phi\nu}[\tau_\sigma] \otimes \text{id}_{m_\sigma} \right)^m | \tilde{M}_{3,\sigma} \rangle \langle Q_{3,\sigma} | \right]$$

for suitable superoperators $\tilde{M}_{3,\sigma}$ and $Q_{3,\sigma}$. Moreover, we can again restrict all operators to their action on Hermitian matrices, and thus consider them as real operators.

First, let us consider the case when the irrep $\sigma \in \text{Irr}(\tau_\lambda^{\otimes 2})$ is *not* contained in ω . Then, the Haar moment operator $\widehat{\omega}[\tau_\sigma]$ is identically zero, so $\widehat{\omega\nu}[\tau_\sigma]$ cannot have an eigenvalue 1. In this case, we may not invoke perturbation theory, but we can simply set

$$O_\sigma := \widehat{\phi\nu}[\tau_\sigma], \quad D_\sigma := \text{tr}_{m_\sigma}(|\tilde{M}_{3,\sigma}\rangle \langle Q_{3,\sigma}|).$$

Hence, we have $\|O_\sigma\|_\infty \leq \|\widehat{\omega\nu}[\tau_\sigma]\|_\infty + \delta_\sigma \leq 1 - \Delta_\sigma + \delta_\sigma$. Analogous to the proof of Thm. 8, we then find

$$|\text{tr}(D_\sigma O_\sigma^m)| \leq \|Y_\sigma^\dagger \tilde{M}_3\|_2 \|T_\sigma^+ Y_\sigma | \rho^{\otimes 2} \rangle (\tilde{\rho})\|_2 \|O_\sigma\|_\infty^m. \quad (45)$$

If $\sigma \in \text{Irr}(\tau_\lambda^{\otimes 2}) \cap \text{Irr}(\omega)$, we proceed analogously to the proof of Thm. 8 and apply perturbation theory to $\widehat{\phi\nu}[\tau_\sigma]$ with parameters $(\delta_\sigma, \Delta_\sigma)$. This results in

$$(\rho^{\otimes 2} | Y_\sigma T_\sigma^+ \widehat{\phi\nu}[\omega_\sigma^{(2)}]^m (Y_\sigma^\dagger \tilde{M}_3) | \tilde{\rho}) = \text{tr}[C_\sigma I_\sigma^m] + \text{tr}[D_\sigma O_\sigma^m],$$

where $I_\sigma \in \mathbb{R}^{n_\sigma \times n_\sigma}$ with n_σ the multiplicity of τ_σ in ω and $C_\sigma = L_{\lambda,1}^\dagger \text{tr}_{m_\sigma}(|\tilde{M}_{3,\sigma}\rangle \langle Q_{3,\sigma}|) R_{\lambda,1}$ and $D_\sigma = L_{\lambda,2}^\dagger \text{tr}_\sigma(|\tilde{M}_{3,\sigma}\rangle \langle Q_{3,\sigma}|) R_{\lambda,2}$. Using $R_{\lambda,1} L_{\lambda,1}^\dagger = \widehat{\omega}[\tau_\sigma]$, we find in particular that

$$\text{tr}(C_\sigma) = \text{tr}(|\tilde{M}_{3,\sigma}\rangle \langle Q_{3,\sigma}| \widehat{\omega}[\tau_\sigma] \otimes \text{id}_{m_\sigma}) = (\rho^{\otimes 2} | Y_\sigma T_\sigma^+ \widehat{\omega}[\omega_\sigma^{(2)}] (Y_\sigma^\dagger \tilde{M}_3) | \tilde{\rho}). \quad (46)$$

Moreover, we have the following bound:

$$|\text{tr}(D_\sigma O_\sigma^m)| \leq g(\delta_\sigma/\Delta_\sigma) \|Y_\sigma^\dagger \tilde{M}_3\|_2 \|T_\sigma^+ Y_\sigma | \rho^{\otimes 2} \rangle (\tilde{\rho})\|_2 \|O_\sigma\|_\infty^m. \quad (47)$$

Finally, we derive the claimed bound on the sum $\sum_{\sigma \in \text{Irr}(\tau_\lambda^{\otimes 2})} \text{tr}(D_\sigma O_\sigma^m)$. To this end, we use Eqs. (45) and (47) for $\sigma \notin \text{Irr}(\omega)$ and $\sigma \in \text{Irr}(\omega)$, respectively. The bounds are almost identical, except for the appearance of the factor $g(\delta_\sigma/\Delta_\sigma)$ in Eq. (47). However, $g(x) \geq 1$ for all $x \geq 0$, hence the prefactor is uniformly bounded by

$$\max_{\sigma \in \text{Irr}(\tau_\lambda^{\otimes 2}) \cap \text{Irr}(\omega)} g(\delta_\sigma/\Delta_\sigma) = g\left(\max_{\sigma \in \text{Irr}(\tau_\lambda^{\otimes 2}) \cap \text{Irr}(\omega)} \delta_\sigma/\Delta_\sigma\right) \leq g\left(\max_{\sigma \in \text{Irr}(\tau_\lambda^{\otimes 2})} \delta_\sigma/\Delta_\sigma\right) = g(r_\lambda^{(3)}),$$

where we additionally used the monotonicity of g . Furthermore, we find the uniform bounds:

$$\begin{aligned} \|T_\sigma^+ Y_\sigma |\rho^{\otimes 2}\rangle(\tilde{\rho})\|_2 &\leq \|T_\sigma^+\|_\infty \sqrt{(\rho^{\otimes 2} | P_\sigma | \rho^{\otimes 2})} \leq \|S_\lambda^+\|_\infty^2 (\rho | P_\lambda | \rho), \\ \max_{\sigma \in \text{Irr}(\tau_\lambda^{\otimes 2})} \|O_\sigma\|_\infty &\leq 1 - \min_{\sigma \in \text{Irr}(\tau_\lambda^{\otimes 2})} \Delta_\sigma \left(1 - 2 \frac{\delta_\sigma}{\Delta_\sigma}\right) \leq 1 - \Delta_\lambda^{(3)} (1 - 2r_\lambda^{(3)}). \end{aligned}$$

Next, we compute, using the concavity of the square root:

$$\begin{aligned} \sum_{\sigma \in \text{Irr}(\tau_\lambda^{\otimes 2})} \|Y_\sigma^\dagger \tilde{M}_3\|_2 &= \sum_{\sigma \in \text{Irr}(\tau_\lambda^{\otimes 2})} \sqrt{\text{tr}(P_\sigma M_3 \mathcal{E}_M^\dagger M_3^\dagger)} \\ &\leq \left(\sum_{\sigma \in \text{Irr}(\tau_\lambda^{\otimes 2})} \sum_{i,j \in [d]} (E_i | \mathcal{E}_M^\dagger | E_j)(E_j \otimes E_j | P_\sigma | E_i \otimes E_i) \right)^{\frac{1}{2}} \\ &= \left(\sum_{i,j \in [d]} (E_i | \mathcal{E}_M^\dagger | E_j)(E_j | P_\lambda | E_i)^2 \right)^{\frac{1}{2}} \\ &\leq \|X_\lambda^\dagger \tilde{M}\|_2. \end{aligned}$$

Here, we have used $\sum_\sigma P_\sigma = P_\lambda^{\otimes 2}$, $(E_i | \mathcal{E}_M^\dagger | E_j) \geq 0$ since \mathcal{E}_M and \mathcal{E}_M^\dagger are completely positive, $(E_i | P_\lambda | E_j)^2 \leq (E_i | P_\lambda | E_j)$, and inserted the expansion as in Eq. (33). Hence, we can use the appropriate bounds from the proof of Thm. 8 for this sum.

Using the definition of c_λ from Thm. 8 and combining the above bounds, we then find the claimed bound:

$$\left| \sum_{\sigma \in \text{Irr}(\tau_\lambda^{\otimes 2})} \text{tr}(D_\sigma O_\sigma^m) \right| \leq c_\lambda \|S_\lambda^+\|_\infty (\rho | P_\lambda | \rho) g(r_\lambda^{(3)}) \left(1 - \Delta_\lambda^{(3)} (1 - 2r_\lambda^{(3)})\right)^m.$$

5.4.4 Sampling complexity of filtering onto trivial irrep

Here, things are slightly simpler: The filter function takes only the values 0 and 1, and hence Hoeffding's inequality guarantees sample efficiency.

5.5 Sufficient sequence lengths

One of the main implications of Theorem 8 is that we can control the ratio between the dominant signal and the subdominant signal in (S). The dominant decays are generally superimposed with “subdominant decays”. Since those are suppressed according to (B) with increasing sequence length m , it is sufficient to choose m large enough to be able to accurately extract the decay parameters with (the isotropic action on) the irreducible representations. In Sec. 5.5.1, we derive and discuss a corresponding lower bound on the sequence length. Let us stress that using too short sequences may involve the danger of *overestimating decay rates* and thus – if interpreted as average gate fidelities – of reporting *too large gate fidelities*. Similar concerns have already been raised in the non-uniform RB literature [17, 21].

We focus here on generally applicable bounds. In particular, we do not make use of any details about the noise in the implementation map, the measure, or even the representation theory of the

group G . We expect that for specific settings, a more refined analysis using more assumptions on the noise and a specific measure and group yield improved the bounds.

Furthermore, the required relative suppression might be relaxed using a more sophisticated data processing. The suitability and limitations of methods like ESPRIT [85] for randomized benchmarking has been previously discussed in Ref. [9]. Note however that the performance of these methods also crucially depend on the separation of poles on the real axis and the total number of poles. We leave the study of their applicability to future work.

In Sec. 5.6, we then proceed by motivating that the bounds derived in Thm. 8 can probably not be substantially improved. To this end, we show that even the noise-free RB signal for common random circuits decays as predicted by Thm. 8.

5.5.1 Exposing the dominant signal

For the extraction of decay parameters, it is certainly sufficient that the subdominant decays are small. If the desired suppression is α , then the suppression bound in Theorem 8 yields the following lower bound on the sequence length m of the RB experiment:

$$m \geq \frac{\log(c_\lambda) + \frac{1}{2} \log((\rho | P_\lambda | \rho)) + \log(g(\delta_\lambda / \Delta_\lambda)) + \log(1/\alpha)}{\log(1/(1 - \Delta_\lambda + 2\delta_\lambda))}. \quad (48)$$

The right hand side of Eq. (48) depends heavily on the group G and the irrep τ_λ on which we filter, on the spectral gap Δ_λ , as well as the SPAM noise and implementation error δ .

The bound (48) only guarantees the suppression by an *additive error* α which is fine as long as $F_\lambda(m) = O(1)$. However, this is not the case for two reasons. First, $F_\lambda(m)$ can be (exponentially) small for small irreps, as it ideally measures the overlap of the initial state with the irrep. Second, $F_\lambda(m)$ decays with m and thus the error should decrease with m , too. Hence, a sensible solution is to require that the subdominant terms are instead suppressed by a *relative error* γ . The derivation of an analogous bound to (48) is postponed to the proof of the following Lemma.

Lemma 18 (Sequence length bounds for extraction of decay parameters). *For any non-trivial irrep $\lambda \in \text{Irr}(\omega)$, the subdominant decay in Thm. 8 is bounded by $\alpha > 0$ provided that*

$$m \geq \Delta_\lambda^{-1} \left(1 - 2 \frac{\delta_\lambda}{\Delta_\lambda}\right)^{-1} \left(\log(c_\lambda) + \frac{1}{2} \log[(\rho | P_\lambda | \rho)] + \log[g(\delta_\lambda / \Delta_\lambda)] + \log(1/\alpha)\right). \quad (49)$$

Moreover, if λ is multiplicity-free, the subdominant decay is smaller than $\gamma |\text{tr}(A_\lambda I_\lambda^m)|$ for $\gamma > 0$ provided that

$$m \geq \Delta_\lambda^{-1} \left(1 - 4 \frac{\delta_\lambda}{\Delta_\lambda}\right)^{-1} \times \left(\log(c_\lambda) + \frac{1}{2} \log[(\rho | P_\lambda | \rho)] + \log[g(\delta_\lambda / \Delta_\lambda)] + \log(1/|F_\lambda(m)_{\text{SPAM}}|) + \log(1/\gamma)\right). \quad (50)$$

Here, $F_\lambda(m)_{\text{SPAM}}$ denotes again the filtered RB signal that one would obtain for perfect unitaries sampled from the Haar measure on G , but subject to SPAM noise.

Proof. The first result follows directly by using the bound $\log(1+x) \leq x$ for $x > -1$ in Eq. (48). Next, let us assume that λ is multiplicity-free. Then, we can rewrite the first term in $F_\lambda(m)$ using Thm. 8 and Eq. (29) as follows:

$$|\text{tr}(A_\lambda I_\lambda^m)| = |F_\lambda(m)_{\text{SPAM}}| I_\lambda^m > |F_\lambda(m)_{\text{SPAM}}| (1 - 2\delta_\lambda)^m.$$

We then find the following bound for the relative suppression:

$$\frac{|F_\lambda(m) - \text{tr}(A_\lambda I_\lambda^m)|}{|\text{tr}(A_\lambda I_\lambda^m)|} < \frac{c_\lambda \sqrt{(\rho | P_\lambda | \rho)} g(\delta_\lambda / \Delta_\lambda)}{|F_\lambda(m)_{\text{SPAM}}|} \left(\frac{1 - \Delta_\lambda + 2\delta_\lambda}{1 - 2\delta_\lambda}\right)^m. \quad (51)$$

We use the following inequality which is valid for all $\delta_\lambda/\Delta_\lambda \in [0, 1/4]$ and $\Delta \in [0, 1)$:

$$\log\left(\frac{1 - \Delta_\lambda + 2\delta_\lambda}{1 - 2\delta_\lambda}\right) \leq \log(1 - \Delta_\lambda) \left(1 - 4\frac{\delta_\lambda}{\Delta_\lambda}\right) \leq -\left(1 - 4\frac{\delta_\lambda}{\Delta_\lambda}\right) \Delta_\lambda. \quad (52)$$

The first inequality follows since the left hand side is strictly monotonically increasing in δ_λ for any $\Delta_\lambda \in [0, 1)$. Thus, it is a convex function which is upper bounded in the interval $[0, \Delta_\lambda/4]$ by a straight line. Requiring that Eq. (51) is less than $\gamma > 0$, and using Eq. (52) yields the claimed bound on m . \square

We proceed by discussing the individual contributions to the bounds in Lem. 18. In general, we conjecture that $\|S_\lambda^+\|_\infty = O(\text{poly}(d_\lambda))$ such that we have $\log c_\lambda = O(\log(d_\lambda))$. Hence, we expect that the sequence length scales at least with $\log(d_\lambda)$ in the worst case. By again specializing λ to be multiplicity-free and aligned with M , we can make this more precise: By Eqs. (25) and (26), we have $d_\lambda \leq d_\lambda/s_\lambda \leq d_\lambda^2$, hence we find $\log(c_\lambda) = \frac{1}{2} \log(d_\lambda/s_\lambda) = \Theta(\log d_\lambda)$. Furthermore, we have $\delta_\lambda/\Delta_\lambda < 1/4$ in the perturbative regime, and hence the prefactor in Eq. (49) cannot exceed $2/\Delta_\lambda$. As discussed in Sec. 5.3.1, $g(x)$ diverges for $x \rightarrow \infty$, and we thus have to assume that the implementation error is actually bounded away from $1/4$, say $\delta_\lambda/\Delta_\lambda \leq 1/5$ such that $\log g(1/5) \approx 1.798 \leq 1.8$. Under this assumption, we can also bound the otherwise diverging prefactor in Eq. (50) as $5/\Delta_\lambda$. Finally, the contribution by $(\rho|P_\lambda|\rho) \leq 1$ is negative and may counter the effect of $\log(d_\lambda)$ in certain regimes. Under the above assumptions, we can then bring Eq. (49) into the simplified form

$$m \geq \frac{2}{\Delta_\lambda} \left(\log(d_\lambda) + \frac{1}{2} \log(\rho|P_\lambda|\rho) + \log(1/\alpha) + 1.8 \right). \quad (53)$$

The same simplification applies to the relative error bound (50). In this case, we have to additionally bound the term depending on $F_\lambda(m)_{\text{SPAM}}$. Assuming that $[P_\lambda, M] = 0$, we can rewrite $F_\lambda(m)_{\text{SPAM}} = v_{\text{SP}} v_M (\rho|P_\lambda|\rho)$ in terms of the SPAM visibilities introduced in Section 5.3.2. We arrive at the bound (assuming $\delta_\lambda/\Delta_\lambda \leq 1/5$):

$$m \geq \frac{5}{\Delta_\lambda} \left(\log(d_\lambda) + \frac{1}{2} \log((\rho|P_\lambda|\rho)^{-1}) + \log(1/\gamma) + \log(1/v_{\text{SP}} v_M) + 1.8 \right). \quad (54)$$

This bound is almost identical to the additive error bound (53), however, it also depends on the amount of SPAM noise relative to the ideal coefficients. This is unavoidable since the SPAM noise typically decreases the strength of the signal as discussed in Section 5.3.2. For example, for depolarizing SPAM noise of strength $1 - p$ we found that $F_\lambda(m)_{\text{SPAM}}$ is suppressed by p^2 . Accordingly, we find a contribution of $2\log(1/p)$ to the sequence length (54) in this situation.

Finally, an important contribution to both bounds (53) and (54) is the inverse spectral gap. For fast-scrambling random circuits, like brickwork circuits, we have $\Delta^{-1} = O(1)$, i.e. the spectral gap is independent of the dimension $d = 2^n$. In this setting, we also have $\log(d_{\text{ad}}) = O(n)$, and thus the sequence length of filtered RB requires *linear circuit depth*. We comment on this in more detail for various random circuits in Sec. 5.7, and give precise scalings with small constants.

However, the scaling depends on both d_λ and Δ_λ^{-1} , allowing for scenarios with even shorter circuit depth for smaller irrep dimensions. For instance, we have $d_\lambda = 1$ for the Heisenberg-Weyl group $\text{HW}_n(p)$, and many irreps of the local Clifford group have sub-exponential dimension. Since these are both local groups, it is also straightforward to obtain large spectral gaps.

5.5.2 Obtaining sampling complexity bounds

As in Sec. 5.5.1, we study the suppression of the subdominant decays in Thm. 10. Our goal is to derive sufficient conditions on the sequence length m under which the assumptions of our sampling complexity theorems 16 and 17 are fulfilled. To this end, the following lemma gives a sufficient condition for the sequence length m in terms of the spectral gap $\Delta_\lambda^{(3)}$, and irrep-specific quantities.

Lemma 19. *The sum of subdominant decays in Thm. 10 is less than $\beta > 0$ provided that*

$$m \geq \frac{1}{\Delta_\lambda^{(3)}} \left(1 - 2r_\lambda^{(3)}\right)^{-1} \left(\log(c_\lambda \|S_\lambda^+\|_\infty) + \log((\rho|P_\lambda|\rho)) + \log(g(r_\lambda^{(3)})) + \log(1/\beta) \right). \quad (55)$$

Proof. The statement follows in complete analogy to the proof of Lem. 18. \square

As for Lemma 18, we expect that the term $\log(c_\lambda \|S_\lambda^+\|_\infty)$ generally scales as $O(\log(d_\lambda))$, however now with a larger prefactor. If $\lambda \in \text{Irr}(\omega)$ is multiplicity-free and $[P_\lambda, M] = 0$, we can use $s_\lambda^{-1} \leq d_\lambda$, c.f. Eq. (26), to obtain $\log(c_\lambda \|S_\lambda^+\|_\infty) = \frac{1}{2} \log(d_\lambda/s_\lambda^3) \leq 2\log(d_\lambda)$. As in Sec. 5.5.1, we want to assume that the implementation error is bounded away from 1/4, say $\delta_\sigma/\Delta_\sigma \leq 1/5$ for all σ , such that we have $r_\lambda^{(3)} \leq 1/5$ and $g(r_\lambda^{(3)}) \leq 1.8$. Then, we can bring Eq. (55) into the more appealing form

$$m \geq \frac{2}{\Delta_\lambda^{(3)}} \left(2\log(d_\lambda) + \log((\rho|P_\lambda|\rho)) + \log(1/\beta) + 1.8 \right).$$

Next, we want to derive a sequence length bound involving relative errors. Compared to Lem. 18, the proof is slightly more delicate since we compare the subdominant decays with the sum of dominant ones $\sum_\sigma \text{tr}(C_\sigma I_\sigma^m)$. Finding a good lower bound for this sum is made difficult by the fact that some of the individual terms may a priori be negative, c.f. the discussion in Sec. 5.4.1. We do not think that this happens in any practically relevant scenario, but include this as an assumption in the following lemma.

Lemma 20. *Assume non-malicious SPAM noise and fix a non-trivial irrep $\lambda \in \text{Irr}(\omega)$ such that all $\sigma \in \text{Irr}(\omega) \cap \text{Irr}(\tau_\lambda^{\otimes 2})$ are multiplicity-free in ω . Then, the sum of subdominant decays in Thm. 10 is suppressed by a relative error $\kappa > 0$ compared to the dominant decays, provided that*

$$m \geq \frac{1}{\Delta_\lambda^{(3)}} \left(1 - 4 \frac{\delta_\lambda^{(3)}}{\Delta_\lambda^{(3)}} \right)^{-1} \times \left(\log(c_\lambda/s_\lambda) + \log((\rho|P_\lambda|\rho)) + \log(g(\delta_\lambda^{(3)}/\Delta_\lambda^{(3)})) + \log(1/\mathbb{E}[f_\lambda^2]_{\text{SPAM}}) + \log(1/\kappa) \right).$$

Here, $\mathbb{E}[f_\lambda^2]_{\text{SPAM}}$ is the second moment of the filter function that one would obtain for the ideal, noiseless implementation $\phi = \omega$ where unitaries are sampled from the Haar measure on G , but subject to SPAM noise, c.f. Eq. (39).

Proof. We use $r_\lambda^{(3)} \leq \delta_\lambda^{(3)}/\Delta_\lambda^{(3)}$ where $\delta_\lambda^{(3)} := \max_\sigma \delta_\sigma$, c.f. Sec. 5.4.1, and $I_\sigma \geq 1 - 2\delta_\sigma \geq 1 - 2\delta_\lambda^{(3)}$. We then have

$$\frac{\left| \sum_{\sigma \in \text{Irr}(\tau_\lambda^{\otimes 2})} \text{tr}(D_\sigma O_\sigma^m) \right|}{\sum_{\sigma \in \text{Irr}(\tau_\lambda^{\otimes 2})} \text{tr}(C_\sigma) I_\sigma^m} \leq \frac{c_\lambda/s_\lambda (\rho|P_\lambda|\rho) g(\delta_\lambda^{(3)}/\Delta_\lambda^{(3)})}{\mathbb{E}[f_\lambda^2]_{\text{SPAM}}} \left(\frac{1 - \Delta_\lambda^{(3)} + 2\delta_\lambda^{(3)}}{1 - 2\delta_\lambda^{(3)}} \right)^m.$$

The statement then follows as in the proof of Lem. 18. \square

As for Lem. 19, assuming that $\delta_\lambda^{(3)}/\Delta_\lambda^{(3)} \leq 1/5$ and $[P_\lambda, M] = 0$, it is sufficient to fulfill the simplified bound

$$\begin{aligned} m &\geq \frac{5}{\Delta_\lambda^{(3)}} \left(2\log(d_\lambda) + \log((\rho|P_\lambda|\rho)) + \log(1/\mathbb{E}[f_\lambda^2]_{\text{SPAM}}) + \log(1/\kappa) + 1.8 \right) \\ &= \frac{5}{\Delta_\lambda^{(3)}} \left(2\log(d_\lambda) + \log((\rho|P_\lambda|\rho)) + \log(1/\mathbb{E}[f_\lambda^2]_{\text{ideal}}) + \log(1/v_{\text{SPAM}}^{(2)}) + \log(1/\kappa) + 1.8 \right). \end{aligned} \quad (56)$$

Hence, we have a similar situation as in Eq. (54). In Sec. 5.4.1, we showed that for weak depolarizing SPAM noise with strength $1 - p$, $v_{\text{SPAM}}^{(2)} \approx p^2$ and thus find the same SPAM noise dependence as in the previous Sec. 5.5.1. We have a more detailed comparison between Eq. (54) and Eq. (56) in the following.

To fulfill the assumptions of our sampling complexity Theorem 17, the sequence length m has to be sufficiently large such that the subdominant terms in the first and second moment are suppressed by relative errors γ and κ . By Lemmas 18 and 20, it is sufficient to choose m as follows

$$m \geq \frac{5}{\Delta_\lambda} \left(\log(d_\lambda) + \frac{1}{2} \log((\rho|P_\lambda|\rho)) + \log(1/F_\lambda(m)_{\text{SPAM}}) + \log(1/\gamma) + 1.8 \right), \quad (57)$$

$$m \geq \frac{5}{\Delta_\lambda^{(3)}} \left(2\log(d_\lambda) + \log((\rho|P_\lambda|\rho)) + \log(1/\mathbb{E}[f_\lambda^2]_{\text{SPAM}}) + \log(1/\kappa) + 1.8 \right). \quad (58)$$

Note that in contrast to Sec. 5.5.1, where the goal was to reliably find the dominant decay parameter, we do not require κ to be small. In principle, it is enough if $\kappa = O(1)$, for instance $\kappa = 1$ would be sufficient. In practice, κ enters linearly in the required number of samples by Thm. 17, but only logarithmically in Eq. (58). Hence, one would try to choose it as small as possible, finding a compromise between number of samples and sequence length.

In general, it is not simple to answer which of the lower bounds (57) and (58) is larger. Typically, we expect that the second bound implies the first one for the following reasons: First, we typically have $\Delta_\lambda^{(3)} \leq \Delta_\lambda$ with equality in many practically relevant cases, see Sec. 5.7. Second, the first two terms in Eq. (58) are twice as large as in Eq. (57). However, the comparison between $F_\lambda(m)_{\text{SPAM}}$ and $\mathbb{E}[f_\lambda^2]_{\text{SPAM}}$ is not as simple. In Prop. 13, we saw examples in which either the first or second moment are larger.

5.5.3 Examples

To be able to make more concrete statements, we specialize to our examples from Sec. 5.2, namely unitary 3-groups, local unitary 3-groups, and the Heisenberg-Weyl group. Recall that for these examples, we have $F_\lambda(m)_{\text{SPAM}} = v_M v_{\text{SP}}(\rho | P_\lambda | \rho)$. If relevant, we assume that the SPAM visibilities are such that $v_{\text{SPAM}}^{(2)} \approx v_M v_{\text{SP}}$ (which is e.g. the case for depolarizing SPAM noise). To achieve tighter bounds, we use the exact values of s_λ and c_λ which we computed in Secs. 5.2 and 5.3.3, instead of the generic upper bounds used before. Thus, we replace the first term in Eqs. (57) and (58) with $\log(c_\lambda)$ and $\log(c_\lambda/s_\lambda)$, respectively, as given in Lems. 18 and 20.

Unitary 3-designs. Suppose G is a unitary 3-design and $d = 2^n$ (i.e. a n -qubit system). Then, we have $c_{\text{ad}} = (d+1)\sqrt{d-1}$ and $c_{\text{ad}}/s_{\text{ad}} = (d+1)^2\sqrt{d-1}$, as well as $(\rho | P_{\text{ad}} | \rho) = (d-1)/d$. To achieve additive error suppression, Lems. 18 and 19 require us to compute the following expressions:

$$\begin{aligned} \log(c_{\text{ad}}) + \frac{1}{2} \log(\rho | P_{\text{ad}} | \rho) &= \log \frac{d^2 - 1}{\sqrt{d}}, \\ \log(c_{\text{ad}}/s_{\text{ad}}) + \log((\rho | P_{\text{ad}} | \rho)) &= \log \frac{\sqrt{d-1}(d^2 - 1)(d+1)}{d}. \end{aligned} \quad (59)$$

Thus, the second expression is always larger than the first, and assuming that the error in Lemma 18 and 19 are chosen as $\alpha \geq \beta$, we find that the following bound on m is sufficient for the assumptions of Thm. 16:

$$m \geq \frac{2}{\Delta_{\text{ad}}^{(3)}} (1.75n + \log(1/\alpha) + 1.8), \quad (\text{additive error}) \quad (60)$$

where we assumed that $d = 2^n$ and used that $\log \frac{\sqrt{d-1}(d^2-1)(d+1)}{d} \leq 1.75n$ for all $n \in \mathbb{N}$.

For relative error suppression by Lems. 18 and 20, we use the exact expression for the second moment, computed in App. C.1, Eq. (103). After a short calculation, we find the expressions

$$\begin{aligned} \log(c_{\text{ad}}) + \frac{1}{2} \log(\rho | P_{\text{ad}} | \rho) + \log(1/F_{\text{ad}}(m)_{\text{ideal}}) &= \log(\sqrt{d}(d+1)), \\ \log(c_{\text{ad}}/s_{\text{ad}}) + \log((\rho | P_{\text{ad}} | \rho)) + \log(1/\mathbb{E}[f_{\text{ad}}^2]_{\text{ideal}}) &= \log \frac{\sqrt{d-1}d(d+1)(d+2)}{3d-2}. \end{aligned}$$

Again, the second expression is always larger than the first. Assuming $\gamma \leq \kappa$, we hence find that it is sufficient for m to fulfill the bound

$$m \geq \frac{5}{\Delta_{\text{ad}}^{(3)}} (1.75n + \log(1/v_M v_{\text{SP}}) + \log(1/\gamma) + 1.8). \quad (\text{relative error})$$

Here, we again used that for $d = 2^n$ and $n \geq 2$, $\log \frac{\sqrt{d-1}d(d+1)(d+2)}{3d-2} \leq 1.75n$.

Local unitary 3-designs. Next, let us assume that G is a local unitary 3-design with local (prime) dimension p . Recall from Sec. 5.2 that the irreps are labelled by $b \in \{0, 1\}^n$ where $b_i = 0$ and $b_i = 1$ mean that we have the adjoint or trivial irrep on the i -th tensor factor, respectively. Moreover, $|b|$ is the Hamming weight of b and $|\bar{b}| = n - |b|$. Then, we have $c_b = [(p+1)\sqrt{p-1}]^{|\bar{b}|}$, $c_b/s_b = [(p+1)^2\sqrt{p-1}]^{|\bar{b}|}$, and $(\rho|P_b|\rho) = [(p-1)/p]^{|\bar{b}|} 1/p^{|b|}$ for pure product states ρ . Hence:

$$\log(c_b) + \frac{1}{2} \log(\rho|P_b|\rho) = |\bar{b}| \log(p^2 - 1) - \frac{n}{2} \log p, \quad (61)$$

$$\log(c_b/s_b) + \log((\rho|P_b|\rho)) = |\bar{b}| \log\left(\sqrt{p-1}(p+1)(p^2-1)\right) - n \log p. \quad (62)$$

For any p , we find a value of $|\bar{b}|/n$, namely $x := \log(p)/2 \log(\sqrt{p-1}(p+1))$, such that Eq. (61) is larger if $|\bar{b}|/n \leq x$, and otherwise smaller than Eq. (62). For instance, if $p = 2$ this is $x = \log(2)/2 \log(3) \approx 0.315$. The case $p = 2$ is also somewhat degenerate as then Eq. (62) is exactly twice Eq. (61), and more importantly, both expressions are negative for $|\bar{b}|/n \leq x$. Hence, in this regime, the irrep-dependent term *reduces* the sequence length. In summary, we can write the sequence length bound for $p = 2$ as

$$m \geq \frac{2}{\Delta_b^{(3)}} \left(\left(\frac{|\bar{b}|}{n} \log(3) - \frac{\log(2)}{2} \right) (1 + \delta_{|\bar{b}| > xn}) n + \log(1/\alpha) + 1.8 \right). \quad (\text{additive error})$$

As before, relative error suppression requires us to compute

$$\log(c_b) + \frac{1}{2} \log(\rho|P_b|\rho) + \log(1/F_b(m)_{\text{ideal}}) = |\bar{b}| \log(\sqrt{p}(p+1)) + \frac{|b|}{2} \log p, \quad (63)$$

$$\log(c_b/s_b) + \log((\rho|P_b|\rho)) + \log(1/\mathbb{E}[f_b^2]_{\text{ideal}}) = |\bar{b}| \log \frac{\sqrt{p-1}p(p+1)(p+2)}{3p-2} + n \log p, \quad (64)$$

where we used the expression for the ideal second moment, c.f. Eq. (109), in the second equation. Here, a detailed analysis reveals that Eq. (64) is always larger than Eq. (63), irrespective of the value of p , n , and $|b|$. Using the upper bound $2.6|\bar{b}| \log p$ for the first term in Eq. (64), we find the following bound for m :

$$m \geq \frac{5}{\Delta_b^{(3)}} ((2.6|\bar{b}| + n) \log p + \log(1/v_M v_{\text{SP}}) + \log(1/\gamma) + 1.8). \quad (\text{relative error})$$

Heisenberg-Weyl group. Finally, if $G = \text{HW}_n(p)$ is the Heisenberg-Weyl group, we have $c_{0,z} = s_{0,z} = 1$, $F_{0,z}(m)_{\text{ideal}} = (\rho|P_{0,z}|\rho) = 1/d$, and $\mathbb{E}[f_{0,z}^2]_{\text{ideal}} = 1/d^2$, hence the irrep-dependent terms in bounds of Lems. 19 and 20 are exactly twice as large as in Lemma 18. Thus it is sufficient for m to fulfill

$$m \geq \frac{2}{\Delta_{0,z}^{(3)}} (-\log d + \log(1/\alpha) + 1.8), \quad (\text{additive error})$$

$$m \geq \frac{5}{\Delta_{0,z}^{(3)}} (\log d + \log(1/v_M v_{\text{SP}}) + \log(1/\gamma) + 1.8). \quad (\text{relative error})$$

5.6 Comparison of bounds to typical random circuit decays

One might wonder whether the upper bounds derived in Thms. 8 and 10 are tight, and if not, how loose they are. A potential leeway in these bounds directly results in sub-optimal lower bounds on the sufficient sequence lengths in Sec. 5.5. To this end, we numerically compute $F_{\text{ad}}(m)$ for a random circuit. Importantly, the characteristic of the decay is already evident in the absence of noise. In particular, the decay associated with the converging random circuit is severely overlaying the actual signal, leading to contributions as predicted by Thm. 8.

A more detailed numerical analysis for linear XEB with different random Clifford circuits was recently presented by Chen, Ding, Huang, and Kong [25], for up to 1225 qubits and different noise models. Since this is a special case of our filtered RB protocol, it nicely shows a typical behavior

of the filtered RB signal. The findings in Ref. [25] for these examples are qualitatively similar to the following discussion (even though much more detailed), and in agreement with the scaling of the bound in Thm. 8.

Here, we consider a *local random circuit* where each layer is obtained by uniformly drawing a pair of qubits $(i, i + 1)$ and applying a Haar-random unitary $U \in \text{U}(4)$ to this pair. Formally, this is described by the following probability measure on $G = \text{U}(2^n)$ (here with “open boundary conditions”):

$$\nu := \frac{1}{n-1} \sum_{i=1}^{n-1} \mu_{(i, i+1)},$$

where $\mu_{(i, i+1)}$ is the local Haar measure on the pair $(i, i + 1)$. Local random circuits form approximate unitary t -designs with an inverse spectral gap $\Delta_t^{-1} = O(\text{poly}(t), n)$, c.f. Sec. 5.7 for more details. In particular, ν^{*m} converges to the Haar measure on $\text{U}(2^n)$ for in the limit $m \rightarrow \infty$ and hence we obtain the ideal signal as

$$\lim_{m \rightarrow \infty} F_{\text{ad}}(m) = (\rho | P_{\text{ad}} | \rho) = 1 - \frac{1}{d}.$$

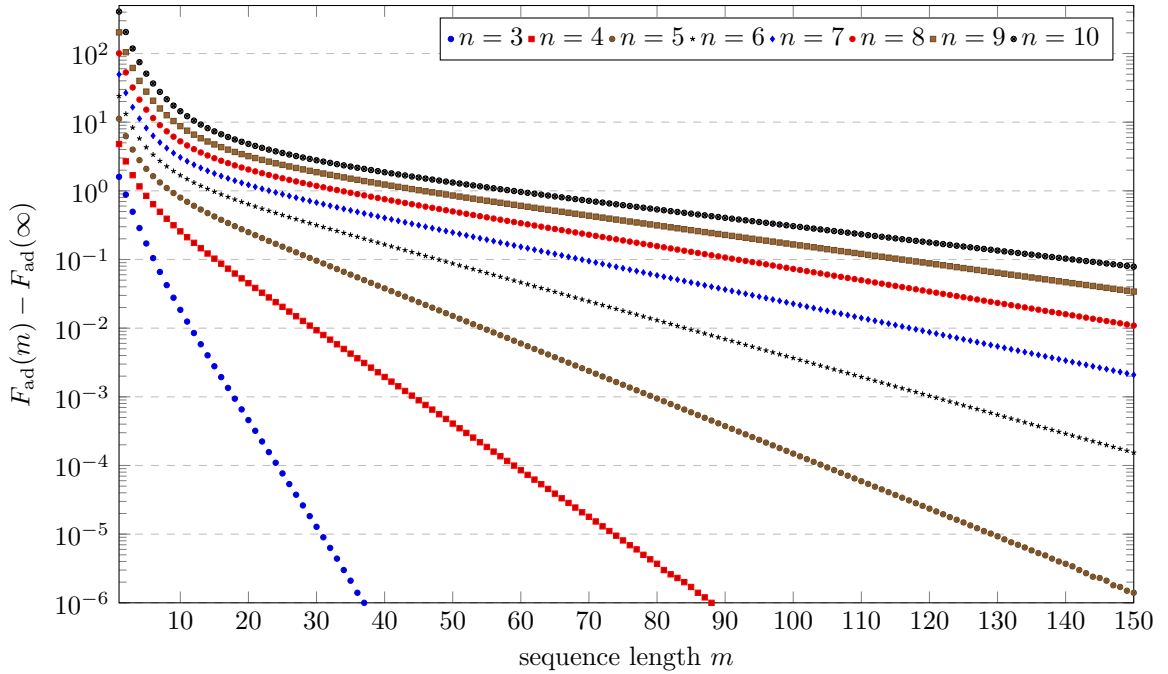


Figure 1: Decay of the contribution to the filtered RB signal $F_{\text{ad}}(m)$ stemming from the use of a random circuit instead of an exact unitary 2-design. The data has been computed numerically for $n = 3, \dots, 10$ qubits using a local random circuit with Haar-random 2-local unitaries in the noise-free setting. The decay is quickly dominated by a single exponential decay given by the second largest eigenvalue $(1 - \Delta)$ of the second moment operator, and thus in good agreement with the bound of Thm. 8. The fast decay in the beginning can be contributed to a superposition of exponential decays associated with smaller eigenvalues. To be able to observe the additional RB decay in the presence of noise, the RB decay must be slower than the ‘mixing decay’ shown here. This is exactly quantified by the condition (A) in Thm. 8.

We have numerically computed the filtered RB signal $F_{\text{ad}}(m)$ for local random circuits on $n = 3, \dots, 10$ qubits and sequence lengths $m = 1, \dots, 150$. To analyze the subdominant contributions to the signal coming from the use of the random circuit in the sense of Thm. 8, we have subtracted the asymptotic value $1 - \frac{1}{d}$ from the data. The difference is shown in Fig. 1. Since we deal with the noise-free case, the signal is given as a linear combination of exponential decays with decay rates corresponding to the eigenvalues of the second moment operator $\mathbf{M}_2(\nu) = \widehat{\omega\nu}[\omega]$ that are smaller than one. Consequently, we can observe two regimes: For small m , all eigenvalues decay quickly except for the second largest one which then dominates the signal for larger values of m .

Indeed, we find that the latter regime is well-approximated by a single exponential decay. Corresponding fits give decay rates that are in very good agreement with the theoretical expectation $(1 - \Delta_2)$ from Thm. 8 (up to relative errors $\leq 10^{-4}$). To this end, we have compared the fit parameters with the numerically obtained spectral gaps Δ_2 of the second moment operator $M_2(\nu)$. Next, we want to compare the magnitude of the subdominant contribution as a function of m with the prediction by Lem. 18. Since we are dealing with the noise-free case, we have $\delta_{\text{ad}} = 0$ and hence find using Eq. (59) that we should take $m \geq \Delta_2^{-1}(\log((d^2 - 1)/\sqrt{d}) + \log(1/\alpha))$ to achieve an additive error $\alpha > 0$. Since $\Delta_2^{-1} \sim 5n$ (see Sec. 5.7) and $\log((d^2 - 1)/\sqrt{d}) \approx 1.05n$, we expect a quadratic dependence on $n = \log_2(d)$. Numerically, we find that the subdominant contribution already falls below a fixed additive error for values of m that are up to nine times smaller than our bound. If we use the exact values for Δ_2^{-1} instead of the asymptotic value $5n$, our bound is only about two times larger. Moreover, our data is compatible with the quadratic dependence on n .

The reason for the sub-optimality of our bound is that it is valid for all m , and thus includes the fast scrambling regime for small m . On the logarithmic scale of Fig. 1, the bound thus corresponds to a shift of the dominant exponential decays in the vertical direction. Nevertheless, the prefactor of the bound in Thm. 8 is still too large when compare with our numerical data: Eq. (B) results in a prefactor $c_{\text{ad}} \sqrt{(\rho | P_{\text{ad}} | \rho)} = (d^2 - 1)/\sqrt{d}$, while it is straightforward to compute $F_{\text{ad}}(1)$, the maximum value of the signal. Indeed, assuming that the initial state ρ is a computational basis state, say $\rho = |0\rangle\langle 0|^{\otimes n}$, and that we measure in the computational basis, we find using $M = M_{\text{loc}}^{\otimes n}$ that

$$\widehat{\omega}_{\mu_{(i,i+1)}}[\omega](M) = M_{\text{loc}}^{\otimes i-1} \otimes S_{\text{loc}} \otimes M_{\text{loc}}^{\otimes n-i-1},$$

where $S_{\text{loc}} = \widehat{\omega}[\omega](M_{\text{loc}}^{\otimes 2})$ is the frame operator on 2 qubits, cp. Eq. (24). We arrive at the following expression:

$$\begin{aligned} F_{\text{ad}}(1) &= \frac{d+1}{n-1} \sum_{i=1}^{n-1} (\rho | P_{\text{ad}} \widehat{\omega}_{\mu_{(i,i+1)}}[\omega](M) | \rho) \\ &= (d+1) \left[\text{tr}(|0\rangle\langle 0| M_{\text{loc}}(|0\rangle\langle 0|))^{n-2} \text{tr}(|0\rangle\langle 0|^{\otimes 2} S_{\text{loc}}(|0\rangle\langle 0|^{\otimes 2})) - \frac{1}{d} \right] \\ &= (d+1) \left(\frac{2}{5} - \frac{1}{d} \right). \end{aligned}$$

Hence, we have $F_{\text{ad}}(1) - (\rho | P_{\text{ad}} | \rho) = (d+1)\frac{2}{5} - 2$.

In general, improving our sequence length bounds requires control over the extent of the fast scrambling regime for small m . To this end, more information about the spectrum of the second moment operator $M_2(\nu)$ beyond its spectral gap is needed. Then, one could bound the contributions coming from different parts of the spectrum individually, which may lead to better sequence length bounds. However, sufficiently large noise will perturb the moment operator in a way that mixes eigenspaces, and thus complicates an analytical treatment. Finally, our example also shows that the n -dependence of our bounds may not be improved, and thus the described approach would only result in smaller constants.

5.7 Application to common random circuits

The signal guarantees for filtered RB presented in Thms. 8 and 10 prominently involve the spectral gap of the used random circuit, and so do the sequence lengths bounds derived in Sec. 5.5. In this section, we want to illustrate these statements by applying our results to common choices of groups G and random circuits ν , resulting in concrete lower bounds on the sequence length for filtered RB in practically relevant cases. As a byproduct, this section may serve as a guideline for the scenarios which are not explicitly covered in this paper.

Concretely, we consider the unitary group $G = \text{U}(2^n)$ and the Clifford group $G = \text{Cl}_n(2)$. For both groups, we can make use of previously derived results for unitary 3-designs. In particular, we have the sequence length bound (60) which we here state in a slightly different form:

$$m \geq \frac{2}{\Delta_3(\nu)} (1.75n + \log(1/\alpha) + 1.8). \quad (65)$$

Here, we use that the t -design spectral gaps $\Delta_t(\nu)$ (i.e. w.r.t. $\omega^{\otimes t}$) for $t = 2, 3$ bound the relevant gaps in Lem. 18 and 19, respectively, and that the gaps are monotonic in t . For sequence lengths m larger than the bound (65), Theorem 8 then guarantees that the expected filtered RB signal $F_{\text{ad}}(m)$ is well-described by a single exponential decay of the form $A_{\text{ad}} I_{\text{ad}}^m$, up to an additive error α . Moreover, Theorem 16 gives a lower bound on the number of samples N sufficient to estimate $F_{\text{ad}}(m)$ within additive error α and with probability $1 - \delta$:

$$N \geq \frac{1}{\varepsilon^2 \delta} (3 + \alpha),$$

Here, we used the bound (104) on the second moment of unitary 3-designs given in App. C.1.

In the following, we discuss the dependence of the above bounds on the spectral gaps $\Delta_t(\nu)$ for various random circuits and $t = 2, 3$. Studies of random circuits usually give spectral gaps that scale as $1/n$ or better in the number of qubits n [35–39].

However, non-asymptotic results with explicit and *small* constants for low designs orders are not so easy to obtain. In the following, we summarize literature results for so-called *local random circuits* and *brickwork circuits* (to be defined shortly), and complement them with own numerical studies for small numbers of qubits. For the design orders we are interested in, $t = 2$ and 3 , the spectral gaps of these random circuits are the same when defined with gates from the unitary group or the Clifford group. We then discuss how the results can be adapted when Haar-random unitaries are replaced by Clifford generators including the case of different probability weights.

5.7.1 A collection of spectral gap bounds

Let us begin by defining local random circuits and brickwork circuits.

Definition 21. Let μ_2 denote the Haar measure on $U(d^2)$.

1. Let $\mathcal{G} = ([n], E)$ be a graph on n vertices. A local random circuit (LRC) on n qudits with connectivity graph \mathcal{G} is a probability measure μ_{LRC} on $U(d^n)$ given by drawing an edge $e \in E$ uniformly at random, and apply a Haar-random unitary $U \sim \mu_2$ to the two qudits connected by e . A nearest-neighbor (NN) local random circuit with open/periodic boundary conditions is a LRC where $E = \{(i, i+1) \mid i \in [n-1]\}$ and $E = \{(i, i+1) \mid i \in [n-1]\} \cup \{(n, 1)\}$, respectively.
2. Let ν_{even} and ν_{odd} be the probability measures on $U(d^n)$ that apply independent Haar-random unitaries $U \sim \mu_2$ in parallel on the qudit pairs $(i, i+1)$ where $i \in [n-1]$ is even or odd, respectively. A brickwork (BW) circuit on n qudits is given by the probability measure $\nu_{\text{BW}} = \nu_{\text{even}} * \nu_{\text{odd}}$.

Exact spectral gaps for NN local random circuits have been computed for $t = 2$ and $n \leq 21$ qubits, as well as for $t = 3$ and $n \leq 11$ by Ćwikliński et al. [86]. For LRCs on a complete graph (i.e. with all-to-all connectivity), Brown and Viola [36] have established the scaling $\Delta_t = \frac{5}{6n} + O(\frac{1}{n^2})$ with a t -independent leading coefficient. A good resource for tight bounds on the spectral gap of NN local random circuit for all n and $t = 2, \dots, 5$ is the work by Haferkamp and Hunter-Jones [38, Sec. IV]. There, the authors use Knabe bounds to promote exact values of the spectral gap for small n to lower bounds for larger n . Since we are particularly interested in spectral gap bounds for $t = 2, 3$, we summarize the relevant results in Table 2.

The spectral gap bound of LRCs can be used to give bounds on the spectral gaps of the corresponding brickwork circuit by using the *detectability lemma* [87, 88]. However, this technique generally results in a loose lower bound on the spectral gap. Hence, for $t = 2$, Haferkamp and Hunter-Jones [38] rely on the explicit computation of the brickwork frame potential by Hunter-Jones [28] to bound the circuit depth. The latter result yields a bound on the difference of the brickwork moment operator $M_2(\nu_{\text{BW}})$ to the Haar projector in the Schatten 2-norm (also called *Frobenius norm*) as follows

$$\|M_2(\nu_{\text{BW}})^m - M_2(\mu)\|_2^2 \leq 2 \left[1 + \left(\frac{4}{5}\right)^{2(2m-1)} \right]^{\lfloor \frac{n}{2} \rfloor - 1} - 2. \quad (66)$$

random circuit	$t = 2$	$t = 3$
NN local random circuit with PBC	$5n$	$5n$
NN local random circuit with OBC	$5n$	$5n$
local random circuit on complete graph	$\sim 6n/5$	$\sim 6n/5$
brickwork (odd number of layers)	$25/9$	42
brickwork (even number of layers)	$50/9$	42

Table 2: Upper bounds on the inverse spectral gap Δ_t^{-1} of the t -th moment operator for certain families of random quantum circuits on n qubits. Here, NN stands for nearest neighbor, and PBC and OBC mean periodic and open boundary conditions, respectively. The results for NN local random circuits is taken from Ref. [38]. The asymptotic scaling $\sim 6n/5$ for local random circuits on complete graphs is shown in Ref. [36]. The brickwork result for $t = 2$ is deduced from the frame potential calculation in Ref. [28], while the result for $t = 3$ follows by applying the detectability lemma to the $t = 3$ spectral gap of local random circuits.

Although the spectral norm is upper bounded by the 2-norm, $\|\cdot\|_\infty \leq \|\cdot\|_2$, there is an obstacle in directly deriving a bound on the spectral gap $\Delta(\nu_{\text{BW}})$ from this result: The moment operator $M_2(\nu_{\text{BW}})$ is not normal and thus there might be a strict inequality in

$$\|M_2(\nu_{\text{BW}})^m - M_2(\mu)\|_\infty \leq \|M_2(\nu_{\text{BW}}) - M_2(\mu)\|_\infty^m = (1 - \Delta(\nu_{\text{BW}}))^m.$$

However, using the symmetrization trick, c.f. Sec. 4.4, we can nevertheless deduce a decent spectral gap bound from Eq. (66). To the best of our knowledge, this is the best bound on the spectral gap of brickwork circuits and it has not been reported in the literature so far (the possibility has occurred to experts though [89]).

To this end, recall that $\nu_{\text{BW}} = \nu_{\text{even}} * \nu_{\text{odd}}$ where the two layers act in parallel on qubit pairs $(i, i+1)$ where i is even or odd, respectively. These two layers are each symmetric and $\nu_{\text{even}}^{*2} = \nu_{\text{even}}$, $\nu_{\text{odd}}^{*2} = \nu_{\text{odd}}$. The ‘inverted measure’ (17) is then given as $\tilde{\nu}_{\text{BW}} = \nu_{\text{odd}} * \nu_{\text{even}}$ such that $\eta_{\text{BW}} := \tilde{\nu}_{\text{BW}} * \nu_{\text{BW}} = \nu_{\text{odd}} * \nu_{\text{even}} * \nu_{\text{odd}}$. Powers then have the form $\eta_{\text{BW}}^{*m} = \nu_{\text{odd}} * (\nu_{\text{even}} * \nu_{\text{odd}})^{*m}$, i.e. they correspond to a brickwork circuit which starts and ends with an odd layer and thus involves an odd number of layers in total. Since the moment operator of the symmetrized measure η_{BW} is self-adjoint, we then find by using the appropriate bound in Ref. [28]:

$$\begin{aligned} (1 - \Delta(\eta_{\text{BW}}))^m &= \|M_2(\eta_{\text{BW}}) - M_2(\mu)\|_\infty^m \\ &= \|M_2(\eta_{\text{BW}})^m - M_2(\mu)\|_\infty \\ &\leq \|M_2(\eta_{\text{BW}})^m - M_2(\mu)\|_2 \\ &\leq \left(2 \left[1 + \left(\frac{4}{5} \right)^{4m} \right]^{\lfloor \frac{n}{2} \rfloor - 1} - 2 \right)^{\frac{1}{2}}. \end{aligned}$$

Taking the m -th root on both sides, we can observe that the left hand side does not depend on m anymore. Hence, we can take the limit $m \rightarrow \infty$ of the resulting right hand side to obtain an upper bound on $1 - \Delta(\eta_{\text{BW}})$. To compute the limit, note that we have the following lower and upper bound for sufficiently large m :

$$2 \left(\left\lfloor \frac{n}{2} \right\rfloor - 1 \right) \left(\frac{4}{5} \right)^{4m} \leq 2 \left[1 + \left(\frac{4}{5} \right)^{4m} \right]^{\lfloor \frac{n}{2} \rfloor - 1} - 2 \leq 4 \left(\left\lfloor \frac{n}{2} \right\rfloor - 1 \right) \left(\frac{4}{5} \right)^{4m}. \quad (67)$$

The lower bound in Eq. (67) follows from Bernoulli’s inequality $(1+x)^r \geq 1+rx$ for $r \in \mathbb{N}_0$ and $x \geq -1$. The upper bound follows from $(1+x)^r \leq e^{rx} \leq 1+2rx$ which holds for any $x \geq 0$ and $r \geq 0$ such that $0 \leq rx \leq 1$. The latter condition is certainly fulfilled for large enough m . Taking the $2m$ -th root of Eq. (67) and the limit $m \rightarrow \infty$, we see that the lower and upper bound both converge to $16/25$, hence we arrive at the result

$$1 - \Delta(\eta_{\text{BW}}) \leq \frac{16}{25} \quad \Rightarrow \quad \Delta(\eta_{\text{BW}}) \geq \frac{9}{25}.$$

By Eq. (18), this implies the following bound on the spectral gap of ν_{BW} (i.e. brickwork circuits with an *even* number of layers):

$$\Delta(\nu_{\text{BW}}) \geq \frac{9}{50}.$$

However, we expect this lower bound to be quite loose and attribute this to the proof technique. Realistically, we do not expect a large difference between the spectral gap of the “symmetric” brickwork circuit η_{BW} and the non-symmetric one ν_{BW} .

There is numerical evidence that the $t = 2$ and $t = 3$ bounds for LRC presented in Tab. 2 are rather tight, at least for moderate to large values of n [38]. For small $n \leq 10$, we have numerically computed the respective spectral gaps and present them in Fig. 2; finding a good agreement with Ref. [38]. In particular, the $t = 2$ and $t = 3$ spectral gaps are identical up to numerical precision. We can observe that the spectral gap for small n deviates notably from the lower bound $1/5n$. This can be used to reduce the sequence lengths of filtered RB experiments on small systems by a factor of 1.3 to 5.

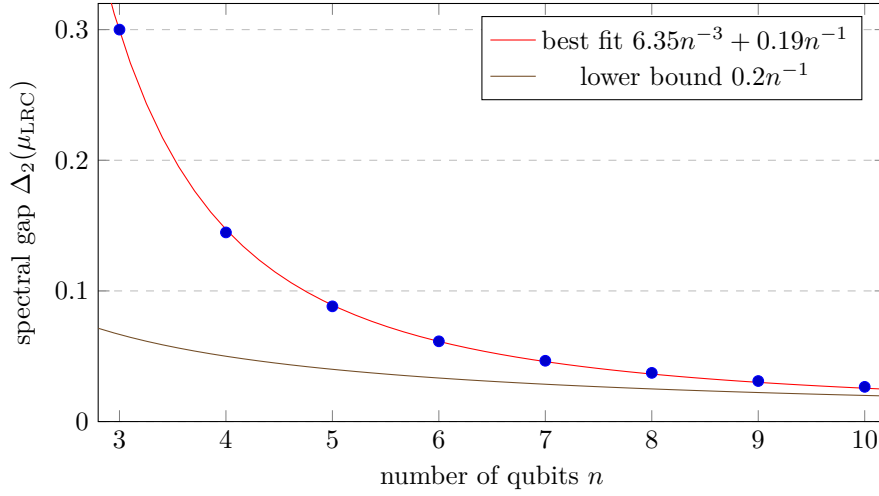


Figure 2: Numerically computed spectral gap of nearest-neighbor local random circuits with open boundary conditions for order $t = 2$. The results are in good agreement with Refs. [38, 86] and asymptotically approach the lower bound $1/5n$.

5.7.2 Spectral gaps for random circuits composed of Clifford generators

We are in particular interested in random circuits where the individual components are not drawn from the local Haar measure μ_2 , but instead from a set of local generators according to the measure ν . For local random circuits, we can lift results on the local spectral gaps of ν to global spectral gaps using the “local-to-global” lemma in Ref. [90].

Lemma 22 ([90, Lem. 16]). *Let ν be a symmetric probability measure on $U(d^2)$ and let $([n], E)$ be a graph on n vertices. Let ν_e be the measure ν with support on the factors corresponding to $e \in E$, and set $\nu_{\text{LRC}} = \sum_{e \in E} p_e \nu_e$ for some probabilities p_e . Let μ_2 be the Haar measure on $U(d^2)$, μ_{LRC} as in Def. 21, and let μ be the Haar measure on $U(d^n)$. Then, we have*

$$\|\mathbf{M}_{\rho_n}(\nu_{\text{LRC}}) - \mathbf{M}_{\rho_n}(\mu)\|_{\infty} \leq 1 - (1 - \|\mathbf{M}_{\rho_2}(\nu) - \mathbf{M}_{\rho_2}(\mu_2)\|_{\infty}) (1 - \|\mathbf{M}_{\rho_n}(\mu_{\text{LRC}}) - \mathbf{M}_{\rho_n}(\mu)\|_{\infty}),$$

for any representation ρ_n of $U(d^n)$ that factorizes for $U(d)^{\times n}$ as $\rho_n(g_1, \dots, g_n) = \rho(g_1) \otimes \dots \otimes \rho(g_n)$.

We have numerically computed the spectral gap of the t -th moment operator $\mathbf{M}_t(\nu_{\mathcal{G}})$ for a probability measure $\nu_{\mathcal{G}}$ which draws from the set of qubit Clifford generators

$$\mathcal{G} := \{PU \mid P \in \{\mathbb{1}, X, Y, Z\}^{\otimes 2}, U \in \{\mathbb{1}, S, H\}^{\otimes 2} \cup \{CX\}\}.$$

To this end, we have varied the probability p of choosing CX as the Clifford component U in the generator set \mathcal{G} , and found that the value $p = 0.35$ maximizes the spectral gap, resulting in

$\Delta_t^{-1}(\nu_{\mathcal{G}}) = 10.99$ for both $t = 2, 3$. Using Lemma 22 and Table 2, we then find the following bound on the inverse spectral gap of the LRC $\nu_{\text{LRC},\mathcal{G}}$ composed of gates from \mathcal{G} :

$$\Delta_t^{-1}(\nu_{\text{LRC},\mathcal{G}}) \leq \Delta_t^{-1}(\nu_{\text{LRC}})\Delta_t^{-1}(\nu_{\mathcal{G}}) \leq \begin{cases} 55n & \text{NN, open/periodic BC,} \\ 14n & \text{all-to-all connectivity,} \end{cases} \quad (68)$$

where $t = 2, 3$. Recall that the obtained upper bound yields a bound on the sequence length m , i.e. the number of generators to be applied, by Eq. (65).

We can now compare this result to the circuit depth that one would obtain for a LRC with Haar-random 2-qubit Clifford unitaries. Note that an arbitrary 2-qubit Clifford unitary can be implemented using at most 3 CX gates in depth ≤ 9 [91, 92]. Hence, the required depth would be at most $9m$ where m is the sequence length for the exact LRC given by Eq. (65). Since this bound differs from the one using generators only by a prefactor, it is sufficient to compare $9 \times 5n = 45n$ (NN) and $9 \times 5n/6 = 15n/2$ (all-to-all) with the respective bounds (68) obtained before. We see that the exact LRC implementation would require a similar circuit depth than our generator-based approach. However, the latter scheme only requires $p = 0.35$ CX gates on average while random 2-qubit Clifford unitaries require an average number of 1.5 CX gates [91]. Moreover, we expect the bound (68) to be rather loose due to the use of Lem. 22, such that the generator-based local random circuits should perform equally well or better in practice.

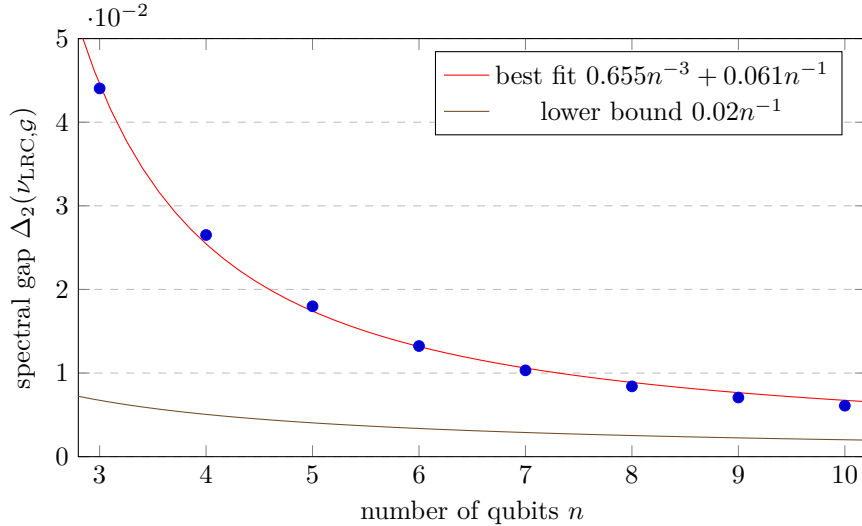


Figure 3: Numerically computed spectral gap $\Delta_2(\nu_{\text{LRC},\mathcal{G}})$ of local random circuits with local gates drawn from the set of Clifford generators \mathcal{G} and CX probability $p = 0.35$. The fit suggests that the derived bound (68) can be reduced by a factor of 3.

For a more precise comparison, we have exactly computed the spectral gap $\Delta_2(\nu_{\text{LRC},\mathcal{G}})$ for NN open boundary conditions. The results for $n \leq 10$ qubits are shown in Fig. 3. Our numerical results suggest that the bound (68) can be improved for NN connectivity by a factor of 3, resulting in $\Delta_t^{-1}(\nu_{\text{LRC},\mathcal{G}}) \leq 16.5n$.

Finally, the detectability lemma [87] in its generalized version [88] gives a bound on the spectral gap of brickwork circuits in terms of the one of a NN local random circuit $\nu_{\text{LRC},\text{NN}}$ as follows (see e.g. Ref. [38, Eq. (33)])

$$\|\mathbf{M}_t(\nu_{\text{BW}}) - \mathbf{M}_t(\mu)\|_{\infty} \leq \left(\frac{n\Delta_t(\nu_{\text{LRC},\text{NN}})}{4} + 1 \right)^{-\frac{1}{2}}.$$

This bound still holds true if the Haar-random 2-qubit unitaries in both random circuits are replaced by gates from \mathcal{G} drawn according to $\nu_{\mathcal{G}}$. Using the conjectured bound $\Delta_t^{-1}(\nu_{\text{LRC},\text{NN},\mathcal{G}}) \leq 16.5n$, we then find

$$\Delta_t(\nu_{\text{BW},\mathcal{G}})^{-1} \leq 134 \quad (t = 2, 3).$$

We suspect that this bound can be significantly improved.

5.8 Towards better filter functions

In Section 5.5, we have argued that filtered randomized benchmarking as presented here needs sufficiently long random sequences in order to suppress the subdominant decay terms. The main source of these terms is the usage of random circuits (with non-uniform measures) instead of the Haar-random unitaries and the decay is, in fact, showing their convergence towards the Haar measure. In particular, this decay also occurs in the noise-free case, c.f. Sec. 5.6.

Instead of increasing the sequence length to achieve sufficient convergence of the random circuit, one might hope that a smart change in the filter function allows to filter on the relevant decays directly. A similar consideration motivated the heuristic estimator for linear XEB proposed in Ref. [22]. In this section, we propose two novel choices of filter functions and provide evidence that they indeed accomplish this goal. We leave a detailed analysis and comparison for future work.

We think that the framework of filtered randomized benchmarking and the following filter functions are of interest for the theory of linear cross-entropy benchmarking (XEB). First, a perturbative analysis has the potential to go beyond the usual white noise assumption [27, 93]. Second, the proposed filter functions might help to resolve some difficulties in finding appropriate estimators for the fidelity that can be equipped with rigorous guarantees when using linear XEB with random circuits [26].

5.8.1 Filtering using the exact frame operator

As sketched in Sec. 2, filtered randomized benchmarking follows a similar idea as shadow tomography. For ideal gates and ideal state preparation and measurement, $\hat{F}_\lambda(m)$ estimates for any sequence length m the expression

$$\begin{aligned} F_\lambda(m) &= \sum_{i \in [d]} \int_{G^m} f_\lambda(i, g_1 \cdots g_m) p(i|g_1, \dots, g_m) d\nu(g_1) \cdots d\nu(g_m) \\ &= \sum_{i \in [d]} \int_G (\rho | P_\lambda S^{-1} \omega(g)^\dagger | E_i) (E_i | \omega(g) | \rho) d\nu^{*m}(g) \\ &= (\rho | P_\lambda S^{-1} S_{\nu^{*m}} | \rho). \end{aligned}$$

Here, we defined the the frame operator associated to a sequence of length m as

$$S_{\nu^{*m}} = \int_G \omega(g)^\dagger M \omega(g) d\nu^{*m}(g).$$

If ν is not the Haar measure (or an appropriate exact design) then S^{-1} does not cancel $S_{\nu^{*m}}$. Since ν^{*m} eventually converges to the Haar measure, S^{-1} becomes a good approximation to the exact inverse frame operator $S_{\nu^{*m}}^{-1}$ with increasing m . The discrepancy between the two frame operators is visible as the additional decay in Thm. 8. Clearly, the solution would be to use the correct frame operator, i.e. to redefine the filter function as

$$f_{\nu, \lambda}(i, g_1, \dots, g_m) := (E_i | \omega(g_1 \cdots g_m) S_{\nu^{*m}}^{-1} P_\lambda | \rho). \quad (69)$$

However, the evaluation of this filter function is, in practice, more challenging than its Haar-random alternative. The analytical and numerical evaluation of the frame operator and the dual frame is an active research topic in shadow tomography [94–98]. The inversion of the frame operator is simplified for measures ν which are invariant under left multiplication with Pauli operators [95], or consist only of Clifford unitaries.⁷ For those, the frame operator is diagonal in the Pauli basis, hence inversion is straightforward. Nevertheless, the computational cost of the classical post-processing increases significantly for the filter function (69).

⁷ M is a Pauli channel and conjugation by Clifford channels maps Pauli channels to Pauli channels. The frame operator is thus a convex combination of Pauli channels, hence a Pauli channel itself and in particular diagonal in the Pauli basis.

5.8.2 The trace filter

Our second proposal is based on the observation that every moment operator is block-diagonal, c.f. Eq. (15). In particular, the exact frame operator $S_\nu = \widehat{\omega\nu}[\omega](M)$ can be decomposed as

$$S_\nu = \widehat{\omega}[\omega](M) + (\widehat{\omega\nu}[\omega] - \widehat{\omega}[\omega])(M) = S + T_\nu,$$

where $S = \widehat{\omega}[\omega](M)$ is the Haar-random frame operator which lies in the commutant of ω and T_ν is orthogonal to S , $\text{tr}(ST_\nu) = 0$. With this notation, the filtered RB signal (4) considered in the previous sections becomes (in the noise-free case)

$$F_\lambda(m) = (\rho | P_\lambda S^+ S_\nu | \rho) = (\rho | P_\lambda S^+ S | \rho) + (\rho | P_\lambda S^+ T_\nu | \rho).$$

Next, we show that – under certain assumptions on the group G and the measure ν – we can change the filter function such that the second term vanishes identically. The idea is to make the RB signal take the form of a *trace inner-product* of super-operators instead of a ‘matrix element’ defined by ρ . This allows us to project exactly on the commutant in the post-processing of ω in the data. We, thereby, filter not only to an irrep but to the specific dominant subspace. In this way, $F_\lambda(m)$ is not affected by the “non-uniformness” of our measure ν and we keep the simple structure of the inverse frame operator S^{-1} in contrast to Sec. 5.8.1.

We exemplify this idea for unitary 2-groups, i.e. essentially the multi-qubit Clifford group and specific subgroups thereof. Let $\omega(g) = U_g(\cdot)U_g^\dagger$ and $G \subset \text{U}(d)$ be a unitary 2-group. In this way, there is only a single non-trivial irrep to consider, namely the adjoint one $\lambda = \text{ad}$, and $P_{\text{ad}} = \text{id} - |\mathbb{1}\rangle\langle\mathbb{1}|/d$. Moreover, we assume that the measure ν is *right-invariant* under the local Clifford group $\text{Cl}_1^{\times n}$, in particular we need $G \supset \text{Cl}_1^{\times n}$. This is not much of a restriction, since we can always perform a layer of Haar-random single-qubit Clifford unitaries (or Haar-random single qubit unitaries) in the beginning of our random circuit at negligible cost. As a consequence of the invariance assumption, the frame operator S_ν is not only diagonal in the Pauli basis, but its diagonal elements depend only on the support of a Pauli operator. (Here, by ‘support’ we mean on which qubits the operator acts non-trivially.) To see this, let $w(u)$ and $w(v)$ be two Pauli operators with equal support, then we can find a local Clifford unitary $C = C_1 \otimes \cdots \otimes C_n$ such that $w(u) = Cw(v)C^\dagger$. Hence:

$$\begin{aligned} (w(u) | S_\nu | w(u)) &= \int_G (w(u) | \omega(g)^\dagger M \omega(g) | w(u)) d\nu(g) \\ &= \int_G (w(v) | \omega(gC)^\dagger M \omega(gC) | w(v)) d\nu(g) \\ &= (w(v) | S_\nu | w(v)), \end{aligned}$$

where we have used the right invariance of ν in the last step. Note that for any superoperator \mathcal{X} with this property, we have

$$\text{tr}(\mathcal{X}) = d^{-1} \sum_{u \in \mathbb{F}_2^{2n}} (w(u) | \mathcal{X} | w(u)) = d^{-1} \sum_{z \in \mathbb{F}_2^n} 3^{|z|} (Z(z) | \mathcal{X} | Z(z)).$$

This is because every $Z(z)$ -operator has support on $|z|$ many qubits and thus can be mapped to $3^{|z|}$ many different Pauli operators with identical support under local Cliffords.

Finally, we define the *trace filter* as

$$f_{\text{tr}}(i, g_1, \dots, g_m) := (E_i | \omega(g_1 \cdots g_m) S^{-1} | \xi) - \text{tr}(\xi), \quad \xi := \frac{1}{d^2} \sum_{z \in \mathbb{F}_2^n} 3^{|z|} Z(z). \quad (70)$$

Suppose we prepare the system in the $|0\rangle$ state such that $\rho = d^{-1} \sum_z Z(z)$. Using the diagonality

of the frame operators, we then find that an ideal implementation yields the RB signal

$$\begin{aligned}
F_{\text{tr}}(m) &= \frac{1}{d^2} \sum_{z \in \mathbb{F}_2^n} 3^{|z|} (Z(z) | S^{-1} S_\nu | \rho) - \text{tr}(\xi) \\
&= \frac{1}{d^3} \sum_{z \in \mathbb{F}_2^n} 3^{|z|} (Z(z) | S^{-1} S_\nu | Z(z)) - \frac{1}{d} \\
&= \frac{1}{d^2} [\text{tr}(S^{-1} S_\nu)] - \frac{1}{d} \\
&= \frac{1}{d^2} [\text{tr}(S^{-1} S) + \text{tr}(S^{-1} T_\nu)] - \frac{1}{d}.
\end{aligned}$$

Now, S is in the commutant of ω , hence so is S^{-1} , and thus $\text{tr}(S^{-1} T_\nu) = 0$. In conclusion, $F_{\text{tr}}(m) = (\rho | P_{\text{ad}} | \rho)$ and is not decaying with the sequence length. Using the trace filter (2) in post-processing, thus, yields an estimator for the state fidelity.

Finally, we note there are also different ways to construct similar trace filters. If one does not want to assume local Clifford invariance, but the frame operators are still diagonal, the scheme can be adapted as follows. Instead of $\rho = |0\rangle\langle 0|$, prepare tensor powers of the ‘facet’ magic state $|F\rangle\langle F| = (\mathbb{1} + (X + Y + Z)/\sqrt{3})/2$ which have the form

$$|F\rangle\langle F|^{\otimes n} = \frac{1}{d} \sum_{u \in \mathbb{F}_2^{2n}} 3^{-\text{wt}(u)/2} w(u),$$

where $\text{wt}(u)$ denotes the Pauli weight of the operator $w(u)$. The ξ operator can then be changed as follows

$$\xi = \frac{1}{d^2} \sum_{u \in \mathbb{F}_2^{2n}} 3^{\text{wt}(u)/2} w(u).$$

It is easy to see that this provides the right result.

5.8.3 In the presence of noise

A priori, it is not clear how these new schemes behave in the presence of general gate-dependent noise. We found that the analysis for the new filter functions (69) and (70) requires some non-trivial extensions to our perturbative approach. In particular, we require a more detailed control on the perturbation of eigenspaces of the moment operator to bound how much $\widehat{\phi\nu}[\omega]^m(\tilde{M})$ can deviate from the frame operator. We leave such an analysis for future work.

Nevertheless, we can provide some evidence that the proposed filter functions detect the noise strength even for sequence length that do not ensure sufficient convergence to the Haar measure when using the *white noise assumption*. This is a wide-spread assumption on the outcome distribution of noisy quantum circuits and a corner stone of the demonstration of quantum supremacy using linear cross-entropy benchmarking (XEB) [10, 93, 99, 100]. We thereby put our proposal on at least comparative theoretical footing as the related existing proposals. The theoretical foundation for this assumption has recently been laid by Ref. [27]. There, the authors show that for local random circuits with gate-independent local noise, the outcome distribution is well approximate in total variation distance by a convex combination of the noise-free distribution and a uniform distribution:

$$p_{\text{noisy}}(i|g_1, \dots, g_m) \approx p_{\text{wn}}(i|g_1, \dots, g_m) := F p_{\text{ideal}}(i|g_1, \dots, g_m) + (1 - F) \frac{1}{d},$$

where F is the relative score in the cross-entropy benchmark. These results hold under the assumption that $m \geq \Omega(n \log(n))$ and that the two-qubit gate error ϵ is small compared to $n \log(n)$.

Then, we can argue that for both proposed filter functions (69) and (70), we have

$$F_{\text{noisy}}(m) = \sum_{i \in [d]} \int f(i, g_1 \cdots g_m) p_{\text{noisy}}(i | g_1, \dots, g_m) d\nu(g_1) \cdots d\nu(g_m) \quad (71)$$

$$\begin{aligned} &\approx F F_{\text{ideal}}(m) + (1 - F) \frac{1}{d} \sum_{i \in [d]} \int f(i, g_1 \cdots g_m) d\nu(g_1) \cdots d\nu(g_m) \\ &= F F_{\text{ideal}}(m). \end{aligned} \quad (72)$$

Here, we have used that the frame operators are unital and hence

$$\sum_{i \in [d]} f(i, g_1 \cdots g_m) = \begin{cases} \text{tr}(P_{\text{ad}}(\rho)) = 0 & \text{for the exact filter function } f, \\ \text{tr}(\xi) - \text{tr}(\xi) = 0 & \text{for the trace filter } f_{\text{tr}}. \end{cases}$$

However, it seems that the results in Ref. [27] are not strong enough to give a decent bound on the approximation error in Eq. (72). In Ref. [27], the total variation distance between p_{noisy} and p_{wn} averaged over the g_i is bounded as $\delta = O(F\epsilon\sqrt{m})$. Note that this error is exactly twice the L^1 -norm error if p_{noisy} and p_{wn} are seen as (integrable) functions on $[d] \times G^m$. Thus, we would require control over the L^∞ -norm of the filter function f in order to bound the inner product in Eq. (71) by Hölder's inequality. In general, the infinity norm of the considered filter functions is of the order of $\|S_{\nu^{*m}}^{-1}\|_\infty$ and $\|S^{-1}\|_\infty$, respectively, leading to a blow-up of the error δ by a dimensional factor in the worst case. See also the recent Ref. [101] in this context.

5.9 Detailed comparison to related works

Here, we want to compare our results, and in particular the assumptions needed for our signal guarantees, with the previously existing work by Helsen et al. [9], Kong [15], Chen, Ding, and Huang [24], and Chen, Ding, Huang, and Kong [25].

The main differences are as follows: Our results hold for RB experiments with gates from an arbitrary compact group G sampled according to an arbitrary (well-behaved) probability measure. The work of Helsen et al. [9] deals with arbitrary finite groups G , and their approach is readily generalized to compact groups with equivalent guarantees [15]. However, for non-uniform sampling with measure ν , their results require that ν^{*m} converges quickly to the Haar measure in total variation distance, which is quite a strong assumption. Moreover, most results in Refs. [9, 15] hold for a RB protocol with inversion gate. However, Ref. [9] introduces the idea of filtered RB, but only for Haar-random sampling and without a proper analysis of its sampling complexity. The works by Chen, Ding, and Huang [24] and Chen, Ding, Huang, and Kong [25] improve on the latter aspects in the sense that no inversion gate is needed and general probability measures ν are admitted under the assumption that ν^{*m} converges to a unitary 2-design. Explicit examples for such random circuits with Clifford gates are discussed in detail in Ref. [25].

To make this more precise, recall the central assumption (A) of our main theorems 8 and 10:

$$\|\widehat{\phi\nu}[\omega_\lambda] - \widehat{\omega\nu}[\omega_\lambda]\|_\infty \leq \delta_\lambda < \frac{\Delta_\lambda}{4}.$$

This can be phrased as the assumption that the implementation function ϕ is sufficiently close to the reference representation ω on average w.r.t. the measure ν . In particular, only the quality of gates in the support of ν matter. This assumption is not only less stringent in several aspects compared to Refs. [9, 15, 24, 25], but our analysis also leads to more profound and tight results, as we will now explain.

1. As a consequence of filtering onto the irrep λ , we only require that the implementation error is small “per irrep” and compared to the irrep-specific spectral gap Δ_λ of $\widehat{\omega\nu}[\omega_\lambda]$. Refs. [9, 15, 24, 25] require conditions on global quantities.
2. We require that the deviation of the Fourier transforms of ϕ and ω is small. These are quantities which are already averaged over the group. In contrast, both Refs. [9, 15, 24,

[25] formally require that the error $\|\phi(g) - \omega(g)\|$, averaged over the group, is small. Closer inspection shows that the proofs in Refs. [24, 25] can be adapted to allow averaging inside the norm. This is not the case for the approach in Refs. [9, 15]. In general, we have the bound (cf. Eq. (28) below):

$$\|\widehat{\phi\nu}[\omega_\lambda] - \widehat{\omega\nu}[\omega_\lambda]\|_\infty \leq \int_G \|\phi(g) - \omega(g)\|_\infty d\nu(g).$$

We expect that the triangle inequality is quite loose in realistic situations and thus “averaging inside the norm” should lead to smaller quantities.

Note that we are using the spectral norm to measure the implementation error while Refs. [24, 25] use the diamond-to-diamond norm for this purpose.⁸ As spectral and diamond-to-diamond norm are not ordered, it is not straightforward to compare the two approaches.

3. We measure errors in *spectral norm* for reasons which we explain shortly. Other norm choices include the diamond-to-diamond norm for the Fourier transforms, and the diamond norm for its vectorized version (13), as well as mixed approaches. The results in Refs. [24, 25] hold for an implementation error that is measured in diamond-to-diamond norm, while ν is assumed to be an approximate unitary 2-design in either diamond-to-diamond norm or the spectral norm, with approximation error less than 1.

In general, norm choices based on the diamond norm imply much stronger notions of approximation for random circuits than for the spectral norm. In Ref. [25], it is shown that in order to constitute an approximate unitary 2-design in diamond-to-diamond norm, a random circuit has to have at least logarithmic depth in the number of qudits n . Moreover, in the same paper, it is also argued that the sequence length m has to be linear in n . This directly implies that the results based on approximation in diamond-to-diamond norm require circuits of depth at least $\Omega(n \log n)$. In contrast, approximation in spectral norm allows for constant-depth random circuits (e.g. brickwork circuits), while the sequence length m is still linear in n . Although not explicitly stated in Refs. [24, 25], the results for the spectral norm in these works thus imply that circuits of depth $O(n)$ are in fact already enough. In practice, the omitted constants and the regime of n eventually decide which scaling is favorable.

We took the generally larger convergence rates in diamond norm as an indication to use the spectral norm instead. Moreover, there is no conceptual difficulty in applying the spectral norm to Fourier transforms evaluated at subrepresentations, c.f. point 1 above. Thus, this norm choice seems to be better suited for our filtering approach which is arguably most relevant for groups with more than one non-trivial irrep. Since we are then able to make the analysis on a per-irrep basis, we can show that it is sufficient to choose the sequence length as $m = O(\log(d_\lambda))$, c.f. Sec. 5.5 (assuming a constant spectral gap). In particular, we recover the results in Refs. [24, 25] for unitary 2-designs, c.f. Sec. 5.7, but obtain more fine-grained and tighter bounds for general compact groups G .

Finally, we also found that choosing the spectral norm naturally involves the spectral gap. Since the spectral gap is a well-studied quantity in the theory of random circuits, there exist plenty of literature results and techniques to bound the spectral gap for the random circuit of interest. In practice, it is to be expected that finding convergence rates in diamond-to-diamond norm is much harder. Indeed, direct results are rare [5, 35], indicating that leveraging spectral gap bounds via norm inequalities at the cost of additional dimensional factors might be the only course of action (as it is often the case for the much better studied diamond norm approximations of the vectorized channel twirl [38, 39, 102, 103]).

4. Consequently, our assumptions on the probability measure ν are minimal. There are no assumptions on the spectral gap Δ_λ except that it is larger than zero. Its value, however, limits the amount of imperfection in ϕ that can be tolerated, as well the required sequence length of the random circuits. An similar limitation can be found for the spectral norm

⁸Note that the diamond-to-diamond norm can only be used for the ‘global’ Fourier transform $\widehat{\phi\nu}[\omega]$ and not on a per-irrep basis. This is because the irreps generally fail to be operator algebras and thus cannot be endowed with Schatten norms.

results in Ref. [24], as well as a qualitatively similar statement for the diamond-to-diamond norm (although the implementation error is measured in a different norm, thus the results are not strictly comparable). Finally, Ref. [9] requires that the probability measure ν is close to the Haar measure in *total variation distance*. This is of course much more stringent than our assumption on the existence of a spectral gap.

5. We take averages with respect to the relevant measure ν . In particular, it is completely irrelevant whether the implementation is good outside the support of ν . This is a desired property, since only gates in $\text{supp}(\nu)$ are ever applied in the RB experiment and hence all other gates should not play a role in the analysis. The work of Chen, Ding, and Huang [24] and Chen, Ding, Huang, and Kong [25] shares this property, while Helsen et al. [9] use Haar averages, even for non-uniform sampling.
6. To the best of our knowledge, our work gives the first sampling complexity bounds for filtered RB for arbitrary groups and random circuits (including linear XEB) that are close to the noise-free situation and in this sense, optimal.

Note that the requirement that the spectral gap Δ_λ is non-zero implies that the measure ν defines an approximate $\tau_\lambda \otimes \omega$ -design. The size of the spectral gap determines the convergence rate of the design and hence strongly influences our sequence length bound, c.f. Lem. 18. For this, it is sufficient that ν defines an approximate $\omega^{\otimes 2}$ -design *for the group G which we actually use for benchmarking*. This is the proper generalization of the *unitary 2-design assumption* made in standard RB literature, when the benchmarking group is not the full unitary group or Clifford group. Likewise, our sampling complexity guarantees require that ν is an approximate $\tau_\lambda^{\otimes 2} \otimes \omega$ -design (or $\omega^{\otimes 3}$ -design), replacing the common unitary 3-design assumption.

6 Conclusion

Filtered randomized benchmarking (RB) is the collection of experimental data obtained by applying random sequences of gates, followed by a suitable post-processing. Summarized by the motto ‘measure first – analyze later’, filtered RB is part of a modern class of characterization protocols such as *shadow tomography* [43, 45, 104], *randomized gate set tomography* [105, 106], and other random sequence protocols [53]. These protocols essentially share their first stage – the data acquisition from random sequences of gates – and only differ in the post-processing of this data. The advantage of such protocols is that different conclusions can be drawn from the same data.

Compared to standard RB, filtered RB has the advantage to avoid the application of the final *inversion gate*. This avoids the problem that the inverse of a unitary can have large circuit depth even if the original unitary does not. Moreover, it relaxes the requirements on the used gate set as it is not needed to efficiently compute the inversion gate. Another advantage is only apparent when the protocol is used for groups G with more than one non-trivial irrep (i.e. groups which are not unitary 2-designs) – in this case, standard RB produces a linear combination of exponential decays in one-to-one correspondence with the irreps of G . In practice, fitting these decays is often not possible and there is no way of attributing them to individual irreps. Filtered RB allows to address specific irreps and produces a single exponential decay that is straightforward to fit.⁹

In this work, we have developed a general theory of filtered RB with random circuits and arbitrary gate-dependent (Markovian and time-stationary) noise. Our theory is based on harmonic analysis on compact groups and neatly combines representation theory with the theory of random circuits. As such, it can be seen as a mathematically elegant advancement of Fourier-based approaches to RB [9, 14], which does not require to implement a Fourier transform ‘by hand’ but instead effectively performs it in the post-processing. We hope that our theory settles the discussion whether a group structure is needed for RB or whether one has to go ‘beyond groups’ [24].

Concretely, we have shown that if the implementation error of the used gates is small enough compared to the spectral gap of the random circuit, the filtered RB signal has the form of a

⁹Assuming that the irrep is multiplicity-free and a random circuit with sufficiently large spectral gap is used.

matrix exponential decay. In general, this decay is superimposed by an additional decay reflecting the convergence of the random circuit to a 2-design for the group G . We have derived sufficient conditions on the depth of the random circuit which guarantee that this additional contribution is negligible and the relevant decays can be extracted. For random circuits which mix sufficiently fast, a *circuit depth which is at most linear in the number of qudits* is sufficient.

Additionally, we have shown that the use of random circuits instead of uniformly drawn unitaries from G does not change the sampling complexity of filtered RB. In particular, filtered RB is *sampling-efficient* if it is sampling-efficient when uniformly distributed unitaries are used. To this end, we have computed the sampling complexity of ideal filtered RB for unitary 3-designs, local unitary 3-designs, and the Pauli group, and found that it is indeed sampling-efficient in these important cases.

To illustrate our general results, we have applied them to commonly used groups and random circuits and have derived concrete, small constants for sufficient sequence lengths. These explicit computation may also serve as a guideline when applying our general results to other groups and random circuits.

Finally, we have discussed other choices of filter functions which should result in a further reduction of the necessary circuit depths for filtered RB. Moreover, we think that these proposals are highly relevant for linear cross-entropy benchmarking (XEB) and the related random circuit sampling benchmark [26, 93]. However, a rigorous analysis for these alternative filter functions requires new techniques beyond the ones used in this paper and we leave such a study for future work. Finally, it remains an open problem to extend our analysis to non-Markovian noise. To this end, future research may combine our methods with the recent results in Ref. [54].

7 Acknowledgements

We thank Jonas Haferkamp for helpful discussions about random circuits and spectral gaps throughout the project, and for pointing out relevant literature and methods for Sec. 5.7. We thank Yelyzaveta Vodovozova and Jadwiga Wilkens for helpful comments on the draft. Furthermore, we would like to thank Jianxin Chen, Cupjin Huang, Linghang Kong, and in particular Dawei Ding for reaching out to us, helping us to improve our summary of Refs. [24, 25], and clarifying its relation to our current work. IR would like to thank Jonas Helsen, Emilio Onorati, Albert Werner and Jens Eisert for countless discussions on randomized benchmarking over the recent years. MH and MK are funded by the Deutsche Forschungsgemeinschaft (DFG, German Research Foundation) within the Emmy Noether program (grant number 441423094) and by the German Federal Ministry of Education and Research (BMBF) within the funding program “quantum technologies – from basic research to market” via the joint project MIQRO (grant number 13N15522).

8 Acronyms

ACES	averaged circuit eigenvalue sampling	5
BW	brickwork	49
LRC	local random circuit	49
NN	nearest-neighbor	49
OVM	operator-valued measure	16
POVM	positive operator-valued measure	7
RB	randomized benchmarking	2
SPAM	state preparation and measurement	2
XEB	cross-entropy benchmarking	3

References

- [1] Jens Eisert, Dominik Hangleiter, Nathan Walk, Ingo Roth, Damian Markham, Rhea Parekh, Ulysse Chabaud, and Elham Kashefi. “Quantum certification and benchmarking”. In: *Nat. Rev. Phys.* 2.7 (2020), pp. 382–390. DOI: [10.1038/s42254-020-0186-4](https://doi.org/10.1038/s42254-020-0186-4). arXiv: [1910.06343](https://arxiv.org/abs/1910.06343) [quant-ph].
- [2] Martin Kliesch and Ingo Roth. “Theory of quantum system certification”. In: *PRX Quantum* 2 (1 2021). Tutorial, p. 010201. DOI: [10.1103/PRXQuantum.2.010201](https://doi.org/10.1103/PRXQuantum.2.010201). arXiv: [2010.05925](https://arxiv.org/abs/2010.05925) [quant-ph].
- [3] Joseph Emerson, Robert Alicki, and Karol Życzkowski. “Scalable noise estimation with random unitary operators”. In: *J. Opt. B* 7.10 (2005), S347. DOI: [10.1088/1464-4266/7/10/021](https://doi.org/10.1088/1464-4266/7/10/021). eprint: [arXiv:quant-ph/0503243](https://arxiv.org/abs/quant-ph/0503243).
- [4] Benjamin Lévi, Cecilia C. López, Joseph Emerson, and D. G. Cory. “Efficient error characterization in quantum information processing”. In: *Phys. Rev. A* 75.2, 022314 (2007), p. 022314. DOI: [10.1103/PhysRevA.75.022314](https://doi.org/10.1103/PhysRevA.75.022314). arXiv: [quant-ph/0608246](https://arxiv.org/abs/quant-ph/0608246) [quant-ph].
- [5] Christoph Dankert, Richard Cleve, Joseph Emerson, and Etera Livine. “Exact and approximate unitary 2-designs and their application to fidelity estimation”. In: *Phys. Rev. A* 80 (1 2009), p. 012304. DOI: [10.1103/PhysRevA.80.012304](https://doi.org/10.1103/PhysRevA.80.012304). arXiv: [quant-ph/0606161](https://arxiv.org/abs/quant-ph/0606161) [quant-ph].
- [6] J. Emerson, M. Silva, O. Moussa, C. Ryan, M. Laforest, J. Baugh, D. G. Cory, and R. Laflamme. “Symmetrized characterization of noisy quantum processes”. In: *Science* 317.5846 (2007), pp. 1893–1896. DOI: [10.1126/science.1145699](https://doi.org/10.1126/science.1145699). arXiv: [0707.0685](https://arxiv.org/abs/0707.0685) [quant-ph].
- [7] E. Knill, D. Leibfried, R. Reichle, J. Britton, R. B. Blakestad, J. D. Jost, C. Langer, R. Ozeri, S. Seidelin, and D. J. Wineland. “Randomized benchmarking of quantum gates”. In: *Phys. Rev. A* 77.1, 012307 (2008), p. 012307. DOI: [10.1103/PhysRevA.77.012307](https://doi.org/10.1103/PhysRevA.77.012307). arXiv: [0707.0963](https://arxiv.org/abs/0707.0963) [quant-ph].
- [8] Easwar Magesan, Jay M. Gambetta, and Joseph Emerson. “Characterizing quantum gates via randomized benchmarking”. In: *Phys. Rev. A* 85 (4 2012), p. 042311. DOI: [10.1103/PhysRevA.85.042311](https://doi.org/10.1103/PhysRevA.85.042311). arXiv: [1109.6887](https://arxiv.org/abs/1109.6887).
- [9] Jonas Helsen, Ingo Roth, Emilio Onorati, Albert H. Werner, and Jens Eisert. “A general framework for randomized benchmarking”. In: *PRX Quantum* 3.2 (2022), p. 020357. DOI: [10.1103/PRXQuantum.3.020357](https://doi.org/10.1103/PRXQuantum.3.020357). arXiv: [2010.07974](https://arxiv.org/abs/2010.07974) [quant-ph].
- [10] Frank Arute et al. “Quantum supremacy using a programmable superconducting processor”. In: *Nature* 574.7779 (2019), pp. 505–510. DOI: [10.1038/s41586-019-1666-5](https://doi.org/10.1038/s41586-019-1666-5). arXiv: [1910.11333](https://arxiv.org/abs/1910.11333) [quant-ph].
- [11] Easwar Magesan, J. M. Gambetta, and Joseph Emerson. “Scalable and robust randomized benchmarking of quantum processes”. In: *Phys. Rev. Lett.* 106 (18 2011), p. 180504. DOI: [10.1103/PhysRevLett.106.180504](https://doi.org/10.1103/PhysRevLett.106.180504). arXiv: [1009.3639](https://arxiv.org/abs/1009.3639) [quant-ph].
- [12] Timothy Proctor, Kenneth Rudinger, Kevin Young, Mohan Sarovar, and Robin Blume-Kohout. “What randomized benchmarking actually measures”. In: *Phys. Rev. Lett.* 119.13, 130502 (2017), p. 130502. DOI: [10.1103/PhysRevLett.119.130502](https://doi.org/10.1103/PhysRevLett.119.130502). arXiv: [1702.01853](https://arxiv.org/abs/1702.01853) [quant-ph].
- [13] Joel J Wallman. “Randomized benchmarking with gate-dependent noise”. In: *Quantum* 2 (2018), p. 47. DOI: [10.22331/q-2018-01-29-47](https://doi.org/10.22331/q-2018-01-29-47). arXiv: [1703.09835](https://arxiv.org/abs/1703.09835) [quant-ph].
- [14] Seth T. Merkel, Emily J. Pritchett, and Bryan H. Fong. “Randomized benchmarking as convolution: Fourier analysis of gate dependent errors”. In: *Quantum* 5 (2021), p. 581. DOI: [10.22331/q-2021-11-16-581](https://doi.org/10.22331/q-2021-11-16-581). arXiv: [1804.05951](https://arxiv.org/abs/1804.05951) [quant-ph].
- [15] Linghang Kong. *A framework for randomized benchmarking over compact groups*. 2021. arXiv: [2111.10357](https://arxiv.org/abs/2111.10357) [quant-ph].
- [16] D. S. França and A. K. Hashagen. “Approximate randomized benchmarking for finite groups”. In: *J. Phys. A* 51.39, 395302 (2018), p. 395302. DOI: [10.1088/1751-8121/aad6fa](https://doi.org/10.1088/1751-8121/aad6fa). arXiv: [1803.03621](https://arxiv.org/abs/1803.03621) [quant-ph].

- [17] Timothy J. Proctor, Arnaud Carignan-Dugas, Kenneth Rudinger, Erik Nielsen, Robin Blume-Kohout, and Kevin Young. “Direct randomized benchmarking for multiqubit devices”. In: *Phys. Rev. Lett.* 123.3, 030503 (2019), p. 030503. DOI: [10.1103/PhysRevLett.123.030503](#). arXiv: [1807.07975 \[quant-ph\]](#).
- [18] Tobias Chasseur and Frank K. Wilhelm. “A complete randomized benchmarking protocol accounting for leakage errors”. In: *Phys. Rev. A* 92.4 (2015), p. 042333. DOI: [10.1103/PhysRevA.92.042333](#). arXiv: [1505.00580 \[quant-ph\]](#).
- [19] Tobias Chasseur, Daniel M. Reich, Christiane P. Koch, and Frank K. Wilhelm. “Hybrid benchmarking of arbitrary quantum gates”. In: *Phys. Rev. A* 95.6 (2017), p. 062335. DOI: [10.1103/PhysRevA.95.062335](#). arXiv: [1606.03927 \[quant-ph\]](#).
- [20] Dominik Hangleiter and Jens Eisert. “Computational advantage of quantum random sampling”. 2022. arXiv: [2206.04079 \[quant-ph\]](#).
- [21] Kristine Boone, Arnaud Carignan-Dugas, Joel J. Wallman, and Joseph Emerson. “Randomized benchmarking under different gate sets”. In: *Phys. Rev. A* 99.3, 032329 (2019), p. 032329. DOI: [10.1103/PhysRevA.99.032329](#). arXiv: [1811.01920 \[quant-ph\]](#).
- [22] Yosef Rinott, Tomer Shoham, and Gil Kalai. “Statistical aspects of the quantum supremacy demonstration”. In: *Statistical Science* 37.3 (2022), pp. 322–347. arXiv: [2008.05177 \[quant-ph\]](#).
- [23] Boaz Barak, Chi-Ning Chou, and Xun Gao. “Spoofing linear cross-entropy benchmarking in shallow quantum circuits”. 2020. arXiv: [2005.02421 \[quant-ph\]](#).
- [24] Jianxin Chen, Dawei Ding, and Cupjin Huang. “Randomized benchmarking beyond groups”. In: *PRX Quantum* 3.3 (2022), p. 030320. DOI: [10.1103/PRXQuantum.3.030320](#). arXiv: [2203.12703 \[quant-ph\]](#).
- [25] Jianxin Chen, Dawei Ding, Cupjin Huang, and Linghang Kong. *Linear Cross Entropy Benchmarking with Clifford Circuits*. 2022. arXiv: [2206.08293](#).
- [26] Yunchao Liu, Matthew Otten, Roozbeh Bassirianjahromi, Liang Jiang, and Bill Fefferman. “Benchmarking near-term quantum computers via random circuit sampling”. 2021. arXiv: [2105.05232 \[quant-ph\]](#).
- [27] Alexander M. Dalzell, Nicholas Hunter-Jones, and Fernando G. S. L. Brandão. “Random quantum circuits transform local noise into global white noise”. 2021. arXiv: [2111.14907 \[quant-ph\]](#).
- [28] Nicholas Hunter-Jones. “Unitary designs from statistical mechanics in random quantum circuits”. 2019. arXiv: [1905.12053 \[quant-ph\]](#).
- [29] Jonas Helsen, Xiao Xue, Lieven M. K. Vandersypen, and Stephanie Wehner. “A new class of efficient randomized benchmarking protocols”. In: *npj Quant. Inf.* 5, 71 (2019), p. 71. DOI: [10.1038/s41534-019-0182-7](#). arXiv: [1806.02048 \[quant-ph\]](#).
- [30] Jonas Helsen, Sepehr Nezami, Matthew Reagor, and Michael Walter. “Matchgate benchmarking: Scalable benchmarking of a continuous family of many-qubit gates”. In: *Quantum* 6 (2022), p. 657. DOI: [10.22331/q-2022-02-21-657](#). arXiv: [2011.13048 \[quant-ph\]](#).
- [31] Steven T. Flammia and Joel J. Wallman. “Efficient estimation of Pauli channels”. In: *ACM Transactions on Quantum Computing* 1 (2020), pp. 1–32. DOI: [10.1145/3408039](#). arXiv: [1907.12976 \[quant-ph\]](#).
- [32] Jay M. Gambetta et al. “Characterization of addressability by simultaneous randomized benchmarking”. In: *Phys. Rev. Lett.* 109.24, 240504 (2012), p. 240504. DOI: [10.1103/PhysRevLett.109.240504](#). arXiv: [1204.6308 \[quant-ph\]](#).
- [33] David C. McKay, Andrew W. Cross, Christopher J. Wood, and Jay M. Gambetta. “Correlated randomized benchmarking”. 2020. arXiv: [2003.02354 \[quant-ph\]](#).
- [34] Hsin-Yuan Huang, Richard Kueng, and John Preskill. “Predicting many properties of a quantum system from very few measurements”. In: *Nature Physics* 16 (2020), pp. 1050–1057. DOI: [10.1038/s41567-020-0932-7](#). arXiv: [2002.08953 \[quant-ph\]](#).

- [35] A. W. Harrow and R. A. Low. “Random quantum circuits are approximate 2-designs”. In: *Commun. Math. Phys.* 291.1 (2009), pp. 257–302. DOI: [10.1007/s00220-009-0873-6](#). arXiv: [0802.1919 \[quant-ph\]](#).
- [36] Winton G. Brown and Lorenza Viola. “Convergence rates for arbitrary statistical moments of random quantum circuits”. In: *Phys. Rev. Lett.* 104.25 (2010), p. 250501. DOI: [10.1103/PhysRevLett.104.250501](#). arXiv: [0910.0913](#).
- [37] Jonas Haferkamp, Felipe Montealegre-Mora, Markus Heinrich, Jens Eisert, David Gross, and Ingo Roth. “Quantum homeopathy works: efficient unitary designs with a system-size independent number of non-Clifford gates”. 2020. arXiv: [2002.09524 \[quant-ph\]](#).
- [38] Jonas Haferkamp and Nicholas Hunter-Jones. “Improved spectral gaps for random quantum circuits: large local dimensions and all-to-all interactions”. In: *Phys. Rev. A* 104.2, 022417 (2021), p. 022417. DOI: [10.1103/PhysRevA.104.022417](#). arXiv: [2012.05259 \[quant-ph\]](#).
- [39] Aram Harrow and Saeed Mehraban. “Approximate unitary t -designs by short random quantum circuits using nearest-neighbor and long-range gates”. 2018. arXiv: [1809.06957 \[quant-ph\]](#).
- [40] E. Derbyshire, J. Yago Malo, A. J. Daley, E. Kashefi, and P. Wallden. “Randomized benchmarking in the analogue setting”. In: *Quantum Sci. Technol.* 5.3, 034001 (2020), p. 034001. DOI: [10.1088/2058-9565/ab7eec](#). arXiv: [1909.01295 \[quant-ph\]](#).
- [41] Ryan Shaffer, Eli Megidish, Joseph Broz, Wei-Ting Chen, and Hartmut Häffner. “Practical verification protocols for analog quantum simulators”. In: *npj Quant. Inf.* 7, 46 (2021), p. 46. DOI: [10.1038/s41534-021-00380-8](#). arXiv: [2003.04500 \[quant-ph\]](#).
- [42] Joel J. Wallman and Joseph Emerson. “Noise tailoring for scalable quantum computation via randomized compiling”. In: *Phys. Rev. A* 94.5, 052325 (2016), p. 052325. DOI: [10.1103/PhysRevA.94.052325](#). arXiv: [1512.01098 \[quant-ph\]](#).
- [43] Andreas Elben, Steven T. Flammia, Hsin-Yuan Huang, Richard Kueng, John Preskill, Benoît Vermersch, and Peter Zoller. “The randomized measurement toolbox”. In: *Nat. Rev. Phys.* (2022). DOI: [10.1038/s42254-022-00535-2](#). arXiv: [2203.11374 \[quant-ph\]](#).
- [44] Kristan Temme, Sergey Bravyi, and Jay M. Gambetta. “Error mitigation for short-depth quantum circuits”. In: *Phys. Rev. Lett.* 119.18, 180509 (2017), p. 180509. DOI: [10.1103/PhysRevLett.119.180509](#). arXiv: [1612.02058 \[quant-ph\]](#).
- [45] Hsin-Yuan Huang, Richard Kueng, and John Preskill. “Predicting many properties of a quantum system from very few measurements”. In: *Nat. Phys.* 16.10 (2020), pp. 1050–1057. DOI: [10.1038/s41567-020-0932-7](#). arXiv: [2002.08953 \[quant-ph\]](#).
- [46] E. Knill. “Quantum computing with realistically noisy devices”. In: *Nature* 434.7029 (2005), pp. 39–44. DOI: [10.1038/nature03350](#). arXiv: [quant-ph/0410199 \[quant-ph\]](#).
- [47] Matthew Ware, Guilhem Ribeill, Diego Ristè, Colm A. Ryan, Blake Johnson, and Marcus P. da Silva. “Experimental Pauli-frame randomization on a superconducting qubit”. In: *Phys. Rev. A* 103.4, 042604 (2021), p. 042604. DOI: [10.1103/PhysRevA.103.042604](#). arXiv: [1803.01818 \[quant-ph\]](#).
- [48] Daniel Stilck França, Sergii Strelchuk, and Michał Studziński. “Efficient benchmarking and classical simulation of quantum processes in the Weyl basis”. In: *Phys. Rev. Lett.* 126.21, 210502 (2021), p. 210502. DOI: [10.1103/PhysRevLett.126.210502](#). arXiv: [2008.12250 \[quant-ph\]](#).
- [49] Alexander Erhard, Joel J. Wallman, Lukas Postler, Michael Meth, Roman Stricker, Esteban A. Martinez, Philipp Schindler, Thomas Monz, Joseph Emerson, and Rainer Blatt. “Characterizing large-scale quantum computers via cycle benchmarking”. In: *Nat. Commun.* 10, 5347 (2019), p. 5347. DOI: [10.1038/s41467-019-13068-7](#). arXiv: [1902.08543 \[quant-ph\]](#).
- [50] Yihong Zhang, Wenjun Yu, Pei Zeng, Guoding Liu, and Xiongfeng Ma. “Scalable fast benchmarking for individual quantum gates with local twirling”. arXiv: [2203.10320 \[quant-ph\]](#).
- [51] Steven T. Flammia. “Averaged circuit eigenvalue sampling”. 2021. arXiv: [2108.05803 \[quant-ph\]](#).

- [52] Timothy Proctor, Stefan Seritan, Kenneth Rudinger, Erik Nielsen, Robin Blume-Kohout, and Kevin Young. “Scalable randomized benchmarking of quantum computers using mirror circuits”. In: *Phys. Rev. Lett.* 129.15, 150502 (2022), p. 150502. DOI: [10.1103/PhysRevLett.129.150502](https://doi.org/10.1103/PhysRevLett.129.150502). arXiv: [2112.09853](https://arxiv.org/abs/2112.09853) [quant-ph].
- [53] Jonas Helsen, Marios Ioannou, Ingo Roth, Jonas Kitzinger, Emilio Onorati, Albert H. Werner, and Jens Eisert. “Estimating gate-set properties from random sequences”. 2021. arXiv: [2110.13178](https://arxiv.org/abs/2110.13178) [quant-ph].
- [54] Pedro Figueroa-Romero, Kavan Modi, and Min-Hsiu Hsieh. “Towards a general framework of randomized benchmarking incorporating non-Markovian noise”. In: *Quantum* 6 (2022), p. 868. DOI: [10.22331/q-2022-12-01-868](https://doi.org/10.22331/q-2022-12-01-868). arXiv: [2202.11338](https://arxiv.org/abs/2202.11338) [quant-ph].
- [55] William Fulton and Joe Harris. *Representation theory*. Vol. 129. Springer Science & Business Media, 2013. DOI: [10.1007/978-1-4612-0979-9](https://doi.org/10.1007/978-1-4612-0979-9).
- [56] T. Bröcker and T. tom Dieck. *Representations of Compact Lie Groups*. Graduate Texts in Mathematics. Berlin Heidelberg: Springer-Verlag, 1985. DOI: [10.1007/978-3-662-12918-0](https://doi.org/10.1007/978-3-662-12918-0).
- [57] Roe Goodman and Nolan R. Wallach. *Symmetry, Representations, and Invariants*. Graduate Texts in Mathematics. New York, NY: Springer, 2009. DOI: [10.1007/978-0-387-79852-3_1](https://doi.org/10.1007/978-0-387-79852-3_1).
- [58] Daniel Bump. *Lie Groups*. 1st ed. Graduate Texts in Mathematics. Springer New York, NY, 2004. DOI: [10.1007/978-1-4757-4094-3](https://doi.org/10.1007/978-1-4757-4094-3).
- [59] Gerald B. Folland. *A Course in Abstract Harmonic Analysis*. 2nd ed. New York: Chapman and Hall/CRC, 2015. 319 pp. DOI: [10.1201/b19172](https://doi.org/10.1201/b19172).
- [60] W. T. Gowers and O. Hatami. “Inverse and stability theorems for approximate representations of finite groups”. In: *Sb. Math.* 208.12 (2017), p. 1784. DOI: [10.1070/SM8872](https://doi.org/10.1070/SM8872). arXiv: [1510.04085](https://arxiv.org/abs/1510.04085) [math.GR].
- [61] Eiichi Bannai, Yoshifumi Nakata, Takayuki Okuda, and Da Zhao. “Explicit construction of exact unitary designs”. 2020. arXiv: [2009.11170](https://arxiv.org/abs/2009.11170) [math.CO].
- [62] John R. Stembridge. “Rational tableaux and the tensor algebra of \mathfrak{gl}_n ”. In: *Journal of Combinatorial Theory, Series A* 46.1 (1987), pp. 79–120. DOI: [10.1016/0097-3165\(87\)90077-X](https://doi.org/10.1016/0097-3165(87)90077-X).
- [63] John R. Stembridge. “A combinatorial theory for rational actions of GL_n ”. In: *Invariant theory (Denton, TX, 1986)*. Vol. 88. Contemp. Math. Amer. Math. Soc., Providence, RI, 1989, pp. 163–176. DOI: [10.1090/conm/088/999989](https://doi.org/10.1090/conm/088/999989).
- [64] G. Benkart, M. Chakrabarti, T. Halverson, R. Leduc, C. Y. Lee, and J. Stroome. “Tensor product representations of general linear groups and their connections with brauer algebras”. In: *Journal of Algebra* 166.3 (1994), pp. 529–567. DOI: [10.1006/jabr.1994.1166](https://doi.org/10.1006/jabr.1994.1166).
- [65] Aidan Roy and A. J. Scott. “Unitary designs and codes”. In: *Des. Codes Cryptogr.* 53.1 (2009), pp. 13–31. DOI: [10.1007/s10623-009-9290-2](https://doi.org/10.1007/s10623-009-9290-2). arXiv: [0809.3813](https://arxiv.org/abs/0809.3813) [math.CO].
- [66] Persi Diaconis and Laurent Saloff-Coste. “Comparison techniques for random walk on finite groups”. In: *The Annals of Probability* 21.4 (1993). Publisher: Institute of Mathematical Statistics, pp. 2131–2156. DOI: [10.1214/aop/1176989013](https://doi.org/10.1214/aop/1176989013).
- [67] Péter Pál Varjú. “Random walks in compact groups”. In: *Doc. Math.* 18 (2012), pp. 1137–1175. arXiv: [1209.1745](https://arxiv.org/abs/1209.1745) [math.GR].
- [68] Markus Heinrich. “On stabiliser techniques and their application to simulation and certification of quantum devices”. PhD thesis. University of Cologne, 2021. URL: <https://kups.ub.uni-koeln.de/50465/>.
- [69] Markus Neuhauser. “An explicit construction of the metaplectic representation over a finite field”. In: *Journal of Lie Theory* 12.1 (2002), pp. 15–30. URL: <http://eudml.org/doc/123051>.
- [70] Gabriele Nebe, E. M. Rains, and N. J. A. Sloane. “The invariants of the Clifford groups”. In: *Des. Codes Cryptogr.* 24 (2001). arXiv: [math/0001038](https://arxiv.org/abs/math/0001038) [math.CO].

- [71] H. Zhu, R. Kueng, M. Grassl, and D. Gross. “The Clifford group fails gracefully to be a unitary 4-design”. 2016. arXiv: [1609.08172 \[quant-ph\]](#).
- [72] D. P. DiVincenzo, D. W. Leung, and B. M. Terhal. “Quantum data hiding”. In: *IEEE Trans. Inf. Th.* 48.3 (2002), pp. 580–598. DOI: [10.1109/18.985948](#). arXiv: [quant-ph/0103098 \[quant-ph\]](#).
- [73] Zak Webb. “The Clifford group forms a unitary 3-design”. In: *Quantum Info. Comput.* 16.15-16 (2016), pp. 1379–1400. arXiv: [1510.02769 \[quant-ph\]](#).
- [74] Huangjun Zhu. “Multiqubit Clifford groups are unitary 3-designs”. In: *Phys. Rev. A* 96 (6 2017), p. 062336. DOI: [10.1103/PhysRevA.96.062336](#). arXiv: [1510.02619 \[quant-ph\]](#).
- [75] Jonas Helsen, Joel J. Wallman, and Stephanie Wehner. “Representations of the multi-qubit Clifford group”. In: *J. Math. Phys.* 59.7 (2018), p. 072201. DOI: [10.1063/1.4997688](#). arXiv: [1609.08188 \[quant-ph\]](#).
- [76] Robert Guralnick and Pham Tiep. “Decompositions of small tensor powers and Larsen’s conjecture”. In: *Represent. Theory* 9.5 (2005), pp. 138–208. DOI: [10.1090/S1088-4165-05-00192-5](#). arXiv: [math/0502080 \[math.GR\]](#).
- [77] Eiichi Bannai, Gabriel Navarro, Noelia Rizo, and Pham Huu Tiep. “Unitary t -groups”. In: *J. Math. Soc. Japan* 72.3 (2020), pp. 909–921. DOI: [10.2969/jmsj/82228222](#). arXiv: [1810.02507 \[math.RT\]](#).
- [78] Felipe Montealegre-Mora and David Gross. “Rank-deficient representations in the theta correspondence over finite fields arise from quantum codes”. In: *Represent. Theory* 25.8 (2021), pp. 193–223. DOI: [10.1090/ert/563](#). arXiv: [1906.07230 \[math.RT\]](#).
- [79] Felipe Montealegre-Mora and David Gross. “Duality theory for Clifford tensor powers”. 2022. arXiv: [2208.01688 \[quant-ph\]](#).
- [80] Shayne F. D. Waldron. *An Introduction to Finite Tight Frames*. 1st ed. Applied and Numerical Harmonic Analysis. Birkhäuser New York, NY, 2018. DOI: [10.1007/978-0-8176-4815-2](#).
- [81] G. W. Stewart and Ji-guang Sun. *Matrix Perturbation Theory*. Elsevier Science, 1990. URL: <https://shop.elsevier.com/books/matrix-perturbation-theory/stewart/978-0-08-092613-1>.
- [82] Robin Harper, Ian Hincks, Chris Ferrie, Steven T. Flammia, and Joel J. Wallman. “Statistical analysis of randomized benchmarking”. In: *Phys. Rev. A* 99 (2019), p. 052350. DOI: [10.1103/PhysRevA.99.052350](#). arXiv: [1901.00535 \[quant-ph\]](#).
- [83] John Watrous. *The Theory of Quantum Information*. Cambridge University Press, 2018. DOI: [10.1017/9781316848142](#).
- [84] Joel J Wallman, Marie Barnhill, and Joseph Emerson. “Robust characterization of leakage errors”. In: *New J. Phys.* 18.4 (2016), p. 043021. DOI: [10.1088/1367-2630/18/4/043021](#). arXiv: [1412.4126 \[quant-ph\]](#).
- [85] R. Roy, A. Paulraj, and T. Kailath. “Estimation of signal parameters via rotational invariance techniques - ESPRIT”. In: *MILCOM 1986 - IEEE Military Communications Conference: Communications-Computers: Teamed for the 90’s*. MILCOM 1986 - IEEE Military Communications Conference: Communications-Computers: Teamed for the 90’s. Vol. 3. 1986, pp. 41.6.1–41.6.5. DOI: [10.1109/MILCOM.1986.4805850](#).
- [86] Piotr Ćwikliński, Michał Horodecki, Marek Mozrzyms, Lukasz Pankowski, and Michał Studziński. “Local random quantum circuits are approximate polynomial-designs - numerical results”. In: *J. Phys. A: Math. Theor.* 46.30 (2013), p. 305301. DOI: [10.1088/1751-8113/46/30/305301](#). arXiv: [1212.2556 \[quant-ph\]](#).
- [87] Dorit Aharonov, Itai Arad, Zeph Landau, and Umesh Vazirani. “The detectability lemma and quantum gap amplification”. In: *Proceedings of the Forty-First Annual ACM Symposium on Theory of Computing*. STOC ‘09, 2009, p. 417. arXiv: [0811.3412 \[quant-ph\]](#).
- [88] Anurag Anshu, Itai Arad, and Thomas Vidick. “A simple proof of the detectability lemma and spectral gap amplification”. In: *Phys. Rev. B* 93.20 (2016), p. 205142. DOI: [10.1103/PhysRevB.93.205142](#). arXiv: [1602.01210](#).

- [89] Jonas Haferkamp. Private Communication. 2022.
- [90] E. Onorati, O. Buerschaper, M. Kliesch, W. Brown, A. H. Werner, and J. Eisert. “Mixing properties of stochastic quantum Hamiltonians”. In: *Comm. Math. Phys.* 355 (2017), pp. 905–947. DOI: [10.1007/s00220-017-2950-6](#). arXiv: [1606.01914 \[quant-ph\]](#).
- [91] Sergey Bravyi, Joseph A. Latone, and Dmitri Maslov. “6-qubit optimal Clifford circuits”. 2020. arXiv: [2012.06074 \[quant-ph\]](#).
- [92] Sergey Bravyi and Dmitri Maslov. “Hadamard-free circuits expose the structure of the Clifford group”. 2020. arXiv: [2003.09412 \[quant-ph\]](#).
- [93] Sergio Boixo, Sergei V. Isakov, Vadim N. Smelyanskiy, Ryan Babbush, Nan Ding, Zhang Jiang, Michael J. Bremner, John M. Martinis, and Hartmut Neven. “Characterizing quantum supremacy in near-term devices”. In: *Nature Physics* 14 (2018), pp. 595–600. DOI: [10.1038/s41567-018-0124-x](#). arXiv: [1608.00263 \[quant-ph\]](#).
- [94] Hong-Ye Hu, Soonwon Choi, and Yi-Zhuang You. “Classical shadow tomography with locally scrambled quantum dynamics”. 2021. arXiv: [2107.04817 \[quant-ph\]](#).
- [95] Kaifeng Bu, Dax Enshan Koh, Roy J. Garcia, and Arthur Jaffe. “Classical shadows with Pauli-invariant unitary ensembles”. 2022. arXiv: [2202.03272 \[quant-ph\]](#).
- [96] Ahmed A. Akhtar, Hong-Ye Hu, and Yi-Zhuang You. “Scalable and flexible classical shadow tomography with tensor networks”. 2022. arXiv: [2209.02093 \[quant-ph\]](#).
- [97] Christian Bertoni, Jonas Haferkamp, Marcel Hinsche, Marios Ioannou, Jens Eisert, and Hakop Pashayan. “Shallow shadows: expectation estimation using low-depth random Clifford circuits”. 2022. arXiv: [2209.12924 \[quant-ph\]](#).
- [98] Mirko Arienzo, Markus Heinrich, Ingo Roth, and Martin Kliesch. *Closed-form analytic expressions for shadow estimation with brickwork circuits*. 2022. DOI: [10.48550/arXiv.2211.09835](#). arXiv: [2211.09835 \[quant-ph\]](#).
- [99] Yulin Wu et al. “Strong quantum computational advantage using a superconducting quantum processor”. In: *Phys. Rev. Lett.* 127.18 (2021), p. 180501. DOI: [10.1103/PhysRevLett.127.180501](#). arXiv: [2106.14734 \[quant-ph\]](#).
- [100] Qingling Zhu et al. *Quantum Computational Advantage via 60-Qubit 24-Cycle Random Circuit Sampling*. 2021. DOI: [10.48550/arXiv.2109.03494](#). arXiv: [2109.03494 \[quant-ph\]](#).
- [101] Abhinav Deshpande, Pradeep Niroula, Oles Shtanko, Alexey V. Gorshkov, Bill Fefferman, and Michael J. Gullans. *Tight bounds on the convergence of noisy random circuits to the uniform distribution*. 2021. arXiv: [2112.00716 \[quant-ph\]](#).
- [102] F. G. S. L. Brandão, A. W. Harrow, and M. Horodecki. “Local random quantum circuits are approximate polynomial-designs”. In: *Commun. Math. Phys.* 346.2 (2016), pp. 397–434. DOI: [10.1007/s00220-016-2706-8](#). arXiv: [1208.0692](#).
- [103] Jonas Haferkamp. “Random quantum circuits are approximate unitary t -designs in depth $O(nt^{5+o(1)})$ ”. In: *Quantum* 6 (2022), p. 795. DOI: [10.22331/q-2022-09-08-795](#).
- [104] Scott Aaronson. “Shadow tomography of quantum states”. In: *Proc. 50th Ann. ACM SIGACT Symp. Th. Comput.* 2018, pp. 325–338. arXiv: [1711.01053 \[quant-ph\]](#).
- [105] Yanwu Gu, Rajesh Mishra, Berthold-Georg Englert, and Hui Khoon Ng. “Randomized linear gate-set tomography”. In: *PRX Quantum* 2 (3 2021), p. 030328. DOI: [10.1103/PRXQuantum.2.030328](#). arXiv: [2010.12235 \[quant-ph\]](#).
- [106] Raphael Brieger, Ingo Roth, and Martin Kliesch. “Compressive gate set tomography”. 2021. arXiv: [2112.05176 \[quant-ph\]](#).
- [107] Persi Diaconis and Mehrdad Shahshahani. “On the eigenvalues of random matrices”. In: *Journal of Applied Probability* 31 (1994), pp. 49–62. DOI: [10.2307/3214948](#).
- [108] E. M. Rains. “Increasing subsequences and the classical groups”. In: *The Electronic Journal of Combinatorics* (1998), R12–R12. DOI: [10.37236/1350](#).

- [109] A. J. Scott. “Optimizing quantum process tomography with unitary 2-designs”. In: *J. Phys. A: Math. Theor.* 41.5 (2008), p. 055308. DOI: [10.1088/1751-8113/41/5/055308](https://doi.org/10.1088/1751-8113/41/5/055308). arXiv: [0711.1017](https://arxiv.org/abs/0711.1017) [quant-ph].
- [110] Alexander M. Dalzell, Nicholas Hunter-Jones, and Fernando G. S. L. Brandão. “Random quantum circuits anti-concentrate in log depth”. In: *PRX Quantum* 3.1 (2022). DOI: [10.1103/PRXQuantum.3.010333](https://doi.org/10.1103/PRXQuantum.3.010333). arXiv: [2011.12277](https://arxiv.org/abs/2011.12277) [quant-ph].
- [111] Ralph Byers and Daniel Kressner. “Structured condition numbers for invariant subspaces”. In: *SIAM J. Matrix Anal. Appl.* 28.2 (2006), pp. 326–347. DOI: [10.1137/050637601](https://doi.org/10.1137/050637601).
- [112] Michael Karow and Daniel Kressner. “On a perturbation bound for invariant subspaces of matrices”. In: *SIAM J. Matrix Anal. Appl.* 35.2 (2014). Publisher: Society for Industrial and Applied Mathematics, pp. 599–618. DOI: [10.1137/130912372](https://doi.org/10.1137/130912372).

Appendices

A Different estimators and their variances

For our analysis, we use a mean estimator, defined in Eq. (3) as

$$\hat{F}_\lambda(m) = \frac{1}{N} \sum_{l=1}^N f_\lambda(i^{(l)}, g_1^{(l)} \cdots g_m^{(l)}). \quad (73)$$

Importantly, we assume that samples are taking iid from the joint distribution $dp(i, g_1, \dots, g_m) = p(i|g_1, \dots, g_m) d\nu(g_1) \dots d\nu(g_m)$, i.e. a random circuit is sampled from $\nu^{\times m}$, and then measured once to obtain a sample from the outcome distribution.

More generally, one may sample N_C random circuits, and then measure each circuit N_M times. Such an approach can have experimental advantages depending on the platform, and the degree and flexibility of control automation. In principle, running the same circuit many times can be optimized for high sampling rates on a hardware level, while changing the circuit in each run may pose an additional classical control overhead. However, many modern quantum devices can be automatically programmed, thus performing a different circuit in each run is not necessarily more resource-intensive. Nevertheless, using a smaller number of random circuits may crucially reduce the runtime and memory consumption required for post-processing in large-scale benchmarking approaches.

That being said, the statistics also behave differently. If each circuit is sampled N_M times, we obtain an estimator of the form

$$\hat{\mathcal{F}}_\lambda(m) = \frac{1}{N_C N_M} \sum_{l=1}^{N_C} \sum_{k=1}^{N_M} f_\lambda(i^{(k,l)}, g_1^{(l)} \cdots g_m^{(l)}).$$

Note that the samples $i^{(k,l)}$ for the same l are conditioned on the same circuit, and thus the variance of $\hat{\mathcal{F}}_\lambda(m)$ is not simply $\text{Var}[f_\lambda]/N_C N_M$. Instead, we have to use the law of total variance, which allows us to use conditional expected values and variances:

$$\text{Var}[\hat{\mathcal{F}}_\lambda(m)] = \frac{1}{N_C} \left(\frac{1}{N_M} \mathbb{E}_{g_j} \text{Var}[f_\lambda(i, g_j) | g_j] + \text{Var}_{g_j} \mathbb{E}_i[f_\lambda(i, g_j) | g_j] \right) \quad (74)$$

$$\begin{aligned} &= \frac{1}{N_C} \left(\frac{1}{N_M} \mathbb{E}_{g_j} (\mathbb{E}_i[f_\lambda(i, g_j)^2 | g_j] - \mathbb{E}_i[f_\lambda(i, g_j) | g_j]^2) + \right. \\ &\quad \left. + \mathbb{E}_{g_j} (\mathbb{E}_i[f_\lambda(i, g_j) | g_j]^2) - (\mathbb{E}_{g_j} \mathbb{E}_i[f_\lambda(i, g_j) | g_j])^2 \right) \\ &= \frac{1}{N_C} \left(\frac{1}{N_M} \mathbb{E}_{g_j} \mathbb{E}_i[f_\lambda(i, g_j)^2 | g_j] + \right. \\ &\quad \left. + \left(1 - \frac{1}{N_M}\right) \mathbb{E}_{g_j} \mathbb{E}_i[f_\lambda(i, g_j) | g_j]^2 - (\mathbb{E}_{g_j} \mathbb{E}_i[f_\lambda(i, g_j) | g_j])^2 \right). \quad (75) \end{aligned}$$

Hence, $\text{Var}[\hat{\mathcal{F}}_\lambda(m)]$ consists of three terms: The first and second moment of the filter function, $\mathbb{E}[f_\lambda]$ and $\mathbb{E}[f_\lambda^2]$, respectively, which give the variance of the estimator (73) and are thus discussed in the main text. The middle term in Eq. (75) gives an additional contribution if $N_M > 1$, i.e. if more than one sample is taken per circuit. In terms of the random circuit ensemble, it corresponds to a *fourth moment*, while the other two terms correspond to second and third moments.

In terms of sample complexity, it does not seem advantageous to choose $N_M > 1$. For instance, if we sample Haar-randomly from the unitary group, then one can check that

$$\begin{aligned}\mathbb{E}_{g_j} \text{Var}[f_\lambda(i, g_j) | g_j] &= 2 \frac{d^2 - 1}{(d+2)(d+3)}, & \text{Var}_{g_j} \mathbb{E}_i[f_\lambda(i, g_j) | g_j] &= 4 \frac{d-1}{(d+2)(d+3)}, \\ \text{Var}[f_\lambda^2] &= 2 \frac{d-1}{d+2}.\end{aligned}$$

(Some of these expressions are computed in App. C.1.) Hence, comparing $\text{Var}[\hat{\mathcal{F}}_\lambda(m)]$ with $\text{Var}[\hat{F}_\lambda(m)] = \text{Var}[f_\lambda^2]/N$ for $N = N_C N_M$, one can readily verify that $\text{Var}[\hat{\mathcal{F}}_\lambda(m)]$ is larger for any value of N_C and N_M . More precisely, the difference is of order $O((1/N_C - 1/N)/d)$. Hence if d is small (say less than 10 qubits) and the total number of samples N is fixed, choosing $N_M = 1$ is clearly optimal. If instead N_C is fixed, then increasing N_M far beyond d does not improve the accuracy of the estimator. Moreover, if d is very large, then the second term in Eq. (74) is negligible and thus $\text{Var}[\hat{\mathcal{F}}_\lambda(m)] = O(1/N) = \text{Var}[\hat{F}_\lambda(m)]$. In this regime, the difference between the two estimators in terms of sampling complexity can be neglected.

In principle, the arguments in Sec. 5.4 can be adapted to also treat the middle term in Eq. (75) perturbatively, as we have done it in Thm. 10. However, in this case many more irreps, and thus terms, appear, which makes the analysis more difficult. We think that a sampling complexity theorem for the estimator $\text{Var}[\hat{\mathcal{F}}_\lambda(m)]$ similar to Thm. 16 can be formulated, but we expect the guarantees to be worse than for $\text{Var}[\hat{F}_\lambda(m)]$.

B Matrix perturbation theory

In this section, we review some results in matrix perturbation theory by Stewart and Sun [81] and derive the corollaries needed to prove our main results. To this end, we introduce some definitions. First, we call a family of norms $\|\cdot\|$ on matrices $\mathbb{C}^{n \times m}$ *matrix norms*, if it is submultiplicative w.r.t. to matrix multiplication; i.e. if $M \in \mathbb{C}^{n \times m}$ and $N \in \mathbb{C}^{m \times k}$, then $\|MN\| \leq \|M\| \|N\|$. The *separation function* between two square matrices $A \in \mathbb{C}^{n \times n}$ and $B \in \mathbb{C}^{m \times m}$ is given by

$$\text{sep}(A, B) := \inf_{\|P\|=1} \|AP - PB\|,$$

where the infimum is taken over all matrices $P \in \mathbb{C}^{n \times m}$. The separation function is stable and continuous in the sense that [81, Theorem 2.5, p. 234]

$$\text{sep}(A, B) - \|E\| - \|F\| \leq \text{sep}(A + E, B + F) \leq \text{sep}(A, B) + \|E\| + \|F\|. \quad (76)$$

Following Ref. [81], we say that $A \in \mathbb{C}^{n \times n}$ has a *spectral resolution* if there is a block-diagonal decomposition of the form

$$[Y_1 \ Y_2]^\dagger A [X_1 \ X_2] = \begin{bmatrix} A_1 & 0 \\ 0 & A_2 \end{bmatrix},$$

for matrices X_i, Y_j with $Y_i^\dagger X_j = \delta_{i,j} \mathbb{1}$, and $A_i = Y_i^\dagger A X_i$. In this context, we write $E_{i,j} := Y_i^\dagger E X_j$ for any matrix E .

The separation function can be used to quantify the effect of small additive perturbations on a spectral resolution as follows.

Theorem 23 ([81, Theorem 2.8, p. 238]). *Let A be a matrix with spectral resolution*

$$[Y_1 \ Y_2]^\dagger A [X_1 \ X_2] = \begin{bmatrix} A_1 & 0 \\ 0 & A_2 \end{bmatrix},$$

$\|\cdot\|$ be a matrix norm and E some other matrix (perturbation). Suppose we have

$$\delta := \text{sep}(A_1, A_2) - \|E_{11}\| - \|E_{22}\| > 0, \quad \text{and} \quad \frac{\|E_{21}\| \|E_{12}\|}{\delta^2} < \frac{1}{4},$$

then there exist a unique matrix P fulfilling

$$P(A_1 + E_{11}) - (A_2 + E_{22})P = E_{21} - PE_{12}P, \quad (77)$$

and $\|P\| < 2 \frac{\|E_{21}\|}{\delta}$, such that the matrices

$$\begin{aligned} \tilde{X}_1 &:= X_1 + X_2 P, & \tilde{A}_1 &:= A_1 + E_{11} + E_{12} P, \\ \tilde{Y}_2 &:= Y_2 - Y_1 P^\dagger, & \tilde{A}_2 &:= A_2 + E_{22} - PE_{12}, \end{aligned}$$

fulfill

$$(A + E)\tilde{X}_1 = \tilde{X}_1\tilde{A}_1, \quad \tilde{Y}_2^\dagger(A + E) = \tilde{A}_2\tilde{Y}_2^\dagger. \quad (78)$$

Remark 1 (Perturbation of real matrices). Note that Theorem 23 can also be used for real matrices: Suppose A is a real matrix with spectral resolution given by real matrices X_i, Y_j with $Y_i^T X_j = \delta_{i,j} \mathbb{1}$, and E is a real perturbation. Let P be the matrix produced by Thm. 23. Then, complex conjugation of the defining Eq. (77) shows that \bar{P} is also a solution to Eq. (77). Since the solution is unique, we have $\bar{P} = P$ and hence P is real, as well as the matrices \tilde{X}_i, \tilde{Y}_i , and \tilde{A}_i .

For the following discussion, we denote $\tilde{Y}_1 := Y_1$ and $\tilde{X}_2 := X_2$. Then also \tilde{X} and \tilde{Y} satisfy the orthogonality relations $\tilde{Y}_i^\dagger \tilde{X}_j = \delta_{i,j} \mathbb{1}$. In block matrix notation we then have

$$[\tilde{X}_1 \tilde{X}_2] := [X_1 X_2] \begin{bmatrix} \mathbb{1} & 0 \\ P & \mathbb{1} \end{bmatrix}, \quad [\tilde{Y}_1 \tilde{Y}_2] := [Y_1 Y_2] \begin{bmatrix} \mathbb{1} & -P^\dagger \\ 0 & \mathbb{1} \end{bmatrix}. \quad (79)$$

Moreover, the subspace conditions (78) translate to

$$\begin{aligned} [\tilde{Y}_1 \tilde{Y}_2]^\dagger (A + E) [\tilde{X}_1 \tilde{X}_2] &= \begin{bmatrix} \tilde{Y}_1^\dagger (A + E) \tilde{X}_1 & \tilde{Y}_1^\dagger (A + E) \tilde{X}_2 \\ \tilde{Y}_2^\dagger (A + E) \tilde{X}_1 & \tilde{Y}_2^\dagger (A + E) \tilde{X}_2 \end{bmatrix} \\ &= \begin{bmatrix} \tilde{Y}_1^\dagger \tilde{X}_1 \tilde{A}_1 & Y_1^\dagger (A + E) X_2 \\ \tilde{Y}_2^\dagger \tilde{X}_1 \tilde{A}_1 & \tilde{A}_2 \tilde{Y}_2^\dagger \tilde{X}_2 \end{bmatrix} = \begin{bmatrix} \tilde{A}_1 & E_{12} \\ 0 & \tilde{A}_2 \end{bmatrix}. \end{aligned}$$

Of course an analogous perturbation theorem holds when changing the roles of perturbed right- and left-invariant subspaces. To keep track of the notation let us write this down explicitly.

Corollary 24 (Flipped version). *Let A be a matrix with spectral resolution*

$$[Y_1 Y_2]^\dagger A [X_1 X_2] = \begin{bmatrix} A_1 & 0 \\ 0 & A_2 \end{bmatrix},$$

$\|\cdot\|$ be a matrix norm and E some other matrix (perturbation). Suppose we have

$$\delta := \text{sep}(A_1, A_2) - \|E_{11}\| - \|E_{22}\| > 0, \quad \text{and} \quad \frac{\|E_{21}\| \|E_{12}\|}{\delta^2} < \frac{1}{4},$$

then there exist a unique matrix P with $\|P\| < 2 \frac{\|E_{12}\|}{\delta}$ such that the matrices

$$\begin{aligned} [\tilde{X}_1 \tilde{X}_2] &:= [X_1 X_2] \begin{bmatrix} \mathbb{1} & P \\ 0 & \mathbb{1} \end{bmatrix}, & [\tilde{Y}_1 \tilde{Y}_2] &:= [Y_1 Y_2] \begin{bmatrix} \mathbb{1} & 0 \\ -P^\dagger & \mathbb{1} \end{bmatrix}, \\ \tilde{A}_1 &:= A_1 + E_{11} - PE_{21}, & \tilde{A}_2 &:= A_2 + E_{22} + E_{21}P. \end{aligned} \quad (80)$$

fulfil $\tilde{Y}_i^\dagger \tilde{X}_j = \delta_{i,j} \mathbb{1}$ and give rise to the following decomposition of the perturbed operator $A + E$:

$$[\tilde{Y}_1 \tilde{Y}_2]^\dagger (A + E) [\tilde{X}_1 \tilde{X}_2] = \begin{bmatrix} \tilde{A}_1 & 0 \\ E_{21} & \tilde{A}_2 \end{bmatrix}. \quad (81)$$

Proof. We apply Theorem 23 to A^\dagger and use the corresponding norm $\|(\cdot)^\dagger\|$. More explicitly, we take adjoints of the equations in the theorem and make the following replacements: $A \rightarrow A^\dagger$, $X \rightarrow Y$, $Y \rightarrow X$, similarly for the quantities with a tilde, $E \rightarrow E^\dagger$, $P \rightarrow -P^\dagger$ and $\|\cdot\| \rightarrow \|(\cdot)^\dagger\|$. This yields the claimed bounds. Moreover,

$$\tilde{Y}_1^\dagger(A + E) = \tilde{A}_1 \tilde{Y}_1^\dagger, \quad (A + E)\tilde{X}_2 = \tilde{X}_2 \tilde{A}_2,$$

where

$$\tilde{Y}_1 := Y_1 - Y_2 P^\dagger, \quad \tilde{A}_1 := A_1 + E_{11} - P E_{21}, \quad (82)$$

$$\tilde{X}_2 := X_2 + X_1 P, \quad \tilde{A}_2 := A_2 + E_{22} + E_{21} P. \quad (83)$$

Denoting $\tilde{X}_1 := X_1$ and $\tilde{Y}_2 := Y_2$ we have again $\tilde{Y}_i^\dagger \tilde{X}_j = \delta_{ij} \mathbb{1}$. Moreover, this yields the result in block matrix notation as stated in the corollary. \square

Concatenating both versions of the perturbation theorem, gives us an expression for the entire spectral resolution of the perturbation (see also the analogous derivation in Ref. [9]).

Theorem 25 (Two-sided version). *Let a matrix A have a spectral resolution*

$$[Y_1 \ Y_2]^\dagger A [X_1 \ X_2] = \begin{bmatrix} A_1 & 0 \\ 0 & A_2 \end{bmatrix},$$

$\|\cdot\|$ be a matrix norm and E some other matrix (perturbation). If

$$\delta := \text{sep}(A_1, A_2) - \|E_{11}\| - \|E_{22}\| > 0, \quad \text{and} \quad \frac{\|E_{21}\| \|E_{12}\|}{\delta^2} < \frac{1}{4}$$

then there exist unique matrices P_1, P_2 satisfying

$$\|P_1\| < 2 \frac{\|E_{21}\|}{\delta}, \quad \|P_2\| < 2 \frac{\|E_{12}\|}{\delta \left(1 - 4 \frac{\|E_{21}\| \|E_{12}\|}{\delta^2}\right)} \quad (84)$$

such that the matrices

$$\begin{aligned} [\tilde{X}_1 \ \tilde{X}_2] &= [X_1 \ X_2] \begin{bmatrix} \text{Id} & 0 \\ P_1 & \text{Id} \end{bmatrix} \begin{bmatrix} \text{Id} & P_2 \\ 0 & \text{Id} \end{bmatrix}, & [\tilde{Y}_1 \ \tilde{Y}_2]^\dagger &= \begin{bmatrix} \text{Id} & -P_2 \\ 0 & \text{Id} \end{bmatrix} \begin{bmatrix} \text{Id} & 0 \\ -P_1 & \text{Id} \end{bmatrix} [Y_1 \ Y_2]^\dagger, \\ \tilde{A}_1 &= A_1 + E_{11} + E_{12} P_1, & \tilde{A}_2 &= A_2 + E_{22} - P_1 E_{12}, \end{aligned}$$

fulfil $\tilde{Y}_i^\dagger \tilde{X}_j = \delta_{ij} \mathbb{1}$ and give rise to the spectral resolution

$$[\tilde{Y}_1 \ \tilde{Y}_2]^\dagger (A + E) [\tilde{X}_1 \ \tilde{X}_2] = \begin{bmatrix} \tilde{A}_1 & 0 \\ 0 & \tilde{A}_2 \end{bmatrix}. \quad (85)$$

Proof. We look at the output of the standard version of the perturbation statement, Theorem 23. There we have

$$[\tilde{Y}_1 \ \tilde{Y}_2]^\dagger (A + E) [\tilde{X}_1 \ \tilde{X}_2] = \begin{bmatrix} \tilde{A}_1 & E_{12} \\ 0 & \tilde{A}_2 \end{bmatrix},$$

with the existence of a matrix P_1 describing the perturbation between the invariant subspaces. In order to deal with the off-diagonal element E_{12} , let $\tilde{A} = \begin{bmatrix} \tilde{A}_1 & 0 \\ 0 & \tilde{A}_2 \end{bmatrix}$ and consider $F = \begin{bmatrix} 0 & E_{12} \\ 0 & 0 \end{bmatrix}$ as its perturbation, i.e., $F_{11} = F_{22} = F_{21} = 0$ and $F_{12} = E_{12}$.

We can apply Corollary 24 (flipped version) if

$$\delta' := \text{sep}(\tilde{A}_1, \tilde{A}_2)$$

is large enough. Using the stability, cp. Eq. (76), of the separation function, i.e.

$$|\text{sep}(A_1 + B_1, A_2 + B_2) - \text{sep}(A_1, A_2)| \leq \|B_1\| + \|B_2\|,$$

and the expressions for \tilde{A}_1 and \tilde{A}_2 from the first perturbation step, we find that

$$\begin{aligned}\delta' &\geq \text{sep}(A_1, A_2) - \|E_{11} + E_{12}P_1\| - \|E_{22} - P_1E_{12}\| \\ &\geq \text{sep}(A_1, A_2) - \|E_{11}\| - \|E_{22}\| - 2\|P_1\|\|E_{12}\| \\ &\geq \delta - 4\frac{\|E_{21}\|\|E_{12}\|}{\delta},\end{aligned}$$

where in the last step we have used the norm-bound for P_1 and the definition of δ from the first step of the perturbation. Thus, $\delta' > 0$ is ensured if

$$\frac{1}{4} > \frac{\|E_{21}\|\|E_{12}\|}{\delta^2},$$

which is the condition from the first perturbation step. The other condition for applying Corollary 24 (flipped version) is trivially fulfilled since $\|F_{21}\| = 0$. Thus, we established the existence of P_2 with

$$\|P_2\| \leq 2\frac{\|E_{12}\|}{\delta'}$$

giving rise to the stated condition.

The final expressions for \tilde{A}_i and the decomposition (85) follow from the fact that $F = \begin{bmatrix} 0 & E_{12} \\ 0 & 0 \end{bmatrix}$ does not contribute in (82), (83) and (81). The statements for the perturbed invariant eigenspaces follows by combining the individual ones (79) and (80). The orthogonality relation follows by straightforward inspection. \square

It will also be useful to have a specialized perturbation result for *moment operators* of random quantum circuits, where the perturbation is controlled in spectral norm.

Theorem 26 (Perturbation of a moment operator). *Consider a moment operator, i.e., an operator A with spectral decomposition*

$$A = [X_1 \ X_2] \begin{bmatrix} \text{Id} & 0 \\ 0 & \Lambda \end{bmatrix} [X_1 \ X_2]^\dagger,$$

where $[X_1 \ X_2]$ is unitary. Suppose that $\|\Lambda\|_\infty \leq 1 - \Delta$ for some $\Delta \in (0, 1]$. Let E be a (potentially non-Hermitian) perturbation bounded as $\|E\|_\infty < \Delta/4$ with blocks $E_{ij} = X_i^\dagger EX_j$ w.r.t. the spectral decomposition of A . Then, there exist unique matrices P_1 and P_2 with $\|P_1\|_\infty < 4\|E\|_\infty/\Delta$ and $\|P_2\|_\infty < \frac{2\|E\|_\infty}{\Delta - 4\|E\|_\infty}$ such that

$$A + E = R_{\lambda,1} I L_{\lambda,1}^\dagger + R_{\lambda,2} O L_{\lambda,2}^\dagger, \quad I = \text{Id} + E_{11} + E_{12}P_1, \quad O = \Lambda + E_{22} - P_1E_{12}, \quad (86)$$

where the operators R_i and L_j are given by

$$[R_{\lambda,1} \ R_{\lambda,2}] = [X_1 \ X_2] \begin{bmatrix} \text{Id} & 0 \\ P_1 & \text{Id} \end{bmatrix} \begin{bmatrix} \text{Id} & P_2 \\ 0 & \text{Id} \end{bmatrix}, \quad [L_{\lambda,1} \ L_{\lambda,2}]^\dagger = \begin{bmatrix} \text{Id} & -P_2 \\ 0 & \text{Id} \end{bmatrix} \begin{bmatrix} \text{Id} & 0 \\ -P_1 & \text{Id} \end{bmatrix} [X_1 \ X_2]^\dagger. \quad (87)$$

In particular, the operators fulfill $R_i^\dagger L_j = \delta_{ij} \text{id}_i$ and $R_i L_j^\dagger = \delta_{ij} \Pi_i$, where $\text{id}_i = X_i^\dagger X_i$ and $\Pi_i = X_i X_i^\dagger$ are the identity on the i -th eigenspace and the projector onto the i -th eigenspace, respectively. Moreover, the following bounds hold:

$$\begin{aligned}\|I - \text{Id}\|_\infty &< 2\|E\|_\infty, \quad \|O - \Lambda\|_\infty < 2\|E\|_\infty, \quad \text{sep}(I, O) \geq \Delta - 4\|E\|_\infty > 0, \\ \|L_{\lambda,2}\|_\infty \|R_{\lambda,2}\|_\infty &\leq \frac{\|E\|_\infty}{\Delta} \left(1 - \frac{\|E\|_\infty}{\Delta}\right) + \frac{1 + \|E\|_\infty/\Delta}{1 - 4\|E\|_\infty/\Delta}.\end{aligned}$$

Finally, if A and E are real matrices, and $[X_1 \ X_2]$ is a real orthogonal matrix, then P_1, P_2 are real matrices and so are $[R_{\lambda,1} \ R_{\lambda,2}]$, $[L_{\lambda,1} \ L_{\lambda,2}]$, I , and O .

Note that for $\|E\|_\infty \rightarrow \Delta/4$ the upper bound on $\|P_2\|_\infty$, and consequently $\|L_{\lambda,2}\|_\infty \|R_{\lambda,2}\|_\infty$, diverges, i.e., the perturbation argument does not work in this limit.

Proof. The proof follows by checking the conditions of Theorem 25. First, we need to bound the separation function between Id and Λ . Using $\text{sep}(\text{Id}, 0) = 1$ and the stability of the separation function (76), we have

$$\text{sep}(\text{Id}, 0 + \Lambda) \geq \text{sep}(\text{Id}, 0) - \|\Lambda\|_\infty \geq 1 - (1 - \Delta) = \Delta.$$

Since isometries have unit spectral norm, we find

$$\|E_{11}\|_\infty, \|E_{21}\|_\infty, \|E_{12}\|_\infty, \|E_{22}\|_\infty \leq \|E\|_\infty. \quad (88)$$

By assumption, we then have

$$\delta := \text{sep}(\text{Id}, \Lambda) - \|E_{11}\|_\infty - \|E_{22}\|_\infty \geq \Delta - 2\|E\|_\infty > \frac{\Delta}{2} > 0 \quad (89)$$

and

$$\frac{\|E_{12}\|_\infty \|E_{21}\|_\infty}{\delta^2} \leq \left(\frac{\|E\|_\infty}{\Delta - 2\|E\|_\infty} \right)^2 \leq \frac{1}{4}.$$

Thus, Theorem 25 implies the existence of matrices P_1 and P_2 such that Eqs. (86) and (87) hold.

Next, we establish the claimed norm bounds on P_1 and P_2 . Since $x - 1 > \frac{x}{2}$ for any $x > 2$, we have with $x = \Delta/(2\|E\|_\infty) > 2$

$$\|P_1\|_\infty \leq 2 \frac{\|E_{21}\|_\infty}{\delta} \leq \frac{2\|E\|_\infty}{\Delta - 2\|E\|_\infty} = \frac{1}{\Delta/(2\|E\|_\infty) - 1} < 4 \frac{\|E\|_\infty}{\Delta}. \quad (90)$$

Using Eq. (88) and repeatedly Eq. (89), the bound (84) on $\|P_2\|_\infty$ becomes

$$\|P_2\|_\infty \leq \frac{2\|E\|_\infty}{\delta - 4\|E\|_\infty^2/\delta} \leq \frac{2\|E\|_\infty}{\Delta - 2\|E\|_\infty - 4\|E\|_\infty^2/(\Delta - 2\|E\|_\infty)} \quad (91)$$

$$\begin{aligned} &= \frac{2\|E\|_\infty(\Delta - 2\|E\|_\infty)}{(\Delta - 2\|E\|_\infty)^2 - 4\|E\|_\infty^2} \\ &= \frac{2\|E\|_\infty(\Delta - 2\|E\|_\infty)}{\Delta^2 - 4\|E\|_\infty\Delta} \leq \frac{2\|E\|_\infty}{\Delta - 4\|E\|_\infty}. \end{aligned} \quad (92)$$

We continue by deriving the remaining bounds. We have

$$\begin{aligned} \|I - \text{Id}\|_\infty &\leq \|E_{11}\|_\infty + \|E_{12}P_1\|_\infty < \|E\|_\infty + 4\frac{\|E\|_\infty^2}{\Delta} < 2\|E\|_\infty, \\ \|O - \Lambda\|_\infty &\leq \|E_{22}\|_\infty + \|P_1E_{12}\|_\infty < \|E\|_\infty + 4\frac{\|E\|_\infty^2}{\Delta} < 2\|E\|_\infty. \end{aligned}$$

Then, by the stability of the separation function,

$$\text{sep}(I, O) \geq \text{sep}(\text{Id}, \Lambda) - 4\|E\|_\infty \geq \Delta - 4\|E\|_\infty.$$

Using the bounds on P_1 and P_2 , we can bound the basis change operators $L_{\lambda,2} = X_2 - X_1P_1^\dagger$ and $R_{\lambda,2} = X_1P_2 + X_2P_1P_2 + X_2$ as

$$\|R_{\lambda,2}\|_\infty \leq 1 + \|P_1\|_\infty\|P_2\|_\infty + \|P_2\|_\infty \quad \|L_{\lambda,2}\|_\infty \leq 1 + \|P_1\|_\infty.$$

We use the first inequalities in (90) and (91) on P_1 and P_2 and then Eq. (89) to obtain

$$\|P_1\|_\infty\|P_2\|_\infty \leq \frac{4\|E\|_\infty^2}{\delta^2 - 4\|E\|_\infty^2} \leq \frac{4\|E\|_\infty^2}{(\Delta - 2\|E\|_\infty)^2 - 4\|E\|_\infty^2} = \frac{4\|E\|_\infty^2}{\Delta^2 - 4\Delta\|E\|_\infty}. \quad (93)$$

Together with the bound (92) on P_2 this yields

$$\begin{aligned} \|L_{\lambda,2}\|_\infty\|R_{\lambda,2}\|_\infty &\leq 1 + (2 + \|P_1\|_\infty)\|P_1\|_\infty\|P_2\|_\infty + \|P_1\|_\infty + \|P_2\|_\infty \\ &\leq 1 + \left(2 + 4\frac{\|E\|_\infty}{\Delta}\right) \frac{4\|E\|_\infty^2}{\Delta^2 - 4\Delta\|E\|_\infty} + 4\frac{\|E\|_\infty}{\Delta} + \frac{2\|E\|_\infty}{\Delta - 4\|E\|_\infty} \\ &= \left(1 - 4\frac{\|E\|_\infty}{\Delta}\right) \frac{\|E\|_\infty}{\Delta} + \frac{1 + \|E\|_\infty/\Delta}{1 - 4\|E\|_\infty/\Delta}. \end{aligned}$$

The final statement for the perturbation of real matrices follows readily from Rem. 1. \square

C Sampling complexity for ideal implementations

In Sec. 5.4, Thm. 17, we have established bounds on the sampling complexity of filtered RB. These involve the second moments of the estimator if an ideal implementation is used for which $\nu = \mu$ is the Haar measure and $\phi = \omega$ is the reference representation. This ideal second moment is given by Eq. (39) as follows

$$\mathbb{E}[f_\lambda^2]_{\text{SPAM}} = (\rho^{\otimes 2} | (X_\lambda S_\lambda^+)^{\otimes 2} \hat{\omega}[\omega_\lambda^{\otimes 2}] (X_\lambda^{\dagger \otimes 2} \tilde{M}_3) | \hat{\rho}). \quad (94)$$

Here,

$$\tilde{M}_3 := \sum_{i \in [d]} |E_i \otimes E_i\rangle \langle \tilde{E}_i| = \sum_{i \in [d]} |E_i \otimes E_i\rangle \langle E_i|_{\mathcal{E}_M},$$

is an operator associated with our measurement basis $E_i = |i\rangle\langle i|$ and the measurement noise \mathcal{E}_M . The second moment involves a projector of the form

$$\hat{\omega}[\omega_\lambda^{\otimes 2}] = \int_G \omega_\lambda(g)^\dagger \otimes \omega_\lambda(g)^\dagger(\cdot) \omega(g) d\mu(g). \quad (95)$$

Note that the above statements also hold if ν is an appropriate design, namely a $\bar{\omega}_\lambda \otimes \bar{\omega}_\lambda \otimes \omega$ -design. Generally, this is a weaker assumption than assuming a $\omega^{\otimes 3}$ -design.

Analogous to the proof of Prop. 2, only the irreps $\tau_\sigma \subset \omega$ which appear in $\tau_\lambda \otimes \tau_\lambda$ contribute to this projection. Compared to Prop. 2, we here use a different formulation which is more practical in the concrete cases below. Let $\Sigma := \text{Irr}(\omega_\lambda \otimes \omega_\lambda) \cap \text{Irr}(\omega)$ be the set of common irreps and let n_σ and m_σ be the multiplicities of τ_σ in ω and $\omega_\lambda \otimes \omega_\lambda$, respectively. Let us label the copies as $\tau_\sigma^{(i)}$. We find

$$\hat{\omega}[\omega_\lambda^{\otimes 2}] = \bigoplus_{\sigma \in \Sigma} \bigoplus_{i=1}^{m_\sigma} \bigoplus_{j=1}^{n_\sigma} \int_G \tau_\sigma^{(i)}(g)^\dagger(\cdot) \tau_\sigma^{(j)}(g) d\mu(g) = \bigoplus_{\sigma} \bigoplus_{i=1}^{m_\sigma} \bigoplus_{j=1}^{n_\sigma} |I_\sigma^{(i,j)}\rangle \langle I_\sigma^{(i,j)}|, \quad (96)$$

where $I_\sigma^{(i,j)}$ is a G -equivariant isometry between the irreps $\tau_\sigma^{(j)}$ and $\tau_\sigma^{(i)}$, a so-called *intertwiner*. In the following, we construct G -equivariant isomorphisms $I_\sigma^{(i,j)}$ which only after normalization with $\|I_\sigma^{(i,j)}\|_2$ become an isometry. We still refer to such maps as *intertwiners*.

Unfortunately, not much more can be said about the common irreps without fixing a specific group and representation. In general, $\tau_\lambda \otimes \tau_\lambda$ contains a trivial irrep if and only if τ_λ is a real representation. For our applications, this is the case, hence the rank of $\hat{\omega}[\omega_\lambda^{\otimes 2}]$ is at least the product of the multiplicity n_λ of τ_λ in ω with the multiplicity of the trivial irrep.

In the following, we consider some concrete cases and assume that $G < \text{U}(d)$. The reference representation is taken as $\omega(g) := U_g(\cdot) U_g^\dagger$ where $g \mapsto U_g$ is the defining representation of $\text{U}(d)$.

The following can alternatively be deduced with appropriate Haar integration formulas, and has already been partially calculated elsewhere, for instance in Ref. [45]. Here, we give a self-contained derivation in consistent notation which might be useful to readers not familiar with other works and can serve as a basis for analogous calculations for other groups.

C.1 Second moment for unitary 3-designs

If G is a unitary 3-design, it is in particular a 2-design and hence ω decomposes into the trivial irrep τ_1 and the adjoint irrep τ_{ad} . We fix $\omega_\lambda \equiv \tau_{\text{ad}}$. The 3-design property implies that the integral in Eq. (95) is the same as over $\text{U}(d)$. For $\text{U}(d)$, the representation $\tau_{\text{ad}} \otimes \tau_{\text{ad}}$ contains the trivial irrep with multiplicity one. A general argument implies that $\tau_{\text{ad}} \otimes \tau_{\text{ad}}$ has to contain the adjoint irrep, too. To find its multiplicity, we compute the character inner product. In the following, χ and χ_{ad} denote the characters of ω and τ_{ad} , respectively.

$$\begin{aligned} m_{\text{ad}} &:= \langle \chi_{\text{ad}}^2, \chi_{\text{ad}} \rangle = \langle (\chi - 1)^2, \chi_{\text{ad}} \rangle = \langle \chi^2, \chi_{\text{ad}} \rangle - 2 \\ &= \langle \chi^3, 1 \rangle - \langle \chi^2, 1 \rangle - 2 = \begin{cases} 1 & \text{if } d = 2, \\ 2 & \text{if } d \geq 3. \end{cases} \end{aligned} \quad (97)$$

Here, we multiply used $\chi = \chi_{\text{ad}} + 1$ and the following combinatorial identity [107–109]:

$$\langle \chi^t, 1 \rangle = \int_{U(d)} |\text{tr } U_g|^{2t} d\mu(g) = \begin{cases} \frac{(2t)!}{t!(t+1)!} & \text{if } d = 2, \\ t! & \text{if } d \geq t. \end{cases}$$

In summary, we find

$$\text{rank } \hat{\omega}[\tau_{\text{ad}}^{\otimes 2}] = \begin{cases} 2 & \text{if } d = 2, \\ 3 & \text{if } d \geq t. \end{cases}$$

Next, we derive the precise contributions of these irreps to $\hat{\omega}[\tau_{\text{ad}}^{\otimes 2}]$ by Eq. (96) and argue that the overlaps of the remaining terms in the second moment (94) with these subspaces are small.

Contribution from the trival irreps. Note that $\tau_{\text{ad}} \otimes \tau_{\text{ad}}$ is the restriction of $\omega \otimes \omega$ to the tensor square $M_0(d)^{\otimes 2}$ of complex traceless $d \times d$ matrices. The trivial subrepresentation of $\omega \otimes \omega$ is spanned by the identity matrix $\mathbb{1} \otimes \mathbb{1}$ and the flip F which can be written as $F = F_0 + \frac{\mathbb{1} \otimes \mathbb{1}}{d}$ for a matrix $F_0 \in M_0(d)^{\otimes 2}$. Hence, the trivial irrep of $\tau_{\text{ad}} \otimes \tau_{\text{ad}}$ is spanned by F_0 and thus equivalent to the trivial irrep of ω , spanned by $\mathbb{1}$, under the intertwiner

$$I_1 := |F_0\rangle\langle \mathbb{1}|.$$

Indeed, $I_1/\|I_1\|_2$ is an G -equivariant isometry. The contribution of the trivial irreps in $\tau_{\text{ad}} \otimes \tau_{\text{ad}}$ and ω is then given as the orthogonal projection onto I_1 :

$$\Pi_1(X) := \int_G \tau_{\text{ad}}(g)^\dagger \otimes \tau_{\text{ad}}(g)^\dagger (\cdot) \tau_1(g) d\mu(g) = \frac{(I_1|X)}{(I_1|I_1)} I_1, \quad (I_1|I_1) = d(d^2 - 1).$$

Here, the normalization follows from $\|\mathbb{1}\|_2^2 = d$ and $\|F_0\|_2^2 = \|F\|_2^2 - d^{-2}\|\mathbb{1} \otimes \mathbb{1}\|_2^2 = d^2 - 1$.

The overlap of $(X_{\text{ad}}^\dagger)^{\otimes 2} \tilde{M}_3$ with I_1 can be computed using the swap trick as follows

$$\begin{aligned} (I_1|(X_{\text{ad}}^\dagger)^{\otimes 2} \tilde{M}_3) &= \sum_{i=1}^d (\tilde{E}_i|\mathbb{1}) ((X_{\text{ad}}^\dagger E_i)^{\otimes 2}|F_0) \\ &= \sum_{i=1}^d \text{tr}(\tilde{E}_i) \text{tr} \left[\left(E_i - \frac{\mathbb{1}}{d} \right)^{\otimes 2} \left(F - \frac{\mathbb{1} \otimes \mathbb{1}}{d} \right) \right] \\ &= \sum_{i=1}^d \text{tr}(\tilde{E}_i) \left[\text{tr} \left(E_i - \frac{\mathbb{1}}{d} \right)^2 - \frac{1}{d} \left(\text{tr} \left(E_i - \frac{\mathbb{1}}{d} \right) \right)^2 \right] \\ &= \sum_{i=1}^d \text{tr}(\tilde{E}_i) \left(1 - \frac{1}{d} \right) \\ &= \left(1 - \frac{1}{d} \right) \text{tr } \mathcal{E}_M^\dagger \left(\sum_i |i\rangle\langle i| \right) \\ &= (d-1) \frac{\text{tr } \tilde{\mathbb{1}}}{d} \leq d-1. \end{aligned}$$

In the last step, we use $\sum_i E_i = \sum_i |i\rangle\langle i| = \mathbb{1}$ and the definition $\tilde{\mathbb{1}} := \mathcal{E}_M^\dagger(\mathbb{1})$. The final bound follows since the measurement noise \mathcal{E}_M is trace non-increasing and thus $\text{tr } \tilde{\mathbb{1}} \leq \text{tr } \mathbb{1} = d$. In particular, if \mathcal{E}_M is trace-preserving, we have equality. Hence, we have the following for the projection of $(X_{\text{ad}}^\dagger)^{\otimes 2} \tilde{M}_3$ onto the trival contribution. Recall that we have found $S_{\text{ad}}^+ = (d+1)\text{id}_{\text{ad}}$ in Sec. 5.2.

$$(S_{\text{ad}}^+)^{\otimes 2} \Pi_1((X_{\text{ad}}^\dagger)^{\otimes 2} \tilde{M}_3) = \frac{\text{tr } \tilde{\mathbb{1}}}{d} \frac{(d-1)(d+1)^2}{d(d^2-1)} |F_0\rangle\langle \mathbb{1}| = \frac{\text{tr } \tilde{\mathbb{1}}}{d} \frac{d+1}{d} |F_0\rangle\langle \mathbb{1}|.$$

Hence, the total contribution by the trivial irrep is

$$\begin{aligned}
(\rho^{\otimes 2} |X_{\text{ad}}^{\otimes 2} (S_{\text{ad}}^+)^{\otimes 2} \Pi_1((X_{\text{ad}}^\dagger)^{\otimes 2} \tilde{M}_3) |\tilde{\rho}) &= \frac{\text{tr } \tilde{\mathbb{1}}}{d} \frac{d+1}{d} (\rho^{\otimes 2} |X_{\text{ad}}^{\otimes 2} |F_0)(\mathbb{1} |\tilde{\rho}) \\
&= \frac{\text{tr } \tilde{\mathbb{1}}}{d} \frac{d+1}{d} \text{tr} \left(\left(\rho - \frac{\mathbb{1}}{d} \right)^{\otimes 2} \left(F - \frac{\mathbb{1} \otimes \mathbb{1}}{d} \right) \right) \\
&= \frac{\text{tr } \tilde{\mathbb{1}}}{d} \frac{d^2 - 1}{d^2} \leq \frac{d^2 - 1}{d^2}
\end{aligned} \tag{98}$$

Contribution from the adjoint irreps. The two adjoint irreps in $\tau_{\text{ad}} \otimes \tau_{\text{ad}}$ come from the identification of certain product operators $A \otimes B \in M_0(d) \otimes M_0(d)$ with their product $AB \in M_0(d)$ or $BA \in M_0(d)$. Clearly, under such maps, the representation $\tau_{\text{ad}} \otimes \tau_{\text{ad}}$ corresponds to τ_{ad} .

To make this precise and explicit, we describe the irreps in the orthogonal basis of Weyl operators. In contrast to Sec. 4.5, we here use the ‘modular definition’ of Weyl operators which is available in any dimension d .¹⁰ To this end, we label the measurement basis as $|x\rangle$ where $x \in \mathbb{Z}_d$. The Weyl operators are then defined as $w(x, z)|y\rangle := \xi^{zy}|y+x\rangle$ where $z, x, y \in \mathbb{Z}_d$, ξ is a primitive d -th root of unity, and all operations are performed in the ring \mathbb{Z}_d . It is convenient to group the arguments as $a = (z, x) \in \mathbb{Z}_d^2$. The Weyl operators are unitary, traceless if $a \neq 0$, and $w(a)w(b) \propto w(a+b)$.

Consider the following linear maps $M_0(d) \rightarrow M_0(d) \otimes M_0(d)$ defined in the Weyl basis:

$$I_{\text{ad}}^{(1)} := \sum_{\substack{a, b \in \mathbb{Z}_d^2 \setminus 0 \\ a+b \neq 0}} |w(a) \otimes w(b)\rangle \langle w(a)w(b)|, \quad I_{\text{ad}}^{(2)} := \sum_{\substack{a, b \in \mathbb{Z}_d^2 \setminus 0 \\ a+b \neq 0}} |w(a) \otimes w(b)\rangle \langle w(b)w(a)|.$$

These maps identify a traceless Weyl operator $w(c) \in M_0(d)$ with the uniform superposition of all $w(a) \otimes w(b) \in M_0(d) \otimes M_0(d)$ such that $a+b=c$. Since the sum is commutative, there are two choices of attributing the summands to tensor factors, leading to the two maps $I_{\text{ad}}^{(1)}$ and $I_{\text{ad}}^{(2)}$. It is straightforward to check (e.g. by computing $I_{\text{ad}}^{(i)\dagger} I_{\text{ad}}^{(i)}$) that both maps are isometries, up to normalization by $\|I_{\text{ad}}^{(i)}\|_2$. The two linear maps are linearly independent, except for the case $d=2$: There, the traceless Pauli operators X, Y, Z mutually anti-commute and hence

$$I_{\text{ad}}^{(1)} = -I_{\text{ad}}^{(2)} \quad (\text{for } d=2).$$

We claim that the images of $I_{\text{ad}}^{(1)}$ and $I_{\text{ad}}^{(2)}$ correspond to a single ($d=2$) or two copies ($d \geq 3$) of τ_{ad} in $\tau_{\text{ad}} \otimes \tau_{\text{ad}}$. In the latter case, the two copies can be mapped onto each other by permuting the tensor factors. Note that this is in perfect alignment with the previously computed multiplicity (97).

The claim can be verified by a simple, but somewhat lengthy calculation which shows that $I_{\text{ad}}^{(1)}$ and $I_{\text{ad}}^{(2)}$ are indeed fixed by the representation $\tau_{\text{ad}}^\dagger \otimes \tau_{\text{ad}}^\dagger(\cdot) \tau_{\text{ad}}$. For $d=2$, we can take either of the two intertwiners, say $I_{\text{ad}}^{(1)}$, as a basis for the range of the projector

$$\Pi_{\text{ad}} := \int_G \tau_{\text{ad}}(g)^\dagger \otimes \tau_{\text{ad}}(g)^\dagger(\cdot) \tau_{\text{ad}}(g) \, d\mu(g).$$

For $d \geq 3$, the two intertwiners are linearly independent, but do not form an orthogonal basis, as

¹⁰However, the resulting groups do not have such nice properties as in the ‘finite field definition’ in prime-power dimensions. Nevertheless, we here only need an orthogonal basis for the traceless subspace.

one can readily compute:

$$\begin{aligned}
(I_{\text{ad}}^{(1)} | I_{\text{ad}}^{(2)}) &= d^2 \sum_{\substack{a, b \in \mathbb{Z}_d^2 \setminus 0 \\ a+b \neq 0}} (w(b)w(a) | w(a)w(b)) \\
&= d^3 \sum_{a \neq 0} \sum_{\substack{b \neq 0 \\ b \neq -a}} \xi^{[a, b]} \\
&= d^3 \sum_{a \neq 0} (d^2 \delta_{a, 0} - 2) \\
&= -2d^3(d^2 - 1).
\end{aligned}$$

Here, $\xi = e^{2\pi i/d}$ and $[a, b] = a_1 b_2 - a_2 b_1$ is the symplectic form measuring whether $w(a)$ and $w(b)$ commute. In the second to last step we used that character orthogonality implies $\sum_{b \in \mathbb{Z}_d^2} \xi^{[a, b]} = d^2 \delta_{a, 0}$. Likewise, we find

$$(I_{\text{ad}}^{(i)} | I_{\text{ad}}^{(i)}) = d^2 \sum_{\substack{a, b \in \mathbb{Z}_d^2 \setminus 0 \\ a+b \neq 0}} (w(a)w(b) | w(a)w(b)) = d^3(d^2 - 1)(d^2 - 2).$$

Hence, for $d \geq 3$, we use Gram-Schmidt orthogonalization to expand the projector:

$$\begin{aligned}
\tilde{I}_{\text{ad}}^{(2)} &:= I_{\text{ad}}^{(2)} - \frac{(I_{\text{ad}}^{(2)} | I_{\text{ad}}^{(1)})}{d^3(d^2 - 1)(d^2 - 2)} I_{\text{ad}}^{(1)} = I_{\text{ad}}^{(2)} + \frac{2}{d^2 - 2} I_{\text{ad}}^{(1)} \\
(\tilde{I}_{\text{ad}}^{(2)} | \tilde{I}_{\text{ad}}^{(2)}) &= (I_{\text{ad}}^{(2)} | I_{\text{ad}}^{(2)}) + \frac{4}{d^2 - 2} (I_{\text{ad}}^{(2)} | I_{\text{ad}}^{(1)}) + \frac{4}{(d^2 - 2)^2} (I_{\text{ad}}^{(1)} | I_{\text{ad}}^{(1)}) \\
&= d^3(d^2 - 1)(d^2 - 2) - \frac{8d^3(d^2 - 1)}{d^2 - 2} + \frac{4d^3(d^2 - 1)}{d^2 - 2} \\
&= d^3(d^2 - 1)(d^2 - 2) \left(1 - \frac{4}{(d^2 - 2)^2} \right) \\
&= d^3(d^2 - 1)(d^2 - 2) \frac{d^2(d^2 - 4)}{(d^2 - 2)^2}.
\end{aligned}$$

For our purposes, it is enough to compute the projection of superoperators $L : M_0(d) \rightarrow M_0(d) \otimes M_0(d)$ which are invariant under the permutation of tensor factors of $M_0(d) \otimes M_0(d)$, this is $\pi L = L$ for $\pi \in S_2$. Since $I_{\text{ad}}^{(2)} = \pi I_{\text{ad}}^{(1)}$ for $\pi \neq \text{id}$, it is then immediate that $(I_{\text{ad}}^{(2)} | L) = (I_{\text{ad}}^{(1)} | L)$ and thus we have the following expansion for $d \geq 3$:

$$\begin{aligned}
\Pi_{\text{ad}}(L) &= \frac{(I_{\text{ad}}^{(1)} | L)}{(I_{\text{ad}}^{(1)} | I_{\text{ad}}^{(1)})} I_{\text{ad}}^{(1)} + \frac{(\tilde{I}_{\text{ad}}^{(2)} | L)}{(\tilde{I}_{\text{ad}}^{(2)} | \tilde{I}_{\text{ad}}^{(2)})} \tilde{I}_{\text{ad}}^{(2)} \\
&= \frac{(I_{\text{ad}}^{(1)} | L)}{d^3(d^2 - 1)(d^2 - 2)} \left(I_{\text{ad}}^{(1)} + \frac{(d^2 - 2)^2}{d^2(d^2 - 4)} \left(1 + \frac{2}{d^2 - 2} \right) \tilde{I}_{\text{ad}}^{(2)} \right) \\
&= \frac{(I_{\text{ad}}^{(1)} | L)}{d^3(d^2 - 1)(d^2 - 2)} \left(I_{\text{ad}}^{(1)} + \frac{d^2 - 2}{d^2 - 4} \left(I_{\text{ad}}^{(2)} + \frac{2}{d^2 - 2} I_{\text{ad}}^{(1)} \right) \right) \\
&= \frac{(I_{\text{ad}}^{(1)} | L)}{d^3(d^2 - 1)(d^2 - 2)} \left(\frac{d^2 - 2}{d^2 - 4} I_{\text{ad}}^{(1)} + \frac{d^2 - 2}{d^2 - 4} I_{\text{ad}}^{(2)} \right) \\
&= \frac{(I_{\text{ad}}^{(1)} | L)}{d^3(d^2 - 1)(d^2 - 4)} \left(I_{\text{ad}}^{(1)} + I_{\text{ad}}^{(2)} \right). \tag{99}
\end{aligned}$$

We find the following for the overlap of $(X_{\text{ad}}^\dagger)^{\otimes 2} \tilde{M}_3$ with $I_{\text{ad}}^{(1)}$:

$$\begin{aligned}
(I_{\text{ad}}^{(1)} | (X_{\text{ad}}^\dagger)^{\otimes 2} \tilde{M}_3) &= \sum_{\substack{a, b \in \mathbb{Z}_d^2 \setminus 0 \\ a+b \neq 0}} \sum_{y \in \mathbb{Z}_d} (w(a) \otimes w(b) | (X_{\text{ad}}^\dagger E_y)^{\otimes 2}) (\tilde{E}_y | w(a) w(b)) \\
&= \sum_{\substack{a, b \in \mathbb{Z}_d^2 \setminus 0 \\ a+b \neq 0}} \sum_{y \in \mathbb{Z}_d} \text{tr}(w(a)^\dagger E_y) \text{tr}(w(b)^\dagger E_y) (\tilde{E}_y | w(a) w(b)) \\
&= \sum_{\substack{z, z' \in \mathbb{Z}_d \setminus 0 \\ z+z' \neq 0}} \sum_{y \in \mathbb{Z}_d} \omega^{-(z+z')y} (\tilde{E}_y | Z(z+z')) \\
&= \sum_{\substack{z, z' \in \mathbb{Z}_d \setminus 0 \\ z+z' \neq 0}} \left(\mathcal{E}_M^\dagger \left(\sum_{y \in \mathbb{Z}_d} \omega^{(z+z')y} |y\rangle \langle y| \right) \middle| Z(z+z') \right) \\
&= \sum_{\substack{z, z' \in \mathbb{Z}_d \setminus 0 \\ z+z' \neq 0}} (Z(z+z') | \mathcal{E}_M | Z(z+z')) \\
&= (d-2) \sum_{z \in \mathbb{Z}_d \setminus 0} (Z(z) | \mathcal{E}_M | Z(z)) \\
&= d(d-2) \text{tr}(P_{\text{ad}} \tilde{M}), \tag{100}
\end{aligned}$$

where we have used that $M = d^{-1} \sum_{z \in \mathbb{Z}_d} |Z(z)\rangle \langle Z(z)|$ and $\tilde{M} = M \mathcal{E}_M$. The expression $\text{tr}(P_{\text{ad}} \tilde{M})$ is discussed in the main text. In particular for λ -multiplicity free and aligned with M , we found the upper bound $\text{tr}(P_{\text{ad}} \tilde{M}) \leq \text{tr}(P_{\text{ad}} M) = d-1$.

Using Eq. (99) with $L = (X_{\text{ad}}^\dagger)^{\otimes 2} \tilde{M}_3$, we find the following expression for the projection onto the adjoint contribution for $d \geq 3$:

$$\Pi_{\text{ad}} \left((X_{\text{ad}}^\dagger)^{\otimes 2} \tilde{M}_3 \right) = \frac{\text{tr}(P_{\text{ad}} \tilde{M})}{d^2(d^2-1)(d+2)} \left(I_{\text{ad}}^{(1)} + I_{\text{ad}}^{(2)} \right). \tag{101}$$

Recall that for $d=2$, the projection is instead given by projecting onto $I_{\text{ad}}^{(1)}$ only. However, since $(I_{\text{ad}}^{(1)} | L) = (I_{\text{ad}}^{(2)} | L) = -(I_{\text{ad}}^{(1)} | L)$ for any symmetric L , the overlap has to vanish. Applied to $L = (X_{\text{ad}}^\dagger)^{\otimes 2} \tilde{M}_3$ this immediately shows that the adjoint contribution to the second moment is zero.

Finally, multiplying Eq. (101) with $S_{\text{ad}}^+ = (d+1)\text{id}_{\text{ad}}$ does only change the prefactor such that we get the contribution of the adjoint irreps to the second moment by contracting Eq. (101) with $\rho^{\otimes 2}$ and $\tilde{\rho}$. Note that the left hand side is again symmetric and thus the contributions of $I_{\text{ad}}^{(1)}$ and $I_{\text{ad}}^{(2)}$ are identical. What is left is to compute the overlap of $I_{\text{ad}}^{(1)}$ with the states. Here, we again assume that ρ is pure, and let $\rho_0 = X_{\text{ad}}^\dagger(\rho) \simeq \rho - \mathbb{1}/d$ be its traceless part. From the definition of $I_{\text{ad}}^{(1)}$, we have $(\rho_0^{\otimes 2} | I_{\text{ad}}^{(1)}) = d^2(\rho_0^2 | X_{\text{ad}})$ and the purity of ρ implies $X_{\text{ad}}^\dagger(\rho_0^2) = (d-2)/d \rho_0$. Hence, we find

$$(\rho^{\otimes 2} | X_{\text{ad}}^{\otimes 2} I_{\text{ad}}^{(1)} | \tilde{\rho}) = d^2(\rho_0^2 | X_{\text{ad}} | \tilde{\rho}) = d(d-2)(\rho | P_{\text{ad}} | \tilde{\rho}).$$

Combining the above results, we obtain

$$\begin{aligned}
(\rho^{\otimes 2} | X_{\text{ad}}^{\otimes 2} (S_{\text{ad}}^+)^{\otimes 2} \Pi_{\text{ad}} \left((X_{\text{ad}}^\dagger)^{\otimes 2} \tilde{M}_3 \right) | \tilde{\rho}) &= \frac{2 \text{tr}(P_{\text{ad}} \tilde{M})(d+1)}{d^2(d-1)(d+2)} (\rho^{\otimes 2} | X_{\text{ad}}^{\otimes 2} I_{\text{ad}}^{(1)} | \tilde{\rho}) \\
&= \frac{2 \text{tr}(P_{\text{ad}} \tilde{M})(d+1)(d-2)}{d(d-1)(d+2)} (\rho | P_{\text{ad}} | \tilde{\rho}). \tag{102}
\end{aligned}$$

Summing the contributions. We have found that the second moment for unitary 3-designs with SPAM noise can be expressed as

$$\begin{aligned}\mathbb{E}[f_{\text{ad}}^2]_{\text{SPAM}} &= \frac{\text{tr } \tilde{\mathbb{I}}}{d} \frac{d^2 - 1}{d^2} + \frac{2 \text{tr}(P_{\text{ad}} \tilde{M})(d+1)(d-2)}{d(d-1)(d+2)} (\rho | P_{\text{ad}} | \tilde{\rho}) \\ &\leq 1 - \frac{1}{d^2} + \frac{2(d+1)(d-1)(d-2)}{d^2(d+2)}\end{aligned}\quad (103)$$

$$\leq \begin{cases} \frac{3}{4} & \text{if } d = 2, \\ 3 - \frac{1}{d^2} & \text{if } d \geq 3. \end{cases}\quad (104)$$

In the second-to-last step we used $\text{tr } \tilde{\mathbb{I}} \leq d$, $(\rho | P_{\text{ad}} | \tilde{\rho}) \leq 1 - 1/d$, and the bound $\text{tr}(P_{\text{ad}} \tilde{M}) \leq d - 1$ from before. Note that the right hand side of Eq. (103) is exactly the expression for $\mathbb{E}[f_{\text{ad}}^2]_{\text{ideal}}$, i.e. the second moment in the absence of SPAM noise.

Subtracting the square of the first moment, $(d-1)^2/d^2$, we thus find the following exact expression for the variance, in the absence of SPAM noise:

$$\text{Var}[f_{\text{ad}}] = 2 \frac{d-1}{d+2}.$$

Analysis of SPAM visibilities From Eq. (103), we can observe that the noise-free contributions coming from the trivial and the adjoint irreps in $\tau_{\text{ad}}^{\otimes 2}$ are modulated by the SPAM visibilities for the first moments. In particular, we have

$$\frac{\text{tr } \tilde{\mathbb{I}}}{d} = \frac{\text{tr}(P_{\text{I}} \tilde{M})}{d} = v_{\text{M},1}, \quad \frac{\text{tr}(P_{\text{ad}} \tilde{M})}{d-1} = v_{\text{M},\text{ad}}, \quad (\rho | P_{\text{ad}} | \tilde{\rho}) = v_{\text{SP},\text{ad}} \frac{d-1}{d}.$$

We have the tight bounds

$$0 \leq v_{\text{M},1} \leq 1, \quad -\frac{1}{d-1} \leq v_{\text{SP},\text{ad}} \leq 1, \quad -\frac{1}{d-1} \leq v_{\text{M},\text{ad}} \leq 1.$$

The first two lower bounds are saturated for \mathcal{E}_{M} being the ‘discard’ operation and $\tilde{\rho}$ being orthogonal to ρ , respectively. Moreover, we have

$$\text{tr}(P_{\text{ad}} \tilde{M}) = \frac{1}{d} \sum_{z \neq 0} (Z(z) | \mathcal{E}_{\text{M}} | Z(z)).$$

Clearly, we can replace \mathcal{E}_{M} with its projection onto Weyl channels. If $\mathcal{E}_{\text{M}} = w(a)(\cdot)w(a)^\dagger$, then we find

$$\frac{1}{d} \sum_{z \neq 0} (Z(z) | \mathcal{E}_{\text{M}} | Z(z)) = \sum_{z \neq 0} \xi^{z \cdot a_x} = \begin{cases} d-1, & \text{if } a_x = 0, \\ -1, & \text{else.} \end{cases}$$

Hence, the lowest value can be achieved if \mathcal{E}_{M} is a convex combination of X -type Weyl operators, which shows the last lower bound.

We see that the contribution from the trivial irrep in Eq. (103) cannot be negative, but the one from the adjoint irrep can, with lower bound $-\frac{2(d+1)(d-2)}{d^2(d+2)} \geq -\frac{2}{d}$.

C.2 Second moment for local unitary 3-designs

Next, we assume that G is a local unitary 3-design, i.e. G factorizes as $G = G_{\text{loc}}^{\times m}$ where each copy of G_{loc} is a unitary 3-design acting on \mathbb{C}^q , and $d = q^m$ (e.g. the single-qubit Clifford group $G_{\text{loc}} = \text{Cl}_1(2)$).¹¹ The irreps of G are then simply the tensor products of the irreps of G_{loc} and hence we can label them by a binary vector $b \in \{0, 1\}^m$ where $b_i = 1$ and $b_i = 0$ correspond to the trivial and adjoint irrep on the i -th factor, respectively.

¹¹The following arguments hold with minor adaptations if $G = G_1 \times \dots \times G_m$ where each G_i is a unitary 3-group, acting on Hilbert spaces of not necessarily equal dimensions.

By Eq. (95), we have to decompose $\tau_b \otimes \tau_b$ into the relevant irreps τ_a appearing in ω . To this end, it is convenient to write $\tau_b \otimes \tau_b \simeq \bigotimes_{i=1}^m \tau_{b_i} \otimes \tau_{b_i}$. Then, $\tau_{b_i} \otimes \tau_{b_i} = 1$ if $b_i = 1$ and otherwise contains exactly one copy of the trivial irrep and m_{ad} copies of the adjoint irrep, where $m_{\text{ad}} = 1$ if $q = 2$ and $m_{\text{ad}} = 2$ else (c.f. Eq. (97)). Hence, the relevant irreps in $\tau_b \otimes \tau_b$ are labelled by $a \in \{0, 1\}^m$ where $a_i = 1$ if $b_i = 1$ and otherwise arbitrary. If $a \circ b$ denotes the bitwise (Hadamard) product, then we can formulate this condition as $|a \circ b| = |b|$. The multiplicity of the irrep τ_a is given as $m_a := m_{\text{ad}}^{|a|}$. Thus, we arrive at the decomposition

$$\tau_b \otimes \tau_b \simeq \bigotimes_{i=1}^m \tau_{b_i} \otimes \tau_{b_i} \simeq \bigoplus_{a: |a \circ b| = |b|} \tau_a^{\oplus m_a} \oplus \text{irrelevant irreps}. \quad (105)$$

We treat each of the $2^{|b|}$ irreps τ_a individually. The rank of the projector $\widehat{\omega}[\tau_a^{\oplus m_a}]$ is $m_a = m_{\text{ad}}^{|a|}$ and we can construct a basis for its range using tensor products of the intertwiners in Sec. C.1. To this end, we also need to define a (local) intertwiner between τ_1 and $\tau_1 \otimes \tau_1$ which we can take as $J_1 := |\mathbb{1} \otimes \mathbb{1}\rangle(\mathbb{1}|$.

For now, let us assume that the first $|b|$ bits of b are set and the remaining ones are zero, and the same holds for a , i. e. its first $|a| \geq |b|$ bits are set and otherwise zero. Similar to Sec. C.1, we want to assume that $L : M(q^m) \rightarrow M(q^m) \otimes M(q^m) \simeq \bigotimes_{i=1}^m M(q) \otimes M(q)$ is symmetric in the sense that it is left-invariant under permutations $\bigotimes_{i=1}^m \pi_i$ for $\pi_i \in S_2$ that permute the factors on every qudit. In this case, we can write

$$\widehat{\omega}[\tau_a^{\oplus m_a}](L) = \frac{(J_1^{\otimes |b|} \otimes I_1^{\otimes |a| - |b|} \otimes I_{\text{ad}}^{(1) \otimes |\bar{a}|} |L\rangle)}{q^{3|b|(q(q^2 - 1))^{|a| - |b|}(q^3(q^2 - 1)(q^2 - 2m_{\text{ad}}))^{|a|}}} J_1^{\otimes |b|} \otimes I_1^{\otimes |a| - |b|} \otimes I_{\text{ad}}^{\otimes |\bar{a}|}, \quad (106)$$

where we define $I_{\text{ad}} := I_{\text{ad}}^{(1)}$ if $q = 2$ and $I_{\text{ad}} := I_{\text{ad}}^{(1)} + I_{\text{ad}}^{(2)}$ for $q \geq 3$.

It seems reasonable to assume that both the measurement basis as well as the initial state share the locality structure of G , however the state preparation and measurement noise might fail to do so. For a local measurement basis $|x\rangle = \bigotimes_{i=1}^m |x_i\rangle$, the measurement operator M_3 becomes

$$M_3 = \sum_{x \in \mathbb{Z}_q^m} |E_x \otimes E_x\rangle\langle E_x| \simeq \bigotimes_{i=1}^m \sum_{x_i \in \mathbb{Z}_q} |E_{x_i} \otimes E_{x_i}\rangle\langle E_{x_i}| =: M_{3, \text{loc}}^{\otimes m}.$$

Retracing the steps from Sec. C.1 carefully, we find that

$$\begin{aligned} J_1^\dagger M_{3, \text{loc}} &= |\mathbb{1}\rangle(\mathbb{1} \otimes \mathbb{1}| M_{3, \text{loc}} = |\mathbb{1}\rangle(\mathbb{1}|, \\ I_1^\dagger M_{3, \text{loc}} &= |\mathbb{1}\rangle(F_0| M_{3, \text{loc}} = \frac{q-1}{q} |\mathbb{1}\rangle(\mathbb{1}|, \\ I_{\text{ad}}^{(1) \dagger} M_{3, \text{loc}} &= (q-2) \sum_{z \in \mathbb{Z}_q \setminus 0} |Z(z)\rangle\langle Z(z)| =: q(q-2)\tau. \end{aligned}$$

Here we have set $\tau := P_{\text{ad}} M_{\text{loc}}$. Taking $L = M_3 \mathcal{E}_M$ in Eq. (106) requires us to evaluate the following inner product:

$$\begin{aligned} (J_1^{\otimes |b|} \otimes I_1^{\otimes |a| - |b|} \otimes I_{\text{ad}}^{(1) \otimes |\bar{a}|} |M_3 \mathcal{E}_M\rangle) &= \left(\frac{q-1}{q}\right)^{|a| - |b|} (q(q-2))^{|a|} \text{tr} \left(|\mathbb{1}\rangle(\mathbb{1}|^{\otimes |a|} \otimes \tau^{\otimes |\bar{a}|} \mathcal{E}_M \right) \\ &\leq \left(\frac{q-1}{q}\right)^{|a| - |b|} (q(q-2))^{|a|} \text{tr} \left(|\mathbb{1}\rangle(\mathbb{1}|^{\otimes |a|} \otimes \tau^{\otimes |\bar{a}|} \right) \\ &= \left(\frac{q-1}{q}\right)^{|a| - |b|} (q(q-2))^{|a|} q^{|a|} (q-1)^{|\bar{a}|} \\ &= q^{|\bar{a}| + |b|} (q-1)^{|\bar{b}|} (q-2)^{|\bar{a}|} \\ &= q^{m + |\bar{a}| - |\bar{b}|} (q-1)^{|\bar{b}|} (q-2)^{|\bar{a}|} \end{aligned} \quad (107)$$

Here, the inequality follows as in Eq. (34), i. e. by the observation that we can replace \mathcal{E}_M by its unital and trace-preserving part with unit spectral norm and apply Hölder's inequality. Note that we have equality in the absence of SPAM noise.

Furthermore, let ρ be a pure product state, w.l.o.g. $\rho = \rho_{\text{loc}}^{\otimes m}$. Then, we have to contract it with the operators in Eq. (106). The necessarily computations have already been performed in Sec. C.1, in particular Eq. (98) and (102).

$$\begin{aligned}
(\rho^{\otimes 2} | J_1^{\otimes |b|} \otimes I_1^{\otimes |a|-|b|} \otimes I_{\text{ad}}^{\otimes |\bar{a}|} | \tilde{\rho}) &= \left(\frac{q-1}{q} \right)^{|a|-|b|} (q-2)^{|\bar{a}|} m_{\text{ad}}^{|\bar{a}|} (\mathbb{1}^{\otimes |a|} \otimes (q\rho_{\text{loc}} - \mathbb{1})^{\otimes |\bar{a}|} | \tilde{\rho}) \\
&\leq \left(\frac{q-1}{q} \right)^{|a|-|b|} (q-2)^{|\bar{a}|} (q-1)^{|\bar{a}|} m_{\text{ad}}^{|\bar{a}|} \\
&= q^{|b|-|a|} (q-1)^{|\bar{b}|} (q-2)^{|\bar{a}|} m_{\text{ad}}^{|\bar{a}|} \\
&= q^{|\bar{a}|-|\bar{b}|} (q-1)^{|\bar{b}|} (q-2)^{|\bar{a}|} m_{\text{ad}}^{|\bar{a}|}, \tag{108}
\end{aligned}$$

where the upper bound follows from Hölder's inequality. Again, we have equality in the absence of SPAM noise.

Recall that we have up to now assumed that only the very first bits of b and a are set and the others are zero. The result for an arbitrary bitstring $b \in \{0,1\}^m$ and $a \in \{0,1\}^m$ such that $|a \circ b| = |b|$ can be obtained by applying a suitable permutation to the basis of the projection in Eq. (106). However, it is straightforward to check that the established upper bounds (107) and (108) still hold, even when such a permutation is applied.

Finally, using $S_b^+ = (q+1)^{n-|b|} \text{id}_b$ from Sec. 5.2, we obtain the following upper bound for the second moment of local unitary 3-designs for $q \geq 3$:

$$\begin{aligned}
\mathbb{E}[f_b^2]_{\text{SPAM}} &= (\rho^{\otimes 2} | (X_b S_b^+)^{\otimes 2} \hat{\omega}[\tau_b \otimes \tau_b] (X_b^{\dagger \otimes 2} \tilde{M}_3) | \tilde{\rho}) \\
&\leq (q+1)^{2|\bar{b}|} \sum_{a: |a \circ b| = |b|} \frac{q^{m+2(|\bar{a}|-|\bar{b}|)} (q-1)^{2|\bar{b}|} (q-2)^{2|\bar{a}|} 2^{|\bar{a}|}}{q^{3(m-|\bar{b}|)} (q(q^2-1))^{|\bar{b}|-|\bar{a}|} (q^3(q^2-1)(q^2-4))^{|\bar{a}|}} \\
&= \frac{(q^2-1)^{|\bar{b}|}}{q^{2m}} \sum_{a: |a \circ b| = |b|} \left(\frac{2(q-2)}{q+2} \right)^{|\bar{a}|} \\
&= \frac{(q^2-1)^{|\bar{b}|}}{q^{2m}} \sum_{k=0}^{|\bar{b}|} \binom{|\bar{b}|}{k} \left(\frac{2(q-2)}{q+2} \right)^k \\
&= \frac{(q^2-1)^{|\bar{b}|}}{q^{2m}} \left(\frac{3q-2}{q+2} \right)^{|\bar{b}|} \tag{109} \\
&\leq \frac{(3q^2)^{|\bar{b}|}}{q^{2m}} = 3^m \left(\frac{3}{q^2} \right)^{|\bar{b}|} \leq 3^{m-|b|}.
\end{aligned}$$

The last inequality follows since we always have $3/q^2 \leq 1/3$ for $q \geq 3$. Hence, the second moment is only reasonably bounded if all but logarithmically many bits in b are set (i.e. we only have a logarithmic number of adjoint irreps). As argued earlier, the inequalities leading to the expression in Eq. (109) are tight in the absence of SPAM noise, and hence this is the result for $\mathbb{E}[f_b^2]_{\text{ideal}}$.

For $q = 2$, we can deduce similarly to Sec. C.1 that all contributions containing an adjoint irrep have to vanish. Concretely, the overlap in Eq. (107) is zero whenever $|\bar{a}| \neq 0$. Hence, the only irrep in Eq. (105) which contributes to the second moment is the one for which $a = (1, \dots, 1)$ is the all-ones vector. We then find

$$\mathbb{E}[f_b^2]_{\text{SPAM}} \leq \frac{q^m (q^2-1)^{2|\bar{b}|}}{q^{3m-|\bar{b}|} (q(q^2-1))^{|\bar{b}|}} = \frac{(q^2-1)^{|\bar{b}|}}{q^{2m}} = \left(\frac{3}{4} \right)^{|\bar{b}|} \left(\frac{1}{4} \right)^{|\bar{b}|} \leq 1.$$

Again, note that we have equality in the first inequality in the absence of SPAM noise.

C.3 Second moment for the Heisenberg-Weyl/Pauli group

As another example, we consider the Heisenberg-Weyl group $G = \text{HW}_n(p)$ as defined in Sec. 4.5, and write the Weyl operators as $w(v)$ with $v \in \mathbb{F}_p^{2n}$. The Heisenberg-Weyl group acts naturally on

$(\mathbb{C}^p)^{\otimes n}$ and its conjugation representation decomposes into one-dimensional irreps since

$$w(v)w(u)w(v)^\dagger = \xi^{[v,u]}w(u),$$

where ξ is a primitive p -th root of unity and $[v, u]$ is the standard symplectic product on \mathbb{F}_p^{2n} . Hence, let us label the irreps of $\text{HW}_n(p)$ by τ_u .

Clearly, $\tau_u \otimes \tau_u \simeq \tau_{2u}$ and hence the projector of the second moment becomes

$$\widehat{\omega}[\tau_u \otimes \tau_u] = \frac{|I_u|(I_u|)}{p^{3n}}, \quad I_u := |w(u) \otimes w(u)(w(2u)|.$$

Thus, we find for $u = (z, x)$, similar to the calculation in Eq. (100):

$$\begin{aligned} (I_u | (X_u^\dagger)^{\otimes 2} \tilde{M}_3) &= \sum_{y \in \mathbb{F}_p^n} (w(u) \otimes w(u) | E_y \otimes E_y) (\tilde{E}_y | w(2u)) \\ &= \delta_{x,0} \sum_{y \in \mathbb{F}_p^n} \xi^{2z \cdot y} (\mathcal{E}_M^\dagger(|y\rangle\langle y|) | Z(2z)) \\ &= \delta_{x,0} (Z(2z) | \mathcal{E}_M | Z(2z)) \leq \delta_{x,0} p^n. \end{aligned}$$

Note that for qubits, $p = 2$, we have $2z = 0$ and hence the last inequality is an equality if \mathcal{E}_M is trace-preserving.

Hence, we find the following bound for the second moment

$$\begin{aligned} \mathbb{E}[f_b^2]_{\text{SPAM}} &= (\rho^{\otimes 2} | (X_u S_u^\dagger)^{\otimes 2} \widehat{\omega}[\tau_u \otimes \tau_u] (X_u^\dagger)^{\otimes 2} \tilde{M}_3 | \tilde{\rho}) \\ &\leq \frac{\delta_{x,0}}{p^{2n}} (\rho | Z(z))^2 (Z(z) | \tilde{\rho}) \leq \frac{\delta_{x,0}}{p^{2n}}, \end{aligned}$$

where we have used Hölder's inequality twice in the last step. Note that all inequalities are saturated in the absence of SPAM noise.